

**Role of Endothelial Potassium Channels in Vasodilation Under Normal and Dyslipidemic Condition**

BY

Sang Joon Ahn

B.S., Kyung-hee University, 2003

M.M.S., Kyung-hee University, 2005

THESIS

Submitted as partial fulfillment of the requirements  
for the degree of Doctor of Philosophy in Bioengineering  
in the Graduate College of the  
University of Illinois at Chicago, 2017

Chicago, Illinois

Defense Committee:

Irena Levitan, Chair and Advisor

David Eddington

James Lee

Shane Phillips, Physical Therapy

Gye Young Park, Pulmonary, Critical Care, Sleep & Allergy

## **Acknowledgements**

I appreciate the supervision and research support from Dr. Levitan and Dr. Phillips during my PhD program. Without the unwavering help and support of Dr. Levitan and Dr. Phillips, this body of work may have not been achieved. I am also grateful for critical and scientific advice from my previous preliminary and current dissertation committee: Dr. Eddington, Dr. Liang, Dr. Wedgewood, Dr. Lee, and Dr. Park. With their advice, my PhD project was enhanced to have a higher impact.

I would also like to thank the staff, professors, and Director of Graduate Studies in the Department of Bioengineering for their support during my time as a student and to pursue my degree program with all convenience. Additionally, I appreciate support and encouragement for my research from the Levitan lab members. Love you guys.

I also want to thank my parents and sister. Their strong support mentally and financially helped me to pursue the doctorate program at the University of Illinois at Chicago. In addition, I would like to thank my friends, cousins and relatives who encouraged me to survive during the PhD program in the United States.

Finally, my beloved fiancé, Gyuri Kim, her great support and love helped me to achieve this accomplishment. I love you and thank you for your support and marrying me.

SJA

## TABLE OF CONTENTS

List of Figures.....	v
List of Abbreviation.....	iiiv
SUMMARY.....	ix
Chapter 1. Introduction.....	1
1.1 Inwardly rectifying potassium channels.....	1
1.2 Expression and Pharmacology of Kir2 channels.....	7
1.3 Endothelial Kir channels.....	8
1.4 Inwardly rectifying potassium channels.....	11
Reference.....	17
Chapter 2. General materials and methods.....	31
2.1 Ethical Approval.....	31
2.2 Reagents and antibodies.....	31
2.3 Isolation of mouse mesenteric arteries.....	32
2.4 Primary mouse mesenteric arterial endothelial cell isolation and culture.....	32
2.5 PCR and Western Blot analysis.....	33
2.6 Vasodilation measurement in mouse mesenteric arteries.....	34
Chapter 3. Inwardly rectifying K <sup>+</sup> channels plays a key role to flow-induced vasodilation in resistance arteries.....	36
3.1 Introduction.....	36
3.2 Methods.....	38
3.3 Results.....	43
3.4 Discussion.....	82
Reference.....	90
Chapter 4. Inwardly rectifying K <sup>+</sup> channels plays a key role to agonist-induced vasodilation in resistance arteries.....	97
4.1 Introduction.....	97
4.2 Methods.....	99
4.3 Results.....	102
4.4 Discussion.....	113

**TABLE OF CONTENTS (continued)**

Reference.....116

Chapter 5. Role of Kir2.1 channels in hyperlipidemia.....117

    5.1 Introduction.....117

    5.2 Methods.....118

    5.3 Results.....119

    5.4 Discussion.....125

    Reference.....127

Chapter 6. Conclusion.....129

    Reference.....134

Appendix.....135

Vitae.....141

## LIST OF FIGURES

Figure 1-1 Schematic structure of inwardly rectifying potassium channels.....	2
Figure 1-2 I-V relation of K <sup>+</sup> channels.....	4
Figure 1-3 Phylogenetic tree of 7 subfamilies of Kir.....	6
Figure 3-1 Mouse mesentery and arterial bed.....	44
Figure 3-2 WT Mouse mesenteric arterial endothelial cell isolation.....	45
Figure 3-3 Kir2 channel expression levels in isolated WT endothelial cells.....	47
Figure 3-4 Kir2.1 channel expression levels in isolated WT and Kir2.1 <sup>+/-</sup> endothelial cell.....	49
Figure 3-5 Schematic feature of pressure gradient induced flow generation.....	51
Figure 3-6 Role of Kir2.1 in flow-induced vasodilation in mouse mesenteric arteries.....	53
Figure 3-7 Loss of Kir2.1 function with dominant-negative Kir2.1 results in the inhibition of FIV in mesenteric arteries.....	55
Figure 3-8 Reversible effect of Ba <sup>2+</sup> in flow-induced vasodilation.....	57
Figure 3-9 Kir2.1 does not affect sodium nitroprusside dependent dilation in endothelium denuded mesenteric arteries.....	58
Figure 3-10 Kir2.1 does not affect K <sup>+</sup> -dependent dilation in endothelium denuded mesenteric arteries.....	60

## LIST OF FIGURES (continued)

Figure 3-11 Loss of Kir2.1 activity reduces K <sup>+</sup> -dependent dilation in endothelium denuded cerebral arteries.....	61
Figure 3-12 Recovery of Kir2.1 function with EC-specific WT Kir2.1-HA adenoviral vector in mesenteric arteries from Kir2.1 <sup>+/-</sup> mice.....	63
Figure 3-13 SK channels regulate flow-induced vasodilation in parallel pathway to Kir channels.....	65
Figure 3-14 Dose-response to apamin of flow-induced vasodilation in WT mesenteric arteries.....	67
Figure 3-15 Kir2.1 regulate flow-induced vasodilation by a NO-dependent and a SK-independent pathway.....	68
Figure 3-16 Kir channels regulate flow-induced eNOS activation by Akt phosphorylation.....	71
Figure 3-17 Recovery of flow-induced eNOS activation by Akt phosphorylation in Kir2.1 <sup>+/-</sup> endothelial cells by the transfection of EC-specific WT-Kir2.1.....	73
Figure 3-18 Kir2.1 controls flow-induced nitric oxide production.....	75
Figure 3-19 Flow-induced nitric oxide production is regulated by SK-independent pathway.....	77
Figure 3-20 Kir2.1 impairment increases blood pressure and peripheral vascular resistance.....	79

## LIST OF FIGURES (continued)

Figure 3-21 Cardiac function does not contribute to increased blood pressure in Kir2.1 deficient mice.....	81
Figure 4-1 Role of Kir2.1 in bradykinin-induced vasodilation in mouse mesenteric arteries.....	103
Figure 4-2 Role of Kir2.1 in acetylcholine-induced vasodilation in mouse mesenteric arteries.....	105
Figure 4-3 Role of Kir2.1 in bradykinin-induced NO production from mesenteric arterial endothelial cells.....	107
Figure 4-4 WT-Kir2.1 transfection recovers bradykinin-induced NO production in endothelial cells from Kir2.1 <sup>+/-</sup> mice.....	110
Figure 4-5 Kir2.1 regulation in Bradykinin-induced NO production from endothelial cells via Akt-dependent pathway.....	112
Figure 5-1 Impaired flow-induced vasodilation in dyslipidemia is due to the loss of Kir2.1 activity.....	120
Figure 5-2 Kir2.1 is essential to prevent lesion formation.....	122
Figure 6-1 Role of endothelial Kir channels in vasodilation under normal and dyslipidemic condition.....	133

## **LIST OF ABBREVIATIONS**

Kir – Inwardly rectifying potassium channels

K<sub>Ca</sub> – Calcium activated potassium channels

Kv – Voltage gated potassium channels

ECs – Endothelial cells

FIV – Flow-induced vasodilation

NO – Nitric oxide

eNOS – Endothelial nitric oxide synthase

ATP/ADP – Adenosine tri/di phosphate

## SUMMARY

Inwardly rectifying potassium (Kir) channels are known to maintain cellular membrane potential and are putatively sensitive to mechanical stimuli. Kir channels are expressed in various cell types including endothelial cells; however, their role in vascular physiology is not well understood. In this thesis, I provide several lines of evidence that Kir channels in endothelial cells are essential for flow-induced vasodilation through NO production: i) flow-induced vasodilation was impaired in genetically deficient Kir2.1 mice, ii) endothelial cells isolated from Kir2.1 deficient mice showed the loss of flow-induced eNOS activation, iii) transfection of endothelial-specific WT Kir2.1 in Kir2.1 deficient endothelial cells recovered flow-induced vasodilation and eNOS activation, and iv) flow-induced NO production was reduced in Kir2.1 impaired mice. Additionally, my data suggest that Kir channels play a key role in receptor-mediated vasodilation through NO production: i) receptor-mediated vasodilation was impaired in genetically deficient Kir2.1 mice, ii) receptor-mediated NO production was impaired in Kir2.1 deficient endothelial cells, and iii) transfection of WT-Kir2.1 channels in endothelial cells from Kir2.1 deficient mice showed the recovery of receptor-mediated NO production.

Our laboratory showed that Kir activity was reduced by cholesterol binding; therefore, I tested the role of Kir channels in impaired flow-induced vasodilation in dyslipidemia. My data suggest that the reduction of flow-induced vasodilation in dyslipidemia was due to the loss of Kir activity. Additionally, I found that Kir deficiency exacerbated lesion formation in aortas of hypercholesterolemic mice. The role of Kir in atherosclerosis is still unclear; however, when we understand the role of Kir in vascular patho-physiology, Kir channels may represent be a new drug target for combating cardiovascular disease.

## Chapter 1. Introduction

### 1.1 Inwardly rectifying potassium channels

Inwardly rectifying potassium (Kir) channels are tetrameric membrane proteins, which selectively transfer K<sup>+</sup> ions across the cellular membrane. Each subunit of Kir channels have a simple structure with two transmembrane-spanning alpha helices (M1 and M2), a pore loop (P), and amino- and carboxy-terminal cytoplasmic domains (Fig. 1-1). The K<sup>+</sup> ion selectivity is conferred by the selectivity filter, which locates in the loop structure with signature sequences (TXGYG or TXGFG) (Bichet *et al.*, 2003). If any of subunits among the tetrameric structure have mutations in the pore loop, the channel loses the ability to transfer K<sup>+</sup> ions (Heginbotham *et al.*, 1994). The first crystal structure of Kir was resolved for KirBac1.1, a bacterial ion channel that is closely related to eukaryotic Kir channels (Kuo *et al.*, 2003). More recent studies also resolved the cytosolic domain of eukaryotic mammalian Kir3.1 and the crystal structure of entire Kir2.2 channels (Nishida & MacKinnon, 2002; Tao *et al.*, 2009). The 3-D structure of the purified Kir6.2-SUR1 complex was also characterized by electron microscopic analysis (Mikhailov *et al.*, 2005). Both homomeric and heteromeric combinations of Kir channel subunits were found to form functional Kir channels. Heteromerization usually appears in the same subfamily members; Kir3.1 can form heteromeric Kir3 channels with any subunit in Kir3 subfamily members, such as Kir3.2, Kir3.3, or Kir3.4 (Liao *et al.*, 1996).

Major roles of Kir channels are known to maintain resting membrane potential and K<sup>+</sup> homeostasis in diverse cell types, including heart, brain, vascular cells and pancreas

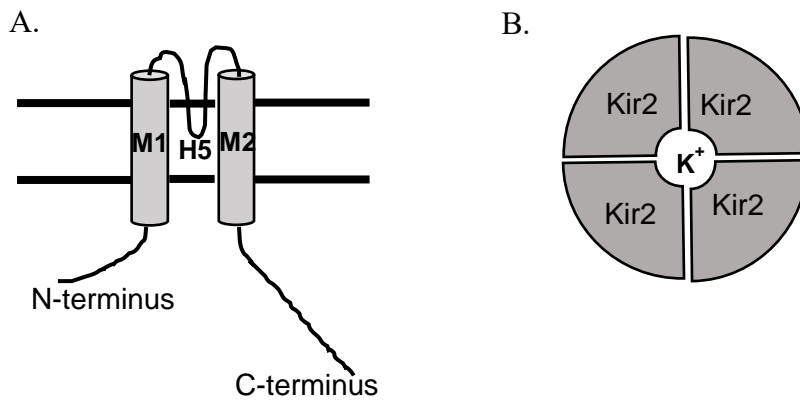


Figure 1-1 Schematic structure of inwardly rectifying potassium channels. (A) Structure of single subunit of Kir channels. Each subunit has two membrane domains (M1 and M2), a pore-forming loop (H5) and cytosolic termini of NH<sub>2</sub> and COOH. (B) 4 subunits consist 1 channel.

(Nichols & Lopatin, 1997; Bichet *et al.*, 2003; Kubo *et al.*, 2005). Kir channels are known to open at resting membrane potential and their major physiological roles are regulating membrane excitability, heart rate and vascular tone (Nichols & Lopatin, 1997; Bichet *et al.*, 2003; Kubo *et al.*, 2005). Downregulation of the Kir current was shown to be associated with heart failure (Beuckelmann *et al.*, 1993). Mutation of Kir channels causes severe genetic syndromes including Bartter's syndrome (loss of function in Kir1.1) (Vollmer *et al.*, 1998), Andersen syndrome (LQT syndrome) (loss of function in Kir2.1) (Tristani-Firouzi *et al.*, 2002), short Q-T syndrome (gain of function in Kir2.1) (Deo *et al.*, 2013), permanent neonatal diabetes (gain of function in Kir6.2) (Remedi *et al.*, 2017).

A characteristic feature of Kir is inward rectification, which plays a key role in its function. The definition of rectification of membrane ionic currents is non-linear relationship between the currents flowing through the channels and membrane potential (*I-V* relationship) (Nichols & Lopatin, 1997). Inward rectification is defined as non-linear *I-V* relationship, in which the influx of ions is higher than the efflux for the same driving force. My work is focused on the subfamily of Kir2 channels considered to be “strong rectifiers,” characterized by significant inward currents and small outward currents (Fig. 1-2). In contrast to Kir channels, most of other potassium channels, such as the family of voltage gated potassium channels (Kv), have outward rectification with outward currents higher than inward currents. Physiologically, however, for both inwardly-rectifying and outwardly-rectifying potassium channels, when the channels open, potassium ions efflux from the cells because intracellular potassium concentration (~145 mM) is higher than extracellular potassium concentration (~4 mM). The efflux of potassium ions causes the hyperpolarization of the membrane potential.

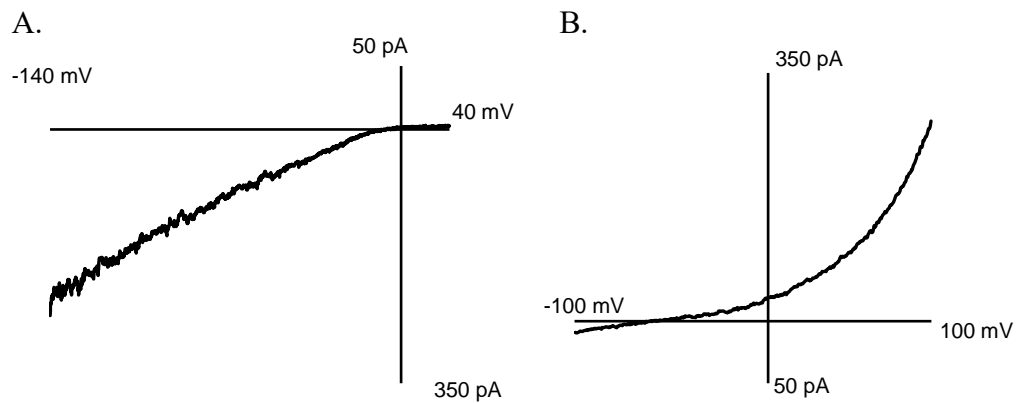


Figure 1-2 I-V relation of  $K^+$  channels. (A) Typical Kir current density curve. Inward rectification is observed under the lower than equilibrium potential of  $K^+$  ( $E_K$ ). Under the membrane potential higher than  $E_K$  causes blocking of channels by divalent cations and/or polyamines. (B) Typical Kv current density curve. Voltage-sensitive M4 subunit transits the location by membrane potential to change the activity of channels. Kv channels are usually blocked under the  $E_K$ , and open when the cells are depolarized.

The mechanism of Kir inward rectification is well studied. At depolarized membrane potential, Kir channels are blocked by the divalent cations, such as magnesium ions, and/or positively charged polyamine molecules, entering the channel pore from the cytosol (Hibino *et al.*, 2010). Applying hyperpolarized potential results in driving the cations out of the channel pore allowing strong currents. In contrast, the outward rectification of Kv channels is based on voltage-sensitive transmembrane domain, which changes conformation in response to membrane depolarization resulting in opening the channels. Physiological role of inward rectification of Kir is preventing the shunt of fast depolarization during the Na<sup>+</sup> or Ca<sup>2+</sup> driven upstroke action potential. Without the mechanism of inward rectification, Kir currents would remain open and shunt the Na<sup>+</sup>/Ca<sup>2+</sup> involved depolarization. Opening of Kv channels during the action potential, however, does not cause the shunt during the upstroke because of the delayed activation. The function of Kv channels is to open at depolarized membrane potential in order to repolarize the membrane potential. Cells that have a large Kir conductance would maintain their resting membrane potential near to E<sub>K</sub>, and would not have impulsive electrical activity (Hibino *et al.*, 2010).

Seven subfamilies with 15 genes of Kir are identified today (Kir1.x to Kir7.x) (Fig. 1-3). These subfamilies can be categorized into four functional groups: 1) strong inwardly rectifying Kir channels (Kir2.x), 2) G protein-gated Kir channels (Kir3.x), 3) ATP-sensitive K<sup>+</sup> channels (Kir6.x), and 4) K<sup>+</sup>-transport channels (Kir1.x, Kir4.x, Kir5.x, and Kir7.x) (Hibino *et al.*, 2010). Kir2 channels are known to maintain the resting membrane potential. Both loss and gain of function mutation of these channels results in severe heart disease. Loss of function in Kir2 channels results in LQT syndrome, and gain of function results in

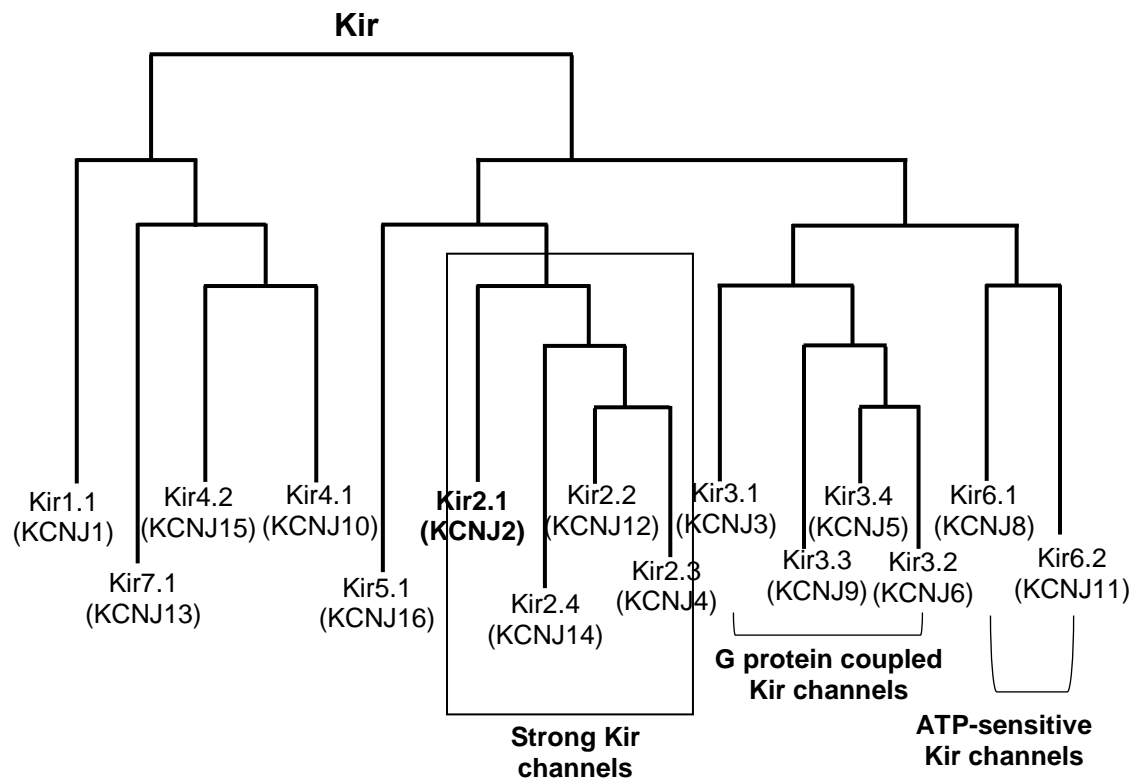


Figure 1-3 Phylogenetic tree of 7 subfamilies of Kir. 15 subtypes of Kir channels are arranged based on similarity of amino acid sequence.

SQT syndrome (Chamberlain *et al.*, 1976; Deo *et al.*, 2013). Kir2.1 is also known as a flow-sensitive channel, which was proposed to play a major role in endothelial function (Olesen *et al.*, 1988). The activity of Kir3 channels is regulated by G protein-coupled receptor, which is activated by muscarinic receptor (Doupnik, 2008). Kir6 channels have regulatory subunits, which are sensitive to ATP/ADP, and are known to regulate metabolic function (Bennett *et al.*, 2010). Kir1, Kir4, Kir5, and Kir7 channels are characterized as transporting K<sup>+</sup> ions in renal, retinal, and neuronal cells (Nagelhus *et al.*, 1999; Kofuji *et al.*, 2002; Yang *et al.*, 2003b; Wang & Giebisch, 2009). My project is focused on the role of Kir2 channels in endothelial function.

## **1.2 Expression and Pharmacology of Kir2 channels**

Numerous cell types express Kir2 channels, such as cardiac myocytes (Rougier *et al.*, 1968; Beeler & Reuter, 1970; Kurachi, 1985), epithelial cells (Greger *et al.*, 1990; Lorenz *et al.*, 2002; Lu *et al.*, 2002; Hebert *et al.*, 2005), neurons (Gahwiler & Brown, 1985; Lacey *et al.*, 1988; Williams *et al.*, 1988; Brown *et al.*, 1990), blood cells (McKinney & Gallin, 1988; Lewis *et al.*, 1991), osteoclasts (Sims & Dixon, 1989), glial cells (Kuffler & Nicholls, 1966; Newman, 1984), and endothelial cells (Forsyth *et al.*, 1997; Leung *et al.*, 2000; Hogg *et al.*, 2002; Yang *et al.*, 2003a).

Ba<sup>2+</sup> and Cs<sup>+</sup> are most commonly used to block Kir2 channels (Hille & Schwarz, 1978; French & Shoukimas, 1985; Isomoto *et al.*, 1997). Kv channel inhibitors, such as Tetraethylammonium and 4-aminopyridine, have little effects on Kir channels (Oonuma *et al.*, 2002). High concentration of Ba<sup>2+</sup> can block Kv channels, but the range of micromolar

concentrations of  $Ba^{2+}$  blocks specifically Kir channels (Quayle *et al.*, 1993; Franchini *et al.*, 2004). Therefore,  $Ba^{2+}$  and  $Cs^{+}$  are generally used as Kir channel blocker to study the Kir channel functions in cells and tissues. Recently, Kir2.1 specific blocker, ML-133, is developed and in use to study physiological functions of Kir2.1 (Wu *et al.*, 2010). Overall, there are only limited pharmacological approaches to determine the roles of Kir2 channels in cellular functions and therefore, most of my work relies on molecular biology approaches: primary endothelial cells from the genetically knocked down mouse models or the cells transfected with viral vectors of WT and dominant negative mutation on Kir2.1.

### **1.3 Endothelial Kir channels**

The endothelium is a single layer of cells, which is the inner layer of blood vessels. Generally, there are two major potassium channels expressed in endothelial cells (ECs): Kir channels, which were known to maintain stable membrane potential and response to flow (Olesen *et al.*, 1988; Hoyer *et al.*, 2002; Fang *et al.*, 2006) and  $Ca^{2+}$ -activated  $K^{+}$  ( $K_{Ca}$ ) channels that are activated by increased intracellular  $Ca^{2+}$  (Ungvari *et al.*, 2002; Wulff & Köhler, 2013). Among Kir channels, Kir2 channels, which are known as strong inward rectifiers with high basal open probability, are mainly expressed in vascular endothelial cells (Forsyth *et al.*, 1997; Yang *et al.*, 2003a; Fang *et al.*, 2005; Millar *et al.*, 2008), and ATP-dependent Kir6 channels (Mederos *et al.*, 2000; Chatterjee *et al.*, 2003; Yoshida *et al.*, 2004; Morrissey *et al.*, 2005; Chatterjee *et al.*, 2006). Endothelial cells are also shown to express mainly two types of  $K_{Ca}$  channels, which are small (SK) and intermediate (IK) conductance  $K_{Ca}$  channels, (Köhler *et al.*, 2000; Bychkov *et al.*, 2002; Köhler & Hoyer, 2007). Additionally, large-conductance (BK) channels are also reported

to be expressed in endothelial cells with some evidence as well (Papassotiriou *et al.*, 2000; Wang *et al.*, 2005).

Kir2 channels are found in aortic, arterial, and microvascular endothelial cells in widely varied species. Particularly, there are functional expression of Kir2 channels in human (Fang *et al.*, 2005), bovine (Romanenko *et al.*, 2002), and porcine (Fang *et al.*, 2005) aortic endothelial cells, and also in bovine pulmonary endothelial cells (Kamouchi *et al.*, 1997; Leung *et al.*, 2000), but are not found in rabbit (Rusko *et al.*, 1992) and mouse (Ledoux *et al.*, 2008a) aortic endothelium. Kir2 channels are also found in microvascular endothelial cells of brain from rat (Yamazaki *et al.*, 2006; Millar *et al.*, 2008) and from bovine cornea (Yang *et al.*, 2003a).

Using a “stamp method,” which can expose the bottom side of endothelial cells to up, the differential distribution of Kir channels between the luminal side and the abluminal of the endothelial cell surfaces were explored. Privileged expression of functional Kir channels were observed on the luminal surface of freshly-isolated cardiac endothelial cells, and there was no visible Kir channel expression on the abluminal surface (Manabe *et al.*, 1995). Meanwhile, bovine aortic endothelial cells express Kir equally on the top and bottom sides of endothelial cells (Colden-Stanfield *et al.*, 1992). These differences may be related to the functional roles of endothelial Kir channels in different tissues.

There are 4 subfamilies in Kir2 channels (Kir2.1 to 4) (Kubo *et al.*, 2005). With Kir2.1 and Kir2.2 are identified as functionally expressed in endothelial cells. Although human aortic endothelial cells express mRNA of all four Kir2 channels, Fang *et al.* showed that Kir2.1 and Kir2.2 are mainly and functionally expressed, and they also observed that Kir2.2 channels strongly contribute to Kir currents in these endothelial cells as assessed using

single-channel analysis and application of dominant negative Kir2 subfamilies (dnKir2.1-4) (Fang *et al.*, 2005). Additionally, this study suggested that Kir2.1 and Kir2.2 subunits may form heteromeric structures in human aortic endothelial cells. It was also observed that Kir2.1 and Kir2.2 mRNA were expressed equivalently in brain capillary endothelial cells from bovine and rat, but there was no further study to distinguish the relative functional distributions between these two channels in these endothelial cells (Yamazaki *et al.*, 2006; Millar *et al.*, 2008).

ATP-dependent Kir channels (Kir6) have similar structure to Kir2 channels except that they have an additional regulatory subunit, which is sulfonylurea receptors (SUR) with ATP-binding affinity; hence, Kir6 channels can be activated/inhibited by the metabolic status of the cells. Kir6 channels are activated by intracellular ADP, and inhibited by intracellular ATP (Ribalet *et al.*, 2005). Kir6 channels are also expressed in multiple types of endothelial cells derived from various tissues (Chatterjee & Fisher, 2014). Among Kir6 family, Kir6.1 and Kir6.2 are known to be expressed in aortic and arterial endothelial cells. In heart capillaries, Kir6.1 and 6.2 are expressed in endothelial cells with higher Kir6.2 expression (Mederos *et al.*, 2000) and also in coronary conduit arteries (Malester *et al.*, 2007). In pulmonary microvascular endothelial cells, the expression of Kir6.2 is also observed, and these channels are shown to be activated by shear stress (Chatterjee *et al.*, 2003; Chatterjee *et al.*, 2006). There was a study that Kir6.2 channels are required in endothelial response to the termination of flow during lung ischemia (Chatterjee *et al.*, 2006).

Michelakis *et al.* demonstrated several lines of evidence for the presence of Kir1 channels and Kir3 channels in endothelial cells from pulmonary vein, but there was no functional

studies performed with these channels in these ECs (Michelakis *et al.*, 2001).

Furthermore, multiple studies demonstrate the expression and functional roles of  $K_{Ca}$  channels in endothelial cells. SK channels are localized mainly in caveolin-rich domains (Absi *et al.*, 2007) and endothelial cell gap junctions (Sandow *et al.*, 2006), and IK channels are located on endothelial protrusions next to myoendothelial junctions (Sandow *et al.*, 2006; Ledoux *et al.*, 2008b). They are activated by  $Ca^{2+}$  influx, and causing endothelial cell hyperpolarization. Endothelial cell hyperpolarization induce the arterial vasodilation by endothelium-derived hyperpolarization of smooth muscle (Kohler & Hoyer, 2007). My study demonstrates the differential role of Kir2 and SK channels in endothelial regulation of vascular function.

#### **1.4 Endothelial regulation of vascular relaxation**

Endothelium plays a critical role in the regulation of blood flow and pressure by controlling vascular tone. Control of vascular tone is critical for maintenance of homeostasis in cardiovascular function. Two major stimuli responsible for the endothelium-dependent vasodilation, relaxation of the blood vessels, are fluid shear stress, a mechanical force generated by blood flow, and vasoactive compounds, such as acetylcholine and bradykinin, that stimulate G-protein coupled receptors in endothelial cells. The first recognition of the importance of the endothelial role in vascular function came from the observation that acetylcholine-mediated relaxation of rabbit aorta was endothelium-dependent (Singer & Peach, 1982). This study also suggested that there was a diffusible factor from endothelial cells which induced vascular relaxation, and defined this factor as

endothelium-derived relaxing factor (EDRF) (Singer & Peach, 1982). In the further study by Ignarro *et al.*, nitric oxide (NO) was identified as the acetylcholine-induced EDRF (Ignarro *et al.*, 1987).

Since NO is a small molecule with no electrical charge, it can diffuse across the cell membrane from endothelial cells to adjacent smooth muscle cells. NO is known to activate GMP cyclase in vascular smooth muscle cells, which is producing cGMP (Kukovetz *et al.*, 1987). Cyclic GMP activates cGMP-dependent myosin light chain phosphatase (MLCP), which removes phosphate from myosin light chains, known to be responsible for vasoconstriction, thus relaxing the smooth muscles (Surks, 2007).

NO is produced by three different types of NOS isoforms: neuronal NO synthase (nNOS), endothelial NO synthase (eNOS), and inducible NO synthase (iNOS). These enzymes share over 50% primary amino acid sequence and have several functional domains, such as N-terminal oxygenase domain, substrate and cofactor binding domains, and calmodulin binding site (Stuehr, 1997). eNOS is the dominant NOS isoform in vascular endothelial cells producing NO to regulate vascular function. N-terminal oxygenase domain with heme, L-arginine, and BH<sub>4</sub> binding domains regulates eNOS coupling and dimerization, which results in NO production.

It is well-known that eNOS is activated by both shear-stress and vasoactive components, such as acetylcholine and bradykinin. There are several mechanisms that are involved in eNOS activation.

1) Both shear-stress and vasoactive compounds described above were shown to increase intracellular Ca<sup>2+</sup> both by inducing release from intracellular stores, and

increasing influx through plasma membrane  $\text{Ca}^{2+}$  channels. Fleming *et al.* showed calcium influx activates calmodulin and calmodulin kinase II, and activated calmodulin kinase II results in S1177 phosphorylation of eNOS, which results in eNOS activation and NO production (Fleming *et al.*, 2001). In addition,  $\text{Ca}^{2+}$  and calmodulins regulate the interaction between eNOS and caveolin-1 (Shaul *et al.*, 1996), which is known to be a negative regulator for eNOS (Michel *et al.*, 1997). Caveolae are invaginated plasma membrane sites that are present in many different cell types, and are more abundantly found in endothelial cells, adipocytes, fibroblasts, and smooth muscle cells (Rafikov *et al.*, 2011). Caveolae are known to be essential sites, which mediate multiple signal transduction pathways (Anderson, 1993). Low calcium level promotes stable interaction of eNOS and caveolin-1, whereas high calcium level dissociates the eNOS from caveolin-1 resulting in eNOS activation (Michel *et al.*, 1997). Garcia-Cardena *et al.* identified the essential caveolin-1 binding site in human eNOS, which is amino acids 350–358 (Garcia-Cardena *et al.*, 1997). Ghosh *et al.* also suggested additional caveolin-1 binding sites in eNOS, which was known to be the electron transport domain, but it is still unclear where the exact residues are (Ghosh *et al.*, 1998). In endothelial cells, calcium influx or shear stress triggers eNOS to be detached from caveolin-1 by the activated calmodulin complex with calcium (Sriram *et al.*, 2016). Caveolin-1 knock-out mouse derived aortic endothelial cells produced increased NO in ex vivo study (Balligand *et al.*, 2009).

2) Another pathway that was shown to activate eNOS is Akt-dependent pathway. Dimmeler *et al.* suggested that shear stress induced eNOS activation is Akt1 dependent and calcium independent, and Akt1 signaling is essential for both receptor-mediated and flow-induced endothelial nitric oxide synthase activation (Dimmeler *et al.*, 1999). Similar

to calmodulin activated kinase II, Akt1 phosphorylates eNOS at the residue, S1177 (Dimmeler *et al.*, 1999). McCabe *et al.* presented evidence for Ca<sup>2+</sup>-independent pathway by showing that substituting S1177 of eNOS to negatively charged residue results in active eNOS even in the low calcium condition (McCabe *et al.*, 2000). Additionally, Hsp90 binds to the eNOS-calmodulin complex resulting in recruitment of Akt1, which phosphorylates S1177 to activate eNOS and produce NO (Brouet *et al.*, 2001).

Although phosphorylation of S1177 residue in eNOS is well-established to be responsible for eNOS activation, several other activation and inactivation sites. The identified sites are S114, S615, S633, and S1177 for serine residues, and the T495 for threonine residue (Rafikov *et al.*, 2011). Phosphorylations of S615, S633, and S1177, which are Akt-dependent, activate eNOS, whereas phosphorylations of S114 and T495 by protein kinase C result in eNOS inactivation and decreased NO production (Chen *et al.*, 1999; Mitchell *et al.*, 2001).

Although NO was identified as EDRF in 1980s, multiple observation suggested the existence of other EDRFs, which contribute to endothelium dependent vasodilation (Kang, 2014). Contribution of different EDRFs varies in different vessel types and species. Studies of flow-mediated vascular relaxation in human forearm brachial arteries and rat cremaster arterioles demonstrated that the prostanoid prostacyclin (PGI<sub>2</sub>) is identified as a major contributor to endothelium-derived vasorelaxation in these vessels (Koller *et al.*, 1993; Duffy *et al.*, 1998). PGI<sub>2</sub> are also known to activate MLCP (Malomvolgyi *et al.*, 1982; Vanhoutte, 1982). In addition to NO and PGI<sub>2</sub>, many other EDRFs are identified, such as hydrogen peroxide (Cherry *et al.*, 1990; Wei & Kontos, 1990; Nishijima *et al.*, 2017), carbon monoxide (Redfors *et al.*, 1983; Kubes *et al.*, 1991), hydrogen sulphide (Leffler *et*

*al.*, 2011; Juman *et al.*, 2016), cytochrome P450 products (White & Marletta, 1992; Liu *et al.*, 1993), sulphur dioxide (Zhang *et al.*, 2014; Bender *et al.*, 2016), and C-type natriuretic peptide (CNP) (Edvinsson *et al.*, 2016).

Another major mechanism of smooth muscle relaxation and vasodilation is hyperpolarization of the membrane potential of smooth muscle cells. Similar to other muscle cells, VSMCs are excitable cells that contract in response to depolarization of membrane potential, which leads to activation of voltage-gated  $\text{Ca}^{2+}$  channels to increase intracellular  $\text{Ca}^{2+}$ , which in turn activates myosin light chain kinase (MLCK), phosphorylating myosin light chains resulting in constriction of vessels (Somlyo & Somlyo, 1968). Conversely, the hyperpolarization of VSMCs causes decrease of intracellular free  $\text{Ca}^{2+}$  by the inactivation of voltage-gated  $\text{Ca}^{2+}$  channels and results in vasodilation (Cohen & Vanhoutte, 1995). Endothelium or endothelial-derived hyperpolarizing factor (EDHF) is also a major regulator for the hyperpolarization of smooth muscle cells. EDHF is defined by two criteria; vasodilation that is independent of NO and  $\text{PGI}_2$ , and endothelial-induced membrane hyperpolarization of smooth muscle cells (Kohler & Hoyer, 2007). Several mechanisms have been proposed to underlie EDHF. In general, Endothelial stimulation, by both fluid shear stress and vasoactive agents, increase  $\text{Ca}^{2+}$  influx, and  $\text{Ca}^{2+}$  activates SK and IK channels to cause hyperpolarization of ECs (Ledoux *et al.*, 2006). Activation of endothelial  $\text{K}_{\text{Ca}}$  channels results in hyperpolarization of smooth muscle cells in 3 different ways; a) The direct propagation of hyperpolarization of endothelial cells to smooth muscle via gap junctions. More specifically, endothelial cells and adjacent smooth cells are connected through myoendothelial gap junctions (MEGJs), which are consisted of connexins, mostly Cx37 and Cx40 with smaller amounts of Cx43 and Cx45 (Ming *et*

*al.*, 2009). MEGJs are known to have very low electrical resistance, so they can facilitate electrical continuity and spread hyperpolarization across the connected cells (de Wit *et al.*, 2008; Nagaraja *et al.*, 2013). Gap junctions also can facilitate the propagation of hyperpolarization between smooth muscle cells (Garland & Dora, 2017). b) The efflux of K<sup>+</sup> through K<sub>Ca</sub> channels of endothelial cells, which in turn activates Kir channels in smooth muscle cells resulting in hyperpolarization of VSMCs. c) The efflux of K<sup>+</sup> can also activate Na<sup>+</sup>-K<sup>+</sup> ATPase in smooth muscle cells which also causes hyperpolarization of VSMCs. The roles of SK and IK channels in vasorelaxation was demonstrated using SK and IK KO mouse model that showed increase of blood pressure and the partial loss of vasodilation in microcirculation (Taylor *et al.*, 2003; Si *et al.*, 2006).

However, in spite of fact that Kir channels are also known to be expressed in ECs and sensitive to flow, their role in endothelial function is not established in vasodilation. So, I focused to figure out the role of endothelial Kir in vasodilation.

## Reference

- Absi M, Burnham MP, Weston AH, Harno E, Rogers M & Edwards G. (2007). Effects of methyl beta-cyclodextrin on EDHF responses in pig and rat arteries; association between SK(Ca) channels and caveolin-rich domains. *Br J Pharmacol*.
- Anderson RG. (1993). Caveolae: where incoming and outgoing messengers meet. *Proc Natl Acad Sci U S A* **90**, 10909-10913.
- Balligand JL, Feron O & Dessy C. (2009). eNOS activation by physical forces: from short-term regulation of contraction to chronic remodeling of cardiovascular tissues. *Physiol Rev* **89**, 481-534.
- Beeler GW, Jr. & Reuter H. (1970). Voltage clamp experiments on ventricular myocardial fibres. *J Physiol* **207**, 165-190.
- Bender SB, de Beer VJ, Tharp DL, Bowles DK, Laughlin MH, Merkus D & Duncker DJ. (2016). Severe familial hypercholesterolemia impairs the regulation of coronary blood flow and oxygen supply during exercise. *Basic Res Cardiol* **111**, 61.
- Bennett K, James C & Hussain K. (2010). Pancreatic beta-cell KATP channels: Hypoglycaemia and hyperglycaemia. *Rev Endocr Metab Disord* **11**, 157-163.
- Beuckelmann DJ, Nabauer M & Erdmann E. (1993). Alterations of K<sup>+</sup> currents in isolated human ventricular myocytes from patients with terminal heart failure. *Circ Res* **73**, 379-385.
- Bichet D, Haass FA & Jan LY. (2003). Merging functional studies with structures of inward-rectifier K(+) channels. *Nat Rev Neurosci* **4**, 957-967.
- Brouet A, Sonveaux P, Dessy C, Balligand JL & Feron O. (2001). Hsp90 ensures the transition from the early Ca<sup>2+</sup>-dependent to the late phosphorylation-dependent activation of the endothelial nitric-oxide synthase in vascular endothelial growth factor-exposed endothelial cells. *J Biol Chem* **276**, 32663-32669.

- Brown DA, Gahwiler BH, Griffith WH & Halliwell JV. (1990). Membrane currents in hippocampal neurons. *Prog Brain Res* **83**, 141-160.
- Bychkov R, Burnham MP, Richards GR, Edwards G, Weston AH, Félétou M & Vanhoutte PM. (2002). Characterization of a charybdotoxin-sensitive intermediate conductance Ca<sup>2+</sup>-activated K<sup>+</sup> channel in porcine coronary endothelium: relevance to EDHF. *British Journal of Pharmacology* **137**, 1346.
- Chamberlain DG, Thomas PC & Wilson AG. (1976). Efficiency of bacterial protein synthesis in the rumen of sheep receiving a diet of sugar beet pulp and barley. *J Sci Food Agric* **27**, 231-238.
- Chatterjee S, Al-Mehdi AB, Levitan I, Stevens T & Fisher AB. (2003). Shear stress increases expression of a KATP channel in rat and bovine pulmonary vascular endothelial cells. *Am J Physiol Cell Physiol* **285**, C959-967.
- Chatterjee S & Fisher AB. (2014). Mechanotransduction in the endothelium: role of membrane proteins and reactive oxygen species in sensing, transduction, and transmission of the signal with altered blood flow. *Antioxid Redox Signal* **20**, 899-913.
- Chatterjee S, Levitan I & Fisher AB. (2006). The KATP channel is an important component of flow sensing in the pulmonary microvasculature. *Microcirculation* **13**, 633-644.
- Chen ZP, Mitchelhill KI, Michell BJ, Stapleton D, Rodriguez-Crespo I, Witters LA, Power DA, Ortiz de Montellano PR & Kemp BE. (1999). AMP-activated protein kinase phosphorylation of endothelial NO synthase. *FEBS Lett* **443**, 285-289.
- Cherry PD, Omar HA, Farrell KA, Stuart JS & Wolin MS. (1990). Superoxide anion inhibits cGMP-associated bovine pulmonary arterial relaxation. *Am J Physiol* **259**, H1056-1062.
- Cohen RA & Vanhoutte PM. (1995). Endothelium-dependent hyperpolarization. Beyond nitric oxide and cyclic GMP. *Circulation* **92**, 3337-3349.
- Colden-Stanfield M, Cramer EB & Gallin EK. (1992). *Comparison of apical and basal surfaces of confluent*

*endothelial cells: patch-clamp and viral studies*, vol. 263.

de Wit C, Boettcher M & Schmidt VJ. (2008). Signaling across myoendothelial gap junctions--fact or fiction? *Cell Commun Adhes* **15**, 231-245.

Deo M, Ruan Y, Pandit SV, Shah K, Berenfeld O, Blaufox A, Cerrone M, Noujaim SF, Denegri M, Jalife J & Priori SG. (2013). KCNJ2 mutation in short QT syndrome 3 results in atrial fibrillation and ventricular proarrhythmia. *Proc Natl Acad Sci U S A* **110**, 4291-4296.

Dimmeler S, Fleming I, Fisslthaler B, Hermann C, Busse R & Zeiher AM. (1999). Activation of nitric oxide synthase in endothelial cells by Akt-dependent phosphorylation. *Nature* **399**, 601-605.

Dougnik CA. (2008). GPCR-Kir channel signaling complexes: defining rules of engagement. *J Recept Signal Transduct Res* **28**, 83-91.

Duffy SJ, Tran BT, New G, Tudball RN, Esler MD, Harper RW & Meredith IT. (1998). Continuous release of vasodilator prostanoids contributes to regulation of resting forearm blood flow in humans. *Am J Physiol* **274**, H1174-1183.

Edvinsson ML, Ahnstedt H, Edvinsson L & Andersson SE. (2016). Characterization of Relaxant Responses to Natriuretic Peptides in the Human Microcirculation In Vitro and In Vivo. *Microcirculation* **23**, 438-446.

Fang Y, Mohler ER, III, Hsieh E, Osman H, Hashemi SM, Davies PF, Rothblat GH, Wilensky RL & Levitan I. (2006). Hypercholesterolemia Suppresses Inwardly Rectifying K<sup>+</sup> Channels in Aortic Endothelium In Vitro and In Vivo. *Circ Res* **98**, 1064-1071.

Fang Y, Schram G, Romanenko VG, Shi C, Conti L, Vandenberg CA, Davies PF, Nattel S & Levitan I. (2005). Functional expression of Kir2.x in human aortic endothelial cells: the dominant role of Kir2.2. *Am J Physiol Cell Physiol* **289**, C1134-1144.

Fleming I, Fisslthaler B, Dimmeler S, Kemp BE & Busse R. (2001). Phosphorylation of Thr(495) regulates Ca(2+)/calmodulin-dependent endothelial nitric oxide synthase activity. *Circ Res* **88**, E68-75.

- Forsyth SE, Hoyer A & Hoyer JH. (1997). Molecular cloning and expression of a bovine endothelial inward rectifier potassium channel. *FEBS Lett* **409**, 277-282.
- Franchini L, Levi G & Visentin S. (2004). Inwardly rectifying K<sup>+</sup> channels influence Ca<sup>2+</sup> entry due to nucleotide receptor activation in microglia. *Cell Calcium* **35**, 449-459.
- French RJ & Shoukimas JJ. (1985). An ion's view of the potassium channel. The structure of the permeation pathway as sensed by a variety of blocking ions. *J Gen Physiol* **85**, 669-698.
- Gahwiler BH & Brown DA. (1985). GABAB-receptor-activated K<sup>+</sup> current in voltage-clamped CA3 pyramidal cells in hippocampal cultures. *Proc Natl Acad Sci U S A* **82**, 1558-1562.
- Garcia-Cardena G, Martasek P, Masters BS, Skidd PM, Couet J, Li S, Lisanti MP & Sessa WC. (1997). Dissecting the interaction between nitric oxide synthase (NOS) and caveolin. Functional significance of the nos caveolin binding domain in vivo. *J Biol Chem* **272**, 25437-25440.
- Garland CJ & Dora KA. (2017). EDH: endothelium-dependent hyperpolarization and microvascular signalling. *Acta Physiol (Oxf)* **219**, 152-161.
- Ghosh S, Gachhui R, Crooks C, Wu C, Lisanti MP & Stuehr DJ. (1998). Interaction between caveolin-1 and the reductase domain of endothelial nitric-oxide synthase. Consequences for catalysis. *J Biol Chem* **273**, 22267-22271.
- Greger R, Bleich M & Schlatter E. (1990). Ion channels in the thick ascending limb of Henle's loop. *Ren Physiol Biochem* **13**, 37-50.
- Hebert SC, Desir G, Giebisch G & Wang W. (2005). Molecular diversity and regulation of renal potassium channels. *Physiol Rev* **85**, 319-371.
- Heginbotham L, Lu Z, Abramson T & MacKinnon R. (1994). Mutations in the K<sup>+</sup> channel signature sequence. *Biophys J* **66**, 1061-1067.

- Hibino H, Inanobe A, Furutani K, Murakami S, Findlay I & Kurachi Y. (2010). Inwardly rectifying potassium channels: their structure, function, and physiological roles. *Physiol Rev* **90**, 291-366.
- Hille B & Schwarz W. (1978). Potassium channels as multi-ion single-file pores. *J Gen Physiol* **72**, 409-442.
- Hoger JH, Ilyin VI, Forsyth S & Hoger A. (2002). Shear stress regulates the endothelial Kir2.1 ion channel. *PNAS* **99**, 7780-7785.
- Hogg DS, McMurray G & Kozlowski RZ. (2002). Endothelial cells freshly isolated from small pulmonary arteries of the rat possess multiple distinct k<sup>+</sup> current profiles. *Lung* **180**, 203-214.
- Ignarro LJ, Buga GM, Wood KS, Byrns RE & Chaudhuri G. (1987). Endothelium-derived relaxing factor produced and released from artery and vein is nitric oxide. *Proc Natl Acad Sci U S A* **84**, 9265-9269.
- Isomoto S, Kondo C & Kurachi Y. (1997). Inwardly rectifying potassium channels: their molecular heterogeneity and function. *Jpn J Physiol* **47**, 11-39.
- Juman S, Nara Y, Yasui N, Negishi H, Okuda H, Takado N & Miki T. (2016). Reduced Production of Hydrogen Sulfide and Sulfane Sulfur Due to Low Cystathionine beta-Synthase Levels in Brain Astrocytes of Stroke-Prone Spontaneously Hypertensive Rats. *Biol Pharm Bull* **39**, 1932-1938.
- Kamouchi M, Van Den Brecht K, Eggermont J, Droogmans G & Nilius B. (1997). Modulation of inwardly rectifying potassium channels in cultured bovine pulmonary artery endothelial cells. *Journal of Physiology* **504**, 545-556.
- Kang KT. (2014). Endothelium-derived Relaxing Factors of Small Resistance Arteries in Hypertension. *Toxicol Res* **30**, 141-148.
- Kofuji P, Biedermann B, Siddharthan V, Raap M, Iandiev I, Milenkovic I, Thomzig A, Veh RW, Bringmann A & Reichenbach A. (2002). Kir potassium channel subunit expression in retinal glial cells:

- implications for spatial potassium buffering. *Glia* **39**, 292-303.
- Kohler R, Degenhardt C, Kahn M, Runkel N, Paul M & Hoyer J. (2000). Expression and Function of Endothelial Ca<sup>2+</sup>-Activated K<sup>+</sup> Channels in Human Mesenteric Artery : A Single-Cell Reverse Transcriptase-Polymerase Chain Reaction and Electrophysiological Study In Situ. *Circulation Research* **87**, 496-503.
- Kohler R & Hoyer J. (2007). The endothelium-derived hyperpolarizing factor: insights from genetic animal models. *Kidney Int* **72**, 145-150.
- Koller A, Sun D & Kaley G. (1993). Role of shear stress and endothelial prostaglandins in flow- and viscosity-induced dilation of arterioles in vitro. *Circ Res* **72**, 1276-1284.
- Kubes P, Nesbitt KA, Cain SM & Chapler CK. (1991). Adrenoceptor regulation of canine skeletal muscle blood flow during carbon monoxide hypoxia. *Can J Physiol Pharmacol* **69**, 1399-1404.
- Kubo Y, Adelman JP, Clapham DE, Jan LY, Karschin A, Kurachi Y, Lazdunski M, Nichols CG, Seino S & Vandenberg CA. (2005). International Union of Pharmacology. LIV. Nomenclature and Molecular Relationships of Inwardly Rectifying Potassium Channels. *Pharmacol Rev* **57**, 509-526.
- Kuffler SW & Nicholls JG. (1966). The physiology of neuroglial cells. *Ergeb Physiol* **57**, 1-90.
- Kukovetz WR, Holzmann S & Romanin C. (1987). Mechanism of vasodilation by nitrates: role of cyclic GMP. *Cardiology* **74 Suppl 1**, 12-19.
- Kuo A, Gulbis JM, Antcliff JF, Rahman T, Lowe ED, Zimmer J, Cuthbertson J, Ashcroft FM, Ezaki T & Doyle DA. (2003). Crystal structure of the potassium channel KirBac1.1 in the closed state. *Science* **300**, 1922-1926.
- Kurachi Y. (1985). Voltage-dependent activation of the inward-rectifier potassium channel in the ventricular cell membrane of guinea-pig heart. *J Physiol* **366**, 365-385.

- Lacey MG, Mercuri NB & North RA. (1988). On the potassium conductance increase activated by GABAB and dopamine D2 receptors in rat substantia nigra neurones. *J Physiol* **401**, 437-453.
- Ledoux J, Bonev AD & Nelson MT. (2008a). Ca<sup>2+</sup>-activated K<sup>+</sup> Channels in Murine Endothelial Cells: Block by Intracellular Calcium and Magnesium. *The Journal of General Physiology* **131**, 125-135.
- Ledoux J, Taylor MS, Bonev AD, Hannah RM, Solodushko V, Shui B, Tallini Y, Kotlikoff MI & Nelson MT. (2008b). Functional architecture of inositol 1,4,5-trisphosphate signaling in restricted spaces of myoendothelial projections. *Proc Natl Acad Sci U S A* **105**, 9627-9632.
- Ledoux J, Werner ME, Brayden JE & Nelson MT. (2006). Calcium-activated potassium channels and the regulation of vascular tone. *Physiology (Bethesda)* **21**, 69-78.
- Leffler CW, Parfenova H, Basuroy S, Jaggar JH, Umstot ES & Fedinec AL. (2011). Hydrogen sulfide and cerebral microvascular tone in newborn pigs. *Am J Physiol Heart Circ Physiol* **300**, H440-447.
- Leung YM, Kwan CY & Daniel EE. (2000). Block of inwardly rectifying K<sup>+</sup> currents by extracellular Mg<sup>2+</sup> and Ba<sup>2+</sup> in bovine pulmonary artery endothelial cells. *Can J Physiol Pharmacol* **78**, 751-756.
- Lewis DL, Ikeda SR, Aryee D & Joho RH. (1991). Expression of an inwardly rectifying K<sup>+</sup> channel from rat basophilic leukemia cell mRNA in *Xenopus* oocytes. *FEBS Lett* **290**, 17-21.
- Liao YJ, Jan YN & Jan LY. (1996). Heteromultimerization of G-protein-gated inwardly rectifying K<sup>+</sup> channel proteins GIRK1 and GIRK2 and their altered expression in weaver brain. *J Neurosci* **16**, 7137-7150.
- Liu Z, Brien JF, Marks GS, McLaughlin BE & Nakatsu K. (1993). Lack of evidence for the involvement of cytochrome P-450 or other hemoproteins in metabolic activation of glyceryl trinitrate in rabbit aorta. *J Pharmacol Exp Ther* **264**, 1432-1439.
- Lorenz JN, Baird NR, Judd LM, Noonan WT, Andringa A, Doetschman T, Manning PA, Liu LH, Miller ML & Shull GE. (2002). Impaired renal NaCl absorption in mice lacking the ROMK potassium channel, a model for type II Bartter's syndrome. *J Biol Chem* **277**, 37871-37880.

- Lu M, Wang T, Yan Q, Yang X, Dong K, Knepper MA, Wang W, Giebisch G, Shull GE & Hebert SC. (2002). Absence of small conductance K<sup>+</sup> channel (SK) activity in apical membranes of thick ascending limb and cortical collecting duct in ROMK (Bartter's) knockout mice. *J Biol Chem* **277**, 37881-37887.
- Malester B, Tong X, Ghiu I, Kontogeorgis A, Gutstein DE, Xu J, Hendricks-Munoz KD & Coetzee WA. (2007). Transgenic expression of a dominant negative K(ATP) channel subunit in the mouse endothelium: effects on coronary flow and endothelin-1 secretion. *Faseb J* **21**, 2162-2172.
- Malomvolgyi B, Hadhazy P, Magyar K, Kanai K & Simonidesz V. (1982). Relaxation by prostacyclin (PGI<sub>2</sub>) and 7-oxo-PGI<sub>2</sub> of isolated cerebral, coronary and mesenteric arteries. *Acta Physiol Acad Sci Hung* **60**, 251-256.
- Manabe K, Ito H, Matsuda H, Noma A & Shibata Y. (1995). Classification of ion channels in the luminal and abluminal membranes of guinea-pig endocardial endothelial cells. *The Journal of Physiology* **484**, 41.
- McCabe TJ, Fulton D, Roman LJ & Sessa WC. (2000). Enhanced electron flux and reduced calmodulin dissociation may explain "calcium-independent" eNOS activation by phosphorylation. *J Biol Chem* **275**, 6123-6128.
- McKinney LC & Gallin EK. (1988). Inwardly rectifying whole-cell and single-channel K currents in the murine macrophage cell line J774.1. *J Membr Biol* **103**, 41-53.
- Mederos Y, Schnitzler M, Derst C, Daut J & Preisig-Müller R. (2000). ATP-sensitive potassium channels in capillaries isolated from guinea-pig heart. *J Physiol* **525**, 307-317.
- Michel JB, Feron O, Sacks D & Michel T. (1997). Reciprocal regulation of endothelial nitric-oxide synthase by Ca<sup>2+</sup>-calmodulin and caveolin. *J Biol Chem* **272**, 15583-15586.
- Michelakis ED, Weir EK, Wu X, Nsair A, Waite R, Hashimoto K, Puttagunta L, Knaus HG & Archer SL. (2001). Potassium channels regulate tone in rat pulmonary veins. *Am J Physiol Lung Cell Mol*

*Physiol* **280**, L1138-1147.

Michell BJ, Chen Z, Tiganis T, Stapleton D, Katsis F, Power DA, Sim AT & Kemp BE. (2001). Coordinated control of endothelial nitric-oxide synthase phosphorylation by protein kinase C and the cAMP-dependent protein kinase. *J Biol Chem* **276**, 17625-17628.

Mikhailov MV, Campbell JD, de Wet H, Shimomura K, Zadek B, Collins RF, Sansom MS, Ford RC & Ashcroft FM. (2005). 3-D structural and functional characterization of the purified KATP channel complex Kir6.2-SUR1. *EMBO J* **24**, 4166-4175.

Millar ID, Wang S, Brown PD, Barrand MA & Hladky SB. (2008). Kv1 and Kir2 potassium channels are expressed in rat brain endothelial cells. *Pflugers Arch* **456**, 379-391.

Ming J, Li T, Zhang Y, Xu J, Yang G & Liu L. (2009). Regulatory effects of myoendothelial gap junction on vascular reactivity after hemorrhagic shock in rats. *Shock* **31**, 80-86.

Morrissey A, Rosner E, Lanning J, Parachuru L, Dhar Chowdhury P, Han S, Lopez G, Tong X, Yoshida H, Nakamura TY, Artman M, Giblin JP, Tinker A & Coetzee WA. (2005). Immunolocalization of KATP channel subunits in mouse and rat cardiac myocytes and the coronary vasculature. *BMC Physiol* **5**, 1.

Nagaraja S, Kapela A, Tran CH, Welsh DG & Tsoukias NM. (2013). Role of microprojections in myoendothelial feedback--a theoretical study. *J Physiol* **591**, 2795-2812.

Nagelhus EA, Horio Y, Inanobe A, Fujita A, Haug FM, Nielsen S, Kurachi Y & Ottersen OP. (1999). Immunogold evidence suggests that coupling of K<sup>+</sup> siphoning and water transport in rat retinal Muller cells is mediated by a coenrichment of Kir4.1 and AQP4 in specific membrane domains. *Glia* **26**, 47-54.

Newman EA. (1984). Regional specialization of retinal glial cell membrane. *Nature* **309**, 155-157.

Nichols CG & Lopatin AN. (1997). Inward rectifier potassium channels. *Annu Rev Physiol* **59**, 171-191.

- Nishida M & MacKinnon R. (2002). Structural basis of inward rectification: cytoplasmic pore of the G protein-gated inward rectifier GIRK1 at 1.8 Å resolution. *Cell* **111**, 957-965.
- Nishijima Y, Cao S, Chabowski DS, Korishettar A, Ge A, Zheng X, Sparapani R, Gutterman DD & Zhang DX. (2017). Contribution of KV1.5 Channel to Hydrogen Peroxide-Induced Human Arteriolar Dilation and Its Modulation by Coronary Artery Disease. *Circ Res* **120**, 658-669.
- Olesen SP, Clapham DE & Davies PF. (1988). Haemodynamic shear stress activates a K<sup>+</sup> current in vascular endothelial cells. *Nature* **331**, 168-170.
- Oonuma H, Iwasawa K, Iida H, Nagata T, Imuta H, Morita Y, Yamamoto K, Nagai R, Omata M & Nakajima T. (2002). Inward rectifier K(+) current in human bronchial smooth muscle cells: inhibition with antisense oligonucleotides targeted to Kir2.1 mRNA. *Am J Respir Cell Mol Biol* **26**, 371-379.
- Papassotiriou J, KÃ–hler R, Prenen J, Krause H, Akbar M, Eggermont J, Paul M, Distler A, Nilius B & Hoyer J. (2000). Endothelial K<sup>+</sup> channel lacks the Ca<sup>2+</sup> sensitivity-regulating  $\hat{I}^2$  subunit. *The FASEB Journal* **14**, 885-894.
- Quayle JM, McCarron JG, Brayden JE & Nelson MT. (1993). Inward rectifier K<sup>+</sup> currents in smooth muscle cells from rat resistance-sized cerebral arteries. *Am J Physiol* **265**, C1363-1370.
- Rafikov R, Fonseca FV, Kumar S, Pardo D, Darragh C, Elms S, Fulton D & Black SM. (2011). eNOS activation and NO function: structural motifs responsible for the posttranslational control of endothelial nitric oxide synthase activity. *J Endocrinol* **210**, 271-284.
- Redfors S, Sjoval H, Jodal M & Lundgren O. (1983). Intramural blood flow distribution in the small intestine of the cat studied by carbon monoxide uptake and 85krypton elimination. *Acta Physiol Scand* **118**, 97-107.
- Remedi MS, Friedman JB & Nichols CG. (2017). Diabetes induced by gain-of-function mutations in the Kir6.1 subunit of the KATP channel. *J Gen Physiol* **149**, 75-84.

- Ribalet B, John SA, Xie LH & Weiss JN. (2005). Regulation of the ATP-sensitive K channel Kir6.2 by ATP and PIP(2). *J Mol Cell Cardiol* **39**, 71-77.
- Romanenko V, Davies PF & Levitan I. (2002). Dual effect of fluid shear stress on volume-regulated anion current in bovine aortic endothelial cells. *J of Am Physiol* **282**, C708-718.
- Rougier O, Vassort G & Stampfli R. (1968). Voltage clamp experiments on frog atrial heart muscle fibres with the sucrose gap technique. *Pflugers Arch Gesamte Physiol Menschen Tiere* **301**, 91-108.
- Rusko J, Tanzi F, van Breemen C & Adams DJ. (1992). Calcium-activated potassium channels in native endothelial cells from rabbit aorta: conductance, Ca<sup>2+</sup> sensitivity and block. *J Physiol* **455**, 601-621.
- Sandow SL, Neylon CB, Chen MX & Garland CJ. (2006). Spatial separation of endothelial small- and intermediate-conductance calcium-activated potassium channels (K(Ca)) and connexins: possible relationship to vasodilator function? *J Anat* **209**, 689-698.
- Shaul PW, Smart EJ, Robinson LJ, German Z, Yuhanna IS, Ying Y, Anderson RG & Michel T. (1996). Acylation targets endothelial nitric-oxide synthase to plasmalemmal caveolae. *J Biol Chem* **271**, 6518-6522.
- Si H, Heyken WT, Wolfle SE, Tysiac M, Schubert R, Grgic I, Vilianovich L, Giebing G, Maier T, Gross V, Bader M, de Wit C, Hoyer J & Kohler R. (2006). Impaired endothelium-derived hyperpolarizing factor-mediated dilations and increased blood pressure in mice deficient of the intermediate-conductance Ca<sup>2+</sup>-activated K<sup>+</sup> channel. *Circ Res* **99**, 537-544.
- Sims SM & Dixon SJ. (1989). Inwardly rectifying K<sup>+</sup> current in osteoclasts. *Am J Physiol* **256**, C1277-1282.
- Singer HA & Peach MJ. (1982). Calcium- and endothelial-mediated vascular smooth muscle relaxation in rabbit aorta. *Hypertension* **4**, 19-25.
- Somlyo AP & Somlyo AV. (1968). Vascular smooth muscle. I. Normal structure, pathology, biochemistry,

- and biophysics. *Pharmacol Rev* **20**, 197-272.
- Sriram K, Laughlin JG, Rangamani P & Tartakovsky DM. (2016). Shear-Induced Nitric Oxide Production by Endothelial Cells. *Biophys J* **111**, 208-221.
- Stuehr DJ. (1997). Structure-function aspects in the nitric oxide synthases. *Annu Rev Pharmacol Toxicol* **37**, 339-359.
- Surks HK. (2007). cGMP-dependent protein kinase I and smooth muscle relaxation: a tale of two isoforms. *Circ Res* **101**, 1078-1080.
- Tao X, Avalos JL, Chen J & MacKinnon R. (2009). Crystal structure of the eukaryotic strong inward-rectifier K<sup>+</sup> channel Kir2.2 at 3.1 Å resolution. *Science* **326**, 1668-1674.
- Taylor MS, Bonev AD, Gross TP, Eckman DM, Brayden JE, Bond CT, Adelman JP & Nelson MT. (2003). Altered expression of small-conductance Ca<sup>2+</sup>-activated K<sup>+</sup> (SK3) channels modulates arterial tone and blood pressure. *Circ Res* **93**, 124-131.
- Tristani-Firouzi M, Jensen JL, Donaldson MR, Sansone V, Meola G, Hahn A, Bendahhou S, Kwiecinski H, Fidzianska A, Plaster N, Fu YH, Ptacek LJ & Tawil R. (2002). Functional and clinical characterization of KCNJ2 mutations associated with LQT7 (Andersen syndrome). *J Clin Invest* **110**, 381-388.
- Ungvari Z, Csiszar A & Kohler A. (2002). Increases in endothelial Ca<sup>2+</sup> activate K<sub>Ca</sub> channels and elicit EDHF-type arteriolar dilation via gap junctions. *Am J Physiol Heart Circ Physiol* **282**, H1760-H1767.
- Vanhoutte PM. (1982). Role of the endothelium in control of vascular smooth muscle function. *Verh K Acad Geneesk Belg* **44**, 411-418.
- Vollmer M, Koehrer M, Topaloglu R, Strahm B, Omran H & Hildebrandt F. (1998). Two novel mutations of the gene for Kir 1.1 (ROMK) in neonatal Bartter syndrome. *Pediatr Nephrol* **12**, 69-71.

- Wang WH & Giebisch G. (2009). Regulation of potassium (K) handling in the renal collecting duct. *Pflügers Arch* **458**, 157-168.
- Wang XL, Ye D, Peterson TE, Cao S, Shah VH, Katusic ZS, Sieck GC & Lee HC. (2005). Caveolae targeting and regulation of large conductance Ca(2+)-activated K<sup>+</sup> channels in vascular endothelial cells. *J Biol Chem* **280**, 11656-11664.
- Wei EP & Kontos HA. (1990). H<sub>2</sub>O<sub>2</sub> and endothelium-dependent cerebral arteriolar dilation. Implications for the identity of endothelium-derived relaxing factor generated by acetylcholine. *Hypertension* **16**, 162-169.
- White KA & Marletta MA. (1992). Nitric oxide synthase is a cytochrome P-450 type hemoprotein. *Biochemistry* **31**, 6627-6631.
- Williams JT, Colmers WF & Pan ZZ. (1988). Voltage- and ligand-activated inwardly rectifying currents in dorsal raphe neurons in vitro. *J Neurosci* **8**, 3499-3506.
- Wu M, Wang H, Yu H, Makhina E, Xu J, Dawson ES, Hopkins CR, Lindsley CW, McManus OB & Li M. (2010). A potent and selective small molecule Kir2.1 inhibitor. In *Probe Reports from the NIH Molecular Libraries Program*. Bethesda (MD).
- Wulff H & Köhler R. (2013). Endothelial small-conductance and intermediate-conductance K<sub>Ca</sub> channels: an update on their pharmacology and usefulness as cardiovascular targets. *J Cardiovasc Pharmacol* **61**, 102-112.
- Yamazaki D, Aoyama M, Ohya S, Muraki K, Asai K & Imaizumi Y. (2006). Novel Functions of Small Conductance Ca<sup>2+</sup>-activated K<sup>+</sup> Channel in Enhanced Cell Proliferation by ATP in Brain Endothelial Cells. *Journal of Biological Chemistry* **281**, 38430-38439.
- Yang D, MacCallum DK, Ernst SA & Hughes BA. (2003a). Expression of the inwardly rectifying K<sup>+</sup> channel Kir2.1 in native bovine corneal endothelial cells. *Invest Ophthalmol Vis Sci* **44**, 3511-3519.

Yang D, Pan A, Swaminathan A, Kumar G & Hughes BA. (2003b). Expression and localization of the inwardly rectifying potassium channel Kir7.1 in native bovine retinal pigment epithelium. *Invest Ophthalmol Vis Sci* **44**, 3178-3185.

Yoshida H, Feig JE, Morrissey A, Ghiu IA, Artman M & Coetzee WA. (2004). K ATP channels of primary human coronary artery endothelial cells consist of a heteromultimeric complex of Kir6.1, Kir6.2, and SUR2B subunits. *J Mol Cell Cardiol* **37**, 857-869.

Zhang Q, Tian J, Bai Y, Lei X, Li M, Yang Z & Meng Z. (2014). Effects of gaseous sulfur dioxide and its derivatives on the expression of KATP, BKCa and L-Ca(2+) channels in rat aortas in vitro. *Eur J Pharmacol* **742**, 31-41.

## **Chapter 2. General materials and Methods**

### **2.1 Ethical Approval**

All mice were housed under pathogen-free conditions at the University of Illinois Animal Care Vivarium and treated humanely in accordance with institutional guidelines (ACC#13-209, 16-183). All experiments were performed based on Guide for the care and use of laboratory animals from NIH.

### **2.2 Reagents and antibodies:**

BaCl<sub>2</sub>, apamin, N $\omega$ -Nitro-L-arginine methyl ester hydrochloride (L-NAME), acetylcholine, sodium nitroprusside (SNP), endothelin-1 (ET-1), ouabain, papaverine hydrochloride, bradykinin, acetylcholine and mouse monoclonal anti- $\alpha$ SMA antibodies were obtained from Sigma-Aldrich (St. Louis, MO, US). Rabbit monoclonal antibodies for mouse inwardly rectifying K<sup>+</sup> channel 2.1 (Kir2.1) were obtained from Abcam (Cambridge, MA, US). Rabbit polyclonal anti-mouse GAPDH, rabbit polyclonal anti-Akt1, rabbit polyclonal anti-pAkt1, rabbit polyclonal anti-peNOS antibodies were purchased from Cell Signaling Technology (Danvers, MA, US) and rabbit polyclonal anti-eNOS antibodies were purchased from Santa Cruz Biotechnology (Paso Robles, CA, US). Rabbit polyclonal anti-mouse vWF antibodies were purchased from Dako (Canada), and rat polyclonal anti-mouse CD31 antibodies were purchased from Beckton Dickinson (Franklin Lakes, NJ, US). Prime Time qPCR predesigned primers for mouse Kir2.1, 2.2, 2.3, CD31,  $\alpha$ SMA and GAPDH were purchased from IDT (Coralville, IA, US). pcDNA3-Kir2.1-HA was a gift from

Dr. Carol Vandenberg (University of California, Santa Barbara). Adenoviral vector expressing Kir2.1-HA with VE-Cadherin EC-specific promoter was generated by Vector BioLabs (Malvern, PA, US). Cells or vessels were transfected with VE-Cad Kir2.1 vector with 100 MOI for 48 hours.

### **2.3 Isolation of mouse mesenteric arteries:**

Mice were euthanized using CO<sub>2</sub> followed by cervical dislocation. The abdominal skin and muscle membrane were opened widely to retain the whole view of mesentery. The whole mesenteric tissues with partial pancreatic tissues were taken out by cutting the edge of mesenteric fat tissues to the intestine. Mesenteric tissues were transferred to HEPES buffer for the careful dissection of isolated arteries. Connective tissue and fat surrounding each blood vessel was carefully removed and the tissues were rinsed to remove any remaining blood cells.

### **2.4 Primary mouse mesenteric arterial endothelial cell isolation and culture:**

Endothelial cell isolation: Six mesenteric arteriole beds were taken from WT and Kir2.1<sup>+/-</sup> mice, respectively. Arteriole beds were washed in Ca<sup>2+</sup>- and Mg<sup>2+</sup>- free PBS and transferred to 1 ml of collagenase/dispase digestion solution (100 mg/ml) (Roche). Using sharp tip scissors, arteriolar branches were broken into small pieces. The tubes were incubated in 37 °C shaking incubator for 1 hour. Digested tissues and cells were spun down in 300xg for 10 mins. Supernatant were removed carefully and 1 ml of 0.05%

trypsin-EDTA was added to the tubes. The tubes were incubated in 37 °C shaking incubator for 15 mins. The solution was gently up-and-downed with 1000p pipette, and sieved through 40- $\mu$ m cell-sieve. The cell-sieve were washed with 10 ml of DMEM, 10% FBS to neutralize the trypsin effect. Cells were spun down in 300xg for 10 mins and then isolated using AutoMACs system and/or MiniMACs system from Miltenyi Biotech with magnetic beads conjugated polyclonal anti-mouse PECAM 1 IgG (Miltenyi Biotech). As recommended by the company protocol (Miltenyi Biotec) to increase the purity of the EC population, we used a two-step separation method, in which cell suspension mixed with the magnetic CD31 beads is run sequentially through two magnetic columns. Purity of the isolated ECs was tested with flow cytometry by staining with monoclonal anti-mouse CD31-PE IgG and with immunofluorescence staining with anti-mouse vWF and PECAM 1 IgGs. Flow cytometry was performed using CyAn ADP (Beckman Coulter). After the isolation, cells were maintained in EGM-2 endothelial cell growth media (Lonza). Cells for experiments were used between passage numbers 5 to 10.

### **2.5 PCR and Western Blot analysis:**

**qPCR:** To measure the mRNA expression of PECAM1 (CD31), smooth muscle  $\alpha$ -actin ( $\alpha$ SMA), Kir2.1, 2.2, and 2.3 in isolated mouse endothelial cells, quantitative PCR was performed. Briefly, endothelial cell RNA from WT and Kir2.1<sup>+/-</sup> mouse arteries were extracted using RNeasy mini kit (Qiagen) according to the manufacturer's instruction including an oncolumn DNase treatment step. The quantity and quality of extracted RNA were measured by Nanodrop (Thermo Fisher). cDNAs were generated with random primers using High Capacity cDNA Reverse Transcription Kit (Applied Biosystems).

Quantitative PCR was performed with Universal SYBR green Supermix (Biorad). Each sample was triplicated for analysis and at least three different sets of cells were tested. After initial denaturation of 95 °C, 40 cycles of 95 °C for 30 sec and annealing temperature of 60 °C for 30 sec, using Viiia 7 real-time PCR system (Applied Biosystems). Acquired fluorescence data were analyzed using  $2^{-\Delta\Delta C_t}$  methods, normalized by GAPDH.

**Western Blot:** Cells were rinsed with ice-cold PBS (pH 7.4) and homogenized in ice-cold RIPA buffer (50 mM Tris–HCl, 150 mM NaCl, NP-40 1%, Na-Doc 0.5%, SDS 0.1%, EDTA 1 mM, pH 7.6) containing 2 mM phenylmethylsulfonyl fluoride with protease inhibitor tablets (Roche). Samples were boiled in SDS sample buffer. Samples were resolved by SDS–PAGE (10% acrylamide gel) and transferred onto a PVDF membrane. The transferred blots were blocked with 4% non-fat milk and then incubated for overnight with primary antibody. After washing, the blots were incubated with peroxidase-conjugated secondary antibodies for 2 hours and developed using the ECL detection system (Thermo Scientific).

## **2.6 Vasodilation measurement in mouse mesenteric arteries:**

Resistance arteries (between 75-150  $\mu\text{m}$ ) from mesenteric arteriole beds were isolated and cannulated to glass micropipettes filled with Krebs solution (pH 7.40). Both ends of the cannulated vessel were connected to two separate Krebs reservoirs, and the vessel was stabilized at 60 cm H<sub>2</sub>O intraluminal pressure by elevating two Krebs-containing reservoirs 60 cm above the organ chamber. The reservoirs and the vessel lumen generate an open circuit. Vessels are equilibrated in this way for 30 minutes. After the 30-min

equilibration period, vessels were constricted (up to 50% of baseline diameter) with endothelin (ET-1) (120 to 160 pM final concentration).

## **Chapter 3. Inwardly rectifying K<sup>+</sup> channels plays a key role to flow-induced vasodilation in resistance arteries**

### **3.1 Introduction**

Olesen *et al.* first showed that Kir channels in endothelial cells are activated by flow (Olesen *et al.*, 1988). They observed that the currents generated by Kir channels increased in bovine aortic endothelial cells exposed to the fluid shear stress. In this study, the ranges of 0.3 to 20 dynes/cm<sup>2</sup> shear stress increased Kir currents. Physiological vascular wall shear stress is reported as the ranges of 5 to 20 dynes/cm<sup>2</sup> (Arfors & Bergqvist, 1974); thus, Olesen *et al.* showed that endothelial Kir channels are activated in the physiological shear stress. In this study, they also showed that the currents increased within a couple seconds after flow exposure; therefore, it was suggested that Kir channels can be a putative flow sensor of ECs. The flow sensitivity of Kir channels were also observed in human aortic endothelial cells (Fang *et al.*, 2006), which shows that Kir channels in endothelial cells are sensitive to flow across the species. Fang *et al.* showed that human aortic endothelial cells express mainly Kir2.1 and Kir2.2, suggesting that Kir2.1 and/or Kir2.2 are sensitive to flow (Fang *et al.*, 2005b). Hoger *et al.* tested the flow-activation of Kir2.1 channels overexpressed in *Xenopus* Oocytes (Hoger *et al.*, 2002). In this study, Hoger *et al.* applied the vertical flow on to Kir2.1 overexpressed oocytes, and observed the increase of Kir currents. Although the application of flow in this preparation was different from the physiological horizontal flow, Hoger *et al.* showed in this study that Kir2.1 is activated by the shear stress without endothelial cell components, which suggests that endothelial cell components may not be required to activate flow-

induced Kir currents.

Based on these studies described above, it suggests that Kir channels are sensitive to flow in endothelial cells, but the Kir channel function in endothelial response to shear stress is still unclear. However, an absence of appropriate genetic models is a critical restriction to study the role of Kir channels in flow-induced endothelial function. Global Kir2.1 knock out mouse model was developed by Zaritsky *et al.* (Zaritsky *et al.*, 2000), but due to a complete cleft of the secondary palate, these mice died 8 to 12 hours after birth.

In order to study the function of endothelial Kir channels, therefore, I used a heterozygous Kir2.1 (Kir2.1<sup>+/-</sup>) mouse model. I tested the functional role of Kir2.1 channels in the microvascular ECs and in flow-induced vasodilation (FIV) of the resistance arteries. Specifically, I tested 1) the contribution of Kir2.1 to FIV, 2) whether Kir channel activation is linked to nitric oxide generation or EDHF by flow and 3) the relevance of Kir and SK channels in FIV of mouse and human resistance arteries. These data suggest novel insights on the role of endothelial Kir channels in the regulation of human and murine vascular tones.

## **3.2 Methods**

### **3.2.1 Immunostaining:**

Briefly, cells were fixed with 4% paraformaldehyde for 15 mins, permeabilized with 0.5% Triton-X100 in PBS for 5 mins and then incubated with the primary anti-bodies (rat anti-mouse PECAM 1 IgG, mouse anti- $\alpha$ SMA IgG and rabbit anti-mouse vWF IgG) in 4 °C for overnight followed by incubation with secondary antibodies (Alexafluor 488 anti-rat IgG, Alexafluor 555 anti-mouse IgG and Alexafluor 568 anti-rabbit IgG, Invitrogen) for 2 hours in room temperature. Fluorescence images were taken through Zeiss Axiovert 200M microscope with AxioCam MRm camera.

### **3.2.2 Exposure to shear stress:**

ECs were exposed to laminar flow using a cone and plate apparatus system described previously (Dai *et al.*, 2004; Wu *et al.*, 2015). Briefly, flow device consisting of a computerized stepper motor UMD-17 (Arcus Technology) and a 1° tapered stainless steel cone. The flow devices were placed in 37°C incubator with 5% CO<sub>2</sub>. 1x10<sup>6</sup> ECs from WT and Kir2.1<sup>+/-</sup> mice were seeded in a gelatin (0.2%) coated well of 6-well plate and cultured in 37 °C for 72 hours. Shear stress (20 dynes/cm<sup>2</sup>) was applied for 30 minutes. Cells were lysed immediately after shear exposure on ice using RIPA buffer with protease and phosphatase inhibitors.

### **3.2.3 Flow-induced vasodilation measurement in mouse mesenteric arteries:**

Vasodilation of mouse mesenteric arteries were measured as described in our previous studies (Miura *et al.*, 2001; Phillips *et al.*, 2007; Liu *et al.*, 2011; Goslawski *et al.*, 2013). Briefly, resistance arteries (between 75-150  $\mu\text{m}$ ) from mesenteric arteriole beds were isolated and cannulated to glass micropipettes filled with Krebs solution (pH 7.40). Both ends of the cannulated vessel were connected to two separate Krebs reservoirs, and the vessel was stabilized at 60 cm H<sub>2</sub>O intraluminal pressure by elevating two Krebs-containing reservoirs 60 cm above the organ chamber. The reservoirs and the vessel lumen generate an open circuit. Vessels are equilibrated in this way for 30 minutes. After the 30-min equilibration period, vessels were constricted (up to 50% of baseline diameter) with endothelin (ET-1) (120 to 160 pM final concentration), and flow-induced vasodilation (FIV) was determined by exposing the vessels to incremental pressure gradients of  $\Delta 10$ ,  $\Delta 20$ ,  $\Delta 40$ ,  $\Delta 60$ , and  $\Delta 100$  cm H<sub>2</sub>O. The rationale to use ET-1 rather than intraluminal pressure is the design of our preparation which generates intraluminal flow by gravity (the reservoirs are moved in equal and opposite directions), I found that pre-constriction with ET-1 provides an alternative and more convenient approach, as described in our previous studies (Phillips *et al.*, 2007). As expected, no difference was observed between WT and Kir2.1<sup>+/-</sup> arteries (pre-constricted by  $49 \pm 0.6\%$  vs.  $49 \pm 0.3\%$ , respectively, n=9), because ET-1 constricts the vessels through G-protein coupled receptor and downstream signaling unrelated to Kir channels. Intraluminal pressure is maintained at 60 cm H<sub>2</sub>O by changing the distance between the reservoirs in equal and opposite directions (e.g. To induce intraluminal flow of  $\Delta 10$  cm H<sub>2</sub>O, one reservoir is elevated to 65 cm H<sub>2</sub>O while the other is lowered to 55 cm H<sub>2</sub>O, simultaneously), as described before (Liu *et al.*, 2003; Goslawski *et al.*, 2013; Grizelj *et al.*, 2015). FIV was determined in the presence and absence of

external perfusion of BaCl<sub>2</sub> (30 and/or 300 μM), L-NAME (100 μM), apamin (20 nM), and combination of BaCl<sub>2</sub> and L-NAME, BaCl<sub>2</sub> and apamin, and apamin and L-NAME. All inhibitors and blockers were incubated with the arteries for 30 mins before the application of flow. Papaverine (100 μM) was added during exposure at the maximal flow (Δ100 cm H<sub>2</sub>O) to test maximal endothelium-independent dilation. Resistance arteries were monitored continuously, and internal diameters were measured at the maximal diameter after each pressure gradient applied. Preparations were visualized with video cameras and monitors (model VIA-100, Boeckeler).

**Endothelium denuded arteries:** Mechanical endothelium denudation was performed by perfusing the artery with 3 ml of air, a common method, previously described (Phillips *et al.*, 2007). Denuded arteries were cannulated in an organ chamber and dose-response to acetylcholine and NO substitute sodium nitroprusside (SNP) (1 nM to 100 μM) were measured. Papaverine (100 μM) was applied with the highest doses of SNP or acetylcholine to confirm the potential of endothelium-independent vessel relaxation.

**EC-specific Kir2.1-HA adenoviral transfection:** EC-specific Kir2.1-HA adenoviral constructs were applied into the lumen of arteries for 48 hours at 37 °C. Then, following pressurization of vessels, FIV was measured with and without BaCl<sub>2</sub> (30 μM).

**Kir2.1 dominant negative (DN) lentiviral transfection:** Kir2.1DN lentiviral constructs were applied into the lumen for overnight at 37 °C. Then, following pressurization of vessels, FIV was measured with and without BaCl<sub>2</sub> (300 μM).

### **3.2.4 NO measurements:**

Resistance arteries (between 75-150  $\mu\text{m}$ ) from mesenteric circulation were isolated and incubated with NO specific fluorescence dye (Diaminorhodamine-4M, DAR4M) (Enzo Scientific) in HEPES at room temperature for 2 hours in the dark. The arteries were cannulated in an organ chamber and incubated for 30 minutes with or without a pressure gradient of 60 cm H<sub>2</sub>O in the dark. Arteries were removed from the chamber and mounted on glass slides for image acquisition by fluorescence microscopy (Nikon eclipse 80i). The NO fluorescent product was excited by 650-nm wavelength light with emission spectrum of 670 nm. Acquired images were analyzed for fluorescence intensity while correcting for background auto fluorescence using NIH image software (NIH Image J).

### **3.2.5 Blood pressure measurement and vascular resistance measurement:**

Blood pressure from WT and Kir2.1<sup>+/-</sup> mice was measured from carotid arteries. Briefly, mice were anesthetized with 3.5% isoflurane in 100% oxygen and carotid arteries were exteriorized for cannulation with polyethylene tubing with a continuous blood pressure experiments blood flow rates and blood pressure were measured by volume-pressure recording with occlusion tail cuff (Sharma *et al.*, 2011). The tail cuff measurements were also done in anesthetized mice. Peripheral vascular resistance is defined as the ratio of Mean blood pressure (mm Hg) to blood flow rate ( $\mu\text{l}/\text{min}$ ) (Rindler *et al.*, 2011).

### **3.2.6 Echocardiogram:**

Wild type mice and Kir2.1<sup>+/-</sup> mice in age of 3-5 months were used for the experiments. Transthoracic echocardiography was conducted using a 40 MHz transducer (MS550D)

on VisualSonics' Vevo 2100 ultrasound machine (VisualSonics, Toronto, Canada). Mice were sedated in an induction chamber using 3.5% isoflurane and then placed in the supine position on a heated stage. The heated stage maintained body temperature at 37° C, measured the electrocardiogram via embedded electrodes and recorded the respiration waveform via impedance pneumography. Anesthetic plane of the mice was maintained using 1.5% isoflurane in 100% oxygen delivered via a nosecone. After the mice were depilated, B-mode and M-mode images from the parasternal short axis view were obtained using the integrated rail system. All cardiac parameters were calculated using VisualSonics' Vevo 2100 analysis software (v. 1.6) with a cardiac measurements package (Pistner *et al.*, 2010).

### **3.2.7 Statistics:**

Data are presented as mean  $\pm$  SEM unless otherwise stated. The calculations for percent vasodilation were performed as described previously (Goslowski *et al.*, 2013). A two-factor ANOVAs with or without repeated measures was used where appropriate to compare FIV generated curves. Bonferroni post hoc analysis revealed significant differences. Linear regression analysis was used to compare the slopes of Ba<sup>2+</sup>-sensitive, current-voltage relationships. When appropriate, Kruskal-Wallis rank tests were performed on group data which had uneven distributions. For all other comparisons, a Student's t-test was performed. Statistical significance was accepted when  $p < 0.05$ .

### 3.3 Results

#### **3.3.1 Functional expression of Kir2.1 in mouse mesenteric arterial ECs**

My first question was which Kir2 channels functionally expressed in mouse endothelial cells. To address this question, I used real-time PCR to profile the mRNA expression levels of three Kir2 major sub-types in ECs.

Mouse mesentery was extracted and the surrounding fat tissues were cleaned to isolate arteriole bed (Fig. 3-1 A and B). Mesenteric arterial ECs were isolated with the endothelial cell marker, platelet-endothelial cell adhesion molecule-1 (PECAM-1, CD31) by the magnetic-bead associated cell sorting system (MACs), and the purity was confirmed by flow cytometry. Cells were labeled by anti-CD31-PE, and figure 3-2 A shows the flow cytometry results: i) unstained population, ii) CD31-PE stained population before MACs separation, iii) CD31-PE stained population after MACs purification, and iv) CD31-PE stained population in not-captured by MACs system. Figure 3-2 A iii shows the increase of CD31-PE signals, which implies the high purity of EC cells after MACs purification. The freshly isolated EC purity was, then, also tested by real-time PCR (Fig. 3-2 B). The expression of endothelial cell marker, PECAM-1, was measured to identify ECs, and the expression of smooth muscle cell marker,  $\alpha$ -smooth muscle actin ( $\alpha$ SMA), was measured to test the contamination of smooth muscle cells in CD31+ and CD31- cell populations after MACs separation. CD31+ cells shows significantly high CD31 mRNA expression levels (~10 fold higher) compared to the expression level in CD31- cell population, and there was almost no detection of  $\alpha$ SMA mRNA expression in CD31+ cell

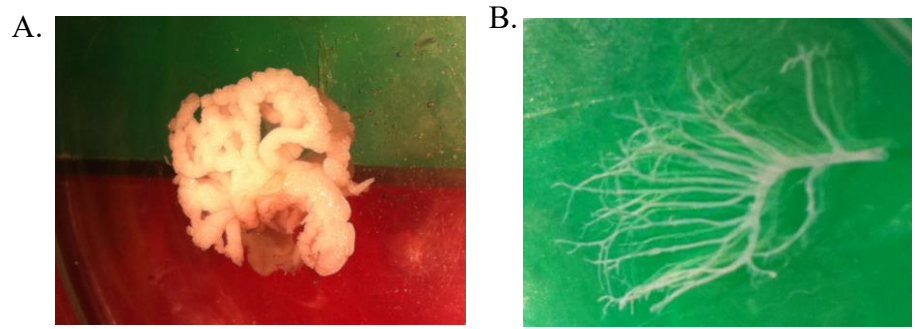


Figure 3-1 Mouse mesentery and arterial bed. A. Extracted mesentery from WT mouse. B. Mesenteric arterial bed after fat removal. Veins were also removed during fat cleaning.

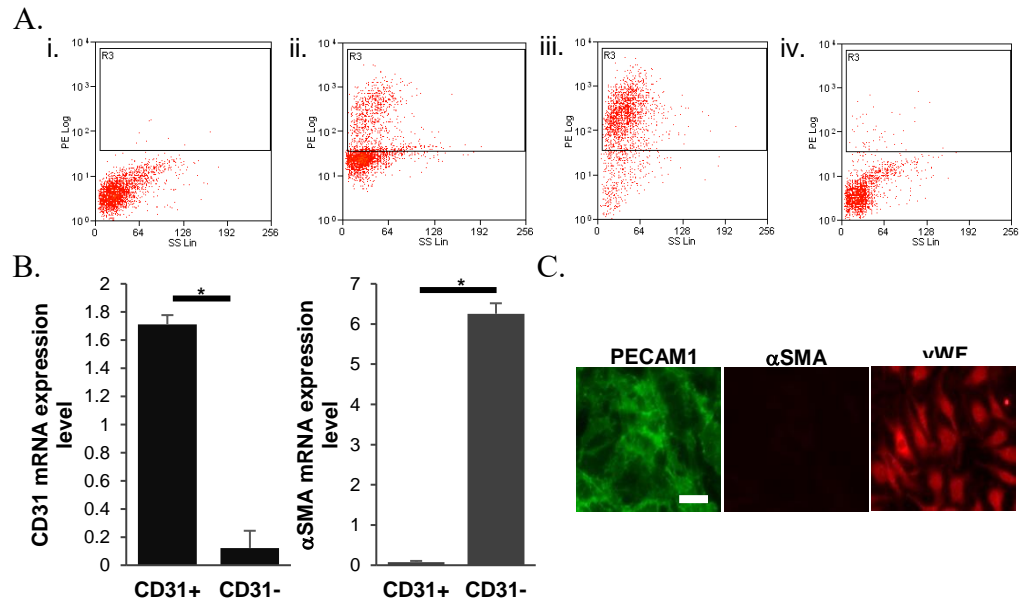


Figure 3-2 WT Mouse mesenteric arterial endothelial cell isolation. (A) Purity of endothelial cells were confirmed by flow cytometry against CD31 (endothelial cell marker). i) unstained, ii) CD31 stained before sorting, iii) CD31+ cells after sorting, iv) CD31- cells after sorting. (B) CD31 and  $\alpha$  smooth muscle actin (smooth muscle cell marker) mRNA levels in isolated CD31+ cells and CD31- cells by real-time PCR. (n=4, \*p<0.05) (C) Fluorescence staining of PECAM1 (endothelial cell marker),  $\alpha$  smooth muscle actin, and von Willebrand Factor (endothelial cell marker) in isolated CD31+ (endothelial) cells.

population. Additionally, primary cultured ECs were further verified by immunofluorescence staining with PECAM1 and von Willebrand Factor (vWF) for ECs and  $\alpha$ SMA for smooth muscle cells (Fig. 3-2 C). Primary cultured ECs showed both PECAM1 and vWF fluorescence signals, but there was no detectable signal for  $\alpha$ SMA. These data confirmed the purity of EC isolation and during primary culture.

According to Smith *et al.*, the expression of Kir2.1 is only observed in ECs but not in smooth muscle cells in mesenteric arteries. Consistent with their study, I observed the significant Kir2.1 mRNA expression in CD31<sup>+</sup> cells but almost no detectable mRNA expression of Kir2.1 in CD31<sup>-</sup> cells (Fig. 3-3 A). In addition, the mRNA expression of other 2 major Kir2 channels, Kir2.2 and 2.3, in ECs were also measured and compared with the expression of Kir2.1 (Fig. 3-3 B and C). The level of Kir2.3 expression was several orders of magnitude lower than Kir2.1. Kir2.2 mRNA expression was not detected. These data indicate that the major Kir2 channel in mouse mesenteric arterial ECs is Kir2.1.

Functional Kir2.1 expression in freshly-isolated/low passage mesenteric ECs was tested with electrophysiologic analysis in our lab. Kir currents in mesenteric ECs were measured and showed the inhibition by Ba<sup>2+</sup> with the IC<sub>50</sub> of 4.8  $\mu$ M, similar to the Ba<sup>2+</sup> sensitivity of Kir in aortic endothelium (Fang *et al.*, 2005a) and typical for Kir2.1 (Liu *et al.*, 2001). These studies verified Kir2.1 constitute the major functional Kir channel in these cells.

My second question is if the Kir2.1<sup>+/-</sup> heterozygous mouse model is suitable to study the role of Kir2.1 in ECs. To address this question, I used real-time PCR to profile the mRNA expression level in ECs isolated from Kir2.1<sup>+/-</sup> heterozygous mice. The Kir2.1 mRNA

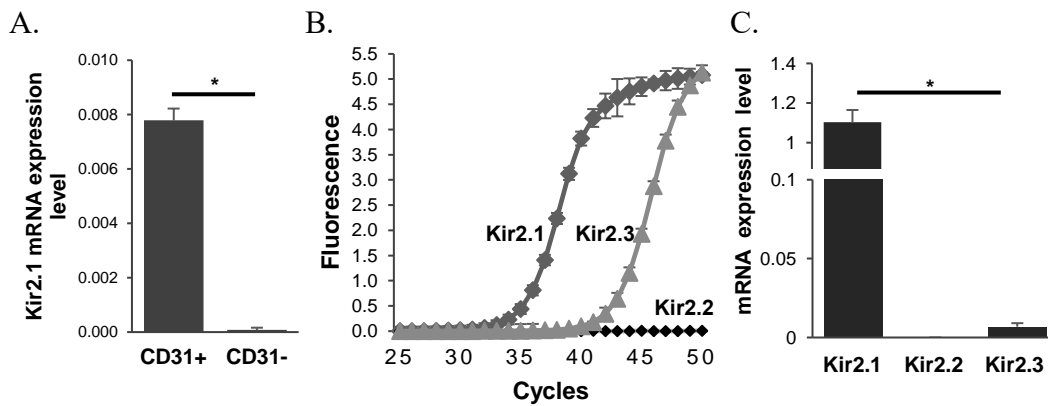


Figure 3-3 Kir2 channel expression levels in isolated WT endothelial cells. (A) Kir2.1 mRNA expression levels in CD31+ and CD31- cells. (n=4, \*p<0.05) (B) Real-time PCR trace of Kir2 channels in WT endothelial cells. (n=4) (C) mRNA expression levels of Kir2 channels. (n=4, \*p<0.05) (Kir2.2 was not measurable.)

expression level was decreased by 60-65% in Kir2.1<sup>+/-</sup> ECs (Fig. 3-4 A a and b). To test if there is any compensatory increase of other two major Kir2 channels by the decrease of Kir2.1 in these ECs, mRNA expression levels of Kir2.2 and Kir2.3 were additionally measured (Fig. 3-4 B). The reduction of Kir2.1 mRNA expression level in Kir2.1<sup>+/-</sup> ECs significantly increased the level of mRNA expression for Kir2.2 and Kir2.3, but overall the expression levels of the both mRNAs were still orders of magnitude lower than the level of Kir2.1. Furthermore, the level of Kir2.1 protein was measured by western blot, and Kir2.1 protein in Kir2.1<sup>+/-</sup> ECs was also decreased around 50%, similar to the reduction of mRNA expression level (Fig. 3-4 C a and b).

To test the functional changes of Kir currents in Kir2.1<sup>+/-</sup> ECs, our lab measured the Kir current in freshly-isolated ECs under both basal static and flow condition, and we observed not only the reduction of Kir currents under static condition but also the loss of flow-induced Kir currents in Kir2.1<sup>+/-</sup> ECs (Ahn *et al.*, 2017).

Taken all data together, I provided evidences that Kir2.1 is the major Kir channels in mouse mesenteric ECs, and the Kir2.1<sup>+/-</sup> mouse model is the powerful genetic model to study the role of Kir2.1 channels in flow-induced endothelial function.

### **3.3.2 Kir2.1 is essential for flow-induced vasodilation**

FIV is one of the major flow-induced functions of endothelium in vessels. My next question was if endothelial Kir2.1 channels plays a role in FIV.

To address this question, I measured FIV in a first order branch of mesenteric arteries. Mesenteric arteries were extracted and cannulated in an organ chamber, which

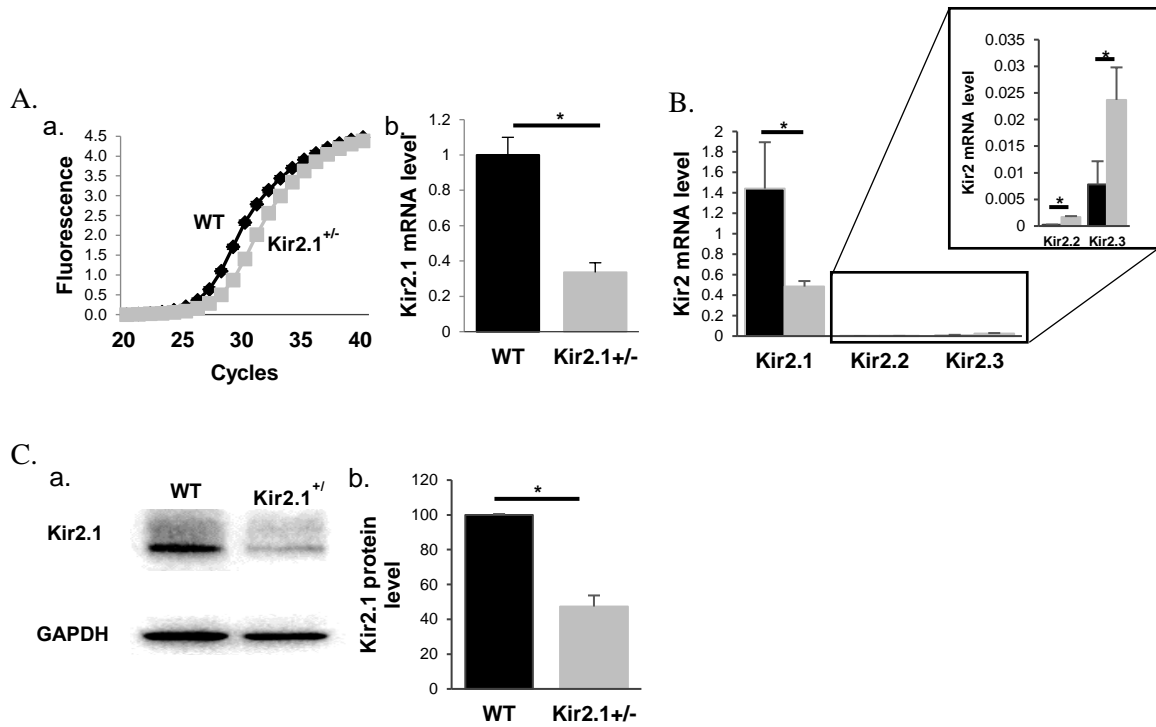
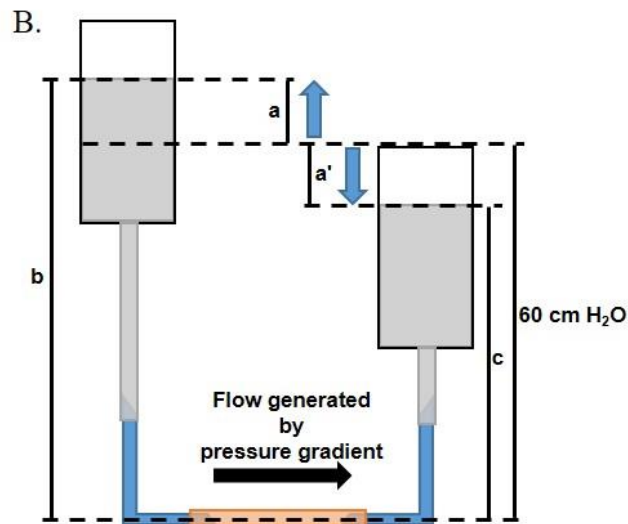
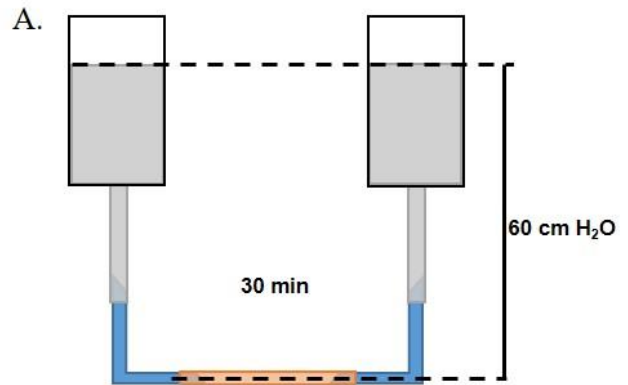


Figure 3-4 Kir2.1 channel expression levels in isolated WT and Kir2.1<sup>+/-</sup> endothelial cells. (A) Kir2.1 expression level in WT and Kir2.1<sup>+/-</sup> cells by real-time PCR. a and b are the trace of real-time PCR and the Kir2.1 mRNA expression levels. (n=4, \*p<0.05) (B) Kir2 channels mRNA expression levels in WT and Kir2.1<sup>+/-</sup> endothelial cells by real-time PCR. (n=4, \*p<0.05) (C) Kir2.1 protein expression levels in isolated WT and Kir2.1<sup>+/-</sup> endothelial cells. a and b are the representative western blot images and the protein expression levels of Kir2.1 in both cells. (n=4, \*p<0.05)

connected with two reservoirs on the both end to generate flow by pressure gradients between reservoirs (Fig. 3-5 A). Arteries were pre-exposed under the pressure of 60 cm H<sub>2</sub>O, which is known to be the physiological intraluminal pressure in resistance arteries. The arteries, then, were pre-constricted by endothelin-1, which is known to be produced by endothelial cells and to cause constriction of vascular smooth muscle through G-protein coupled receptors on smooth muscle cells. In order to generate flow in the cannulated arteries,  $\Delta 10$ ,  $\Delta 20$ ,  $\Delta 40$ ,  $\Delta 60$  and  $\Delta 100$  cm H<sub>2</sub>O pressure gradients were made by changing the heights of two reservoirs (Fig. 3-5 B). From the height of 60 cm, one side of the reservoir went up and the other side of the reservoir went down by equal lengths of 5, 10, 20, 30, and 50 cm. The height difference of two reservoirs made pressure gradients by gravity, and these pressure gradients generated the intraluminal flow in the cannulated mesenteric arteries. Two reservoirs were moved with equal amounts for each of the pressure gradients; therefore, the intraluminal pressure was always maintained as 60 cm H<sub>2</sub>O during the experiments, which provides the environment to measure the vasodilation purely induced by flow. To calculate the wall shear stress generated by pressure gradients in cannulated mesenteric arteries, I measured the volumetric flow rates in each pressure gradients by measuring the volume of flow-through after the cannulated arteries in 1 min. Based on these flow rates, I calculated the average intraluminal wall shear stress level of cannulated arteries (Fig. 3-5 C). The calculated range of shear stress levels generated by  $\Delta 40$  to  $\Delta 100$  cm H<sub>2</sub>O pressure gradients in cannulated mesenteric arteries were shown in the range of 9 to 28 dynes/cm<sup>2</sup>, which is relatively close to physiological shear stress level in resistance arteries. Lower than 40 cm H<sub>2</sub>O, no measurable volume of flow-through were collected in 1 min. These results



$a=a'$ ,  $a$  increases by 5, 10, 20, 30, or 50 cm from 60 cm point, and  $a'$  decrease in same manner  
 $b+c=120$  cm H<sub>2</sub>O, intra-luminal pressure =  $(b+c)/2 = 60$  cm H<sub>2</sub>O  
 $a+a' = \Delta$  Pressure gradient ( $\Delta 10, \Delta 20, \Delta 40, \Delta 60,$  and  $\Delta 100$  cm H<sub>2</sub>O)

C.

	Vessel diameter ( $\mu\text{m}$ )
	131.3 $\pm$ 17.2
Pressure gradient	Shear Stress (dyns/cm <sup>2</sup> )
$\Delta 40$ cm H <sub>2</sub> O	9 $\pm$ 0.4
$\Delta 60$ cm H <sub>2</sub> O	17.6 $\pm$ 1.4
$\Delta 100$ cm H <sub>2</sub> O	28 $\pm$ 0.6

Figure 3-5 Schematic feature of pressure gradient induced flow generation. (A) Mesenteric arteries are stabilized under 60 cm H<sub>2</sub>O of intraluminal pressure. (B) Pressure gradient between two reservoir generates flow in arteries with 60 cm H<sub>2</sub>O of intraluminal pressure. (C) Calculated shear-stress levels under  $\Delta 40$ ,  $\Delta 60$ , and  $\Delta 100$  cm H<sub>2</sub>O pressure gradients.

imply that the experimental design of FIV measurement using an organ chamber mimics relatively close to the in vivo condition.

Barium ( $\text{Ba}^{2+}$ ) is a well-known pharmaceutical inhibitor for Kir channels. In order to study the role of Kir in FIV, I measured FIV in pressurized WT mesenteric arteries, of which the diameters were 140 to 180  $\mu\text{m}$ , with the ranges of 0, 0.3, 3, 10, 30, and 300  $\mu\text{M}$  of  $\text{Ba}^{2+}$ . Figure 3-6 A showed the representative trace of FIV in a WT mesenteric artery without  $\text{Ba}^{2+}$ . As expected, WT mesenteric arteries were dilated by the pressure gradient generated flow, and higher flows increased the intraluminal diameters more. FIV was decreased by the increase of  $\text{Ba}^{2+}$  concentration, and there was no further decrease of FIV after 30  $\mu\text{M}$  of  $\text{Ba}^{2+}$  (Fig. 3-6 B). Maximal FIVs at  $\Delta 100$  cm  $\text{H}_2\text{O}$  were summarized in figure 3-6 C, and I calculated the  $\text{IC}_{50}$  (7.2  $\mu\text{M}$ ) based on these data. In the study of electrophysiological Kir current measurement, the dose dependent inhibition of  $\text{Ba}^{2+}$  was tested in our lab, and the inhibition of  $\text{Ba}^{2+}$  was observed with the  $\text{IC}_{50}$  of 4.8  $\mu\text{M}$  in WT ECs, which is similar to  $\text{IC}_{50}$  in FIV. Although  $\text{Ba}^{2+}$  is a well-known inhibitor for Kir channels,  $\text{Ba}^{2+}$  is not a specific inhibitor of Kir2.1 channels; hence, I tested FIV in Kir2.1<sup>+/-</sup> mesenteric arteries to see if Kir2.1 plays a role in FIV. FIV was measured in pressurized mesenteric arteries of 100-200  $\mu\text{m}$  isolated from WT and Kir2.1<sup>+/-</sup> mice. Figure 3-6 D showed representative traces of FIV in WT and Kir2.1<sup>+/-</sup> mesenteric arteries. FIV was significantly reduced (~40% of FIV in WT arteries) in Kir2.1<sup>+/-</sup> mesenteric arteries (Fig. 3-6 E and F). To verify further that the reduction of FIV in Kir2.1<sup>+/-</sup> resistance arteries was due to the loss of Kir channel function,  $\text{Ba}^{2+}$  (300  $\mu\text{M}$ ) was applied and there was no further FIV decrease observed in these arteries, which suggested that Kir2.1 were the only  $\text{Ba}^{2+}$ -sensitive channels in these arteries. Papaverine was used at the end of each

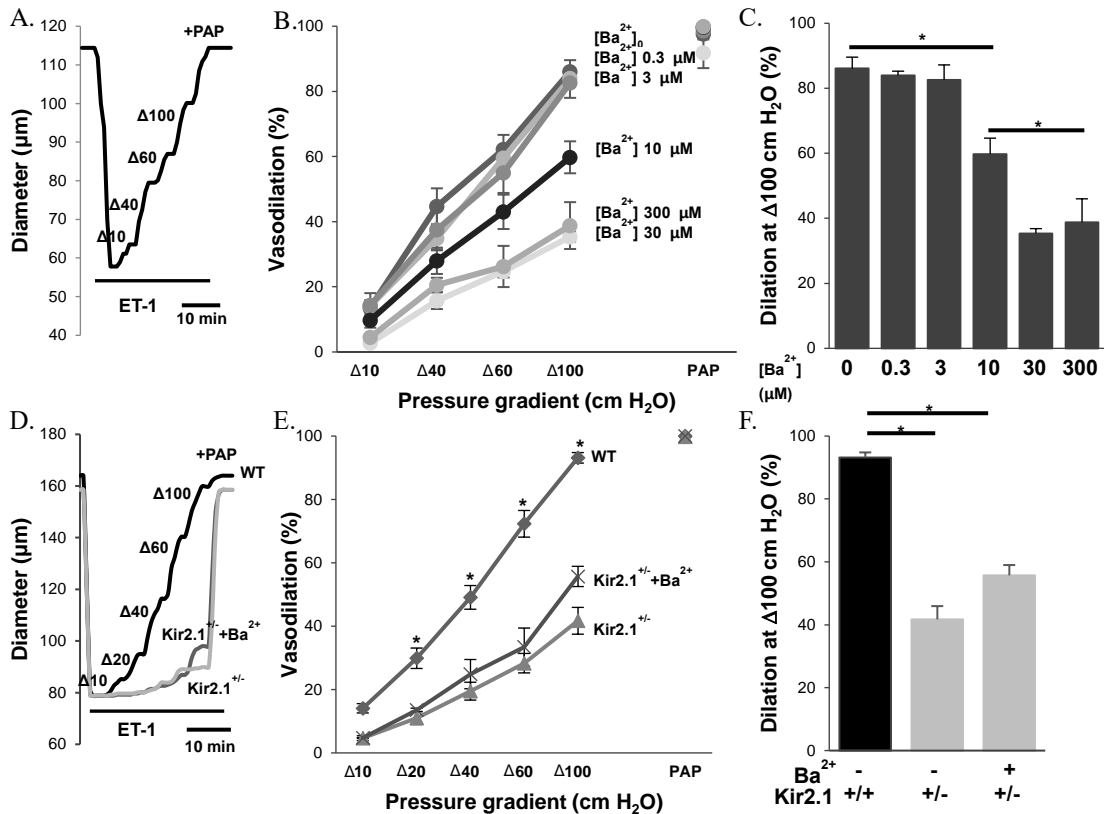


Figure 3-6 Role of Kir2.1 in flow-induced vasodilation in mouse mesenteric arteries. (A) Representative FIV trace in the absence of Ba<sup>2+</sup> ([Ba<sup>2+</sup>]<sub>0</sub>). Ba<sup>2+</sup> is perfused extravascularly. (B) Average flow-induced dilation (%) of pre-constricted mesenteric arteries harvested from WT mice with Ba<sup>2+</sup>-dose variation. (n=5, \*p<0.05) (D) Representative FIV trace of pre-constricted mesenteric arteries harvested from WT or Kir2.1<sup>+/-</sup> mice with and without 300 µM Ba<sup>2+</sup>, as a function of pressure gradient. (E) Average flow-induced dilation (%) of mesenteric arteries harvested from WT or Kir2.1<sup>+/-</sup> mice with and without 300 µM Ba<sup>2+</sup>, as a function of pressure gradient. (n=6 per group, \*p<0.05) C, F: Maximal dilation at Δ100 cm H<sub>2</sub>O pressure gradient for the same experimental conditions as described in B and E respectively. (ET-1=endothelin-1, PAP=Papaverine, added at the end of experiments to test the vessels' maximal dilation.)

experiments to verify that the reduction of FIV was due to the endothelium-dependent pathways. Papaverine is an endothelium-independent vasodilator, which activates the GMP cyclase in smooth muscle cells and induces vasodilation. The application of papaverine at  $\Delta 100$  cm H<sub>2</sub>O increased FIV to ~100% in both of WT and Kir2.1<sup>+/-</sup> mesenteric arteries, which proves that the loss of Kir2.1 channels in endothelium caused the reduction of FIV in Kir2.1<sup>+/-</sup> arteries. Therefore, these data suggest that Kir2.1 channels in ECs plays an important role in FIV.

To eliminate the possibility that the loss of FIV in Kir2.1<sup>+/-</sup> mice could be a result of non-specific changes in this genetic model, I also tested FIV in WT mouse mesenteric arteries, which were transfected with dominant negative mutant of Kir2.1 in lentiviral vectors. It is well established that the substitution of GYG to AAA amino acids sequence in the region of the pore loop of the Kir2.1 channel, which breaks the K<sup>+</sup> selectivity filter, results in the disruption of Kir2.1 current by specific dominant negative effect (Schram *et al.*, 2002). Specifically, transfecting the cells with dnKir2.1 subunits abrogates the activity of the endogenous Kir2.1 channels. Kir currents reduction by dominant negative transfection on human aortic endothelial cells were confirmed in our lab (Fang *et al.*, 2005b).

A WT mesenteric artery was cannulated one side, and the lentiviral vectors were applied into the lumen of the artery. After the lumen was filled up with viral vector containing media, the other side of artery was tied to prevent the leakage, and incubated for 24 hours in 37 °C. FIV was measured in WT mesenteric arteries transfected with empty lentiviral vector or dnKir2.1 lentiviral vectors. FIV in arteries transfected with dnKir2.1 was significantly lower than that in vessels transfected with empty vector (Fig. 3-7 A and B)

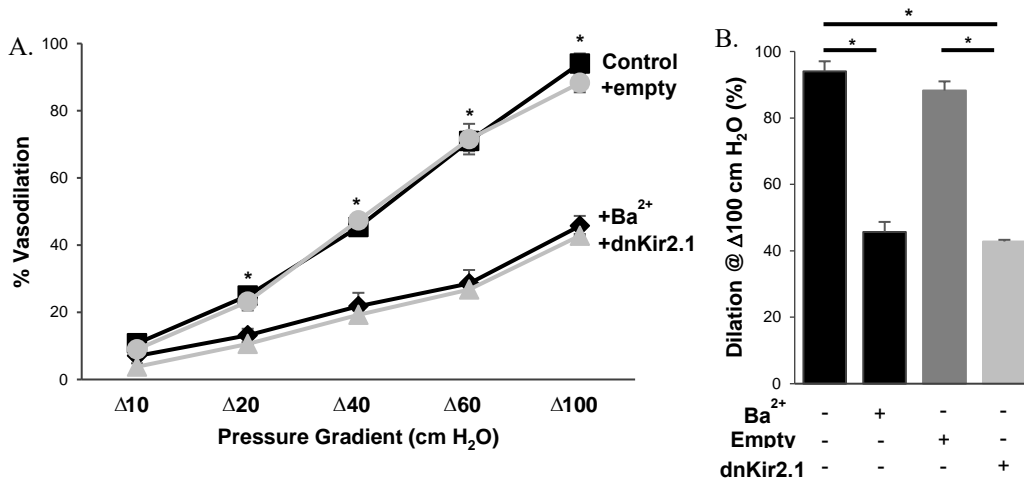


Figure 3-7 Loss of Kir2.1 function with dominant-negative Kir2.1 results in the inhibition of FIV in mesenteric arteries. (A) dnKir2.1 or empty lentiviral constructs are intraluminally treated to intact mesenteric arteries for 24 hours. Average flow-induced dilation of pre-constricted lentiviral constructs-treated and non-treated mesenteric arteries harvested from WT mice, as a function of pressure gradient. Vessel diameters are normalized to diameters stabilized at 60 cm H<sub>2</sub>O and the intraluminal pressure is maintained at the same pressure. Ba<sup>2+</sup> (300 μM) is perfused extravascularly to WT mesenteric arteries without the transfection of lentiviral constructs. (n=3 per group, \*p<0.05) (B) Average dilations at Δ100 cm H<sub>2</sub>O of A.

indicating that the loss of Kir activity causes the reduction of FIV in mesenteric arteries.

To determine if the inhibition of FIV by blocking Kir channels with  $Ba^{2+}$  was reversible, I tested whether the effect of  $Ba^{2+}$  on FIV could be recovered by the washout of  $Ba^{2+}$  (Fig. 3-8 A, B, and C). FIV was measured in WT arteries by increasing pressure gradients as described above before and after the application of  $Ba^{2+}$ . My data showed that  $Ba^{2+}$  significantly reduced FIV. After washout of  $Ba^{2+}$  from the organ chamber, FIV was completely recovered. This data show that  $Ba^{2+}$  induced inhibition of FIV is reversible.

My next goal to determine whether the effect of Kir2.1 channels in FIV is endothelial dependent. The Kir2.1<sup>+/-</sup> heterozygous genetic mouse model is a global knock down model; hence, not only endothelial cells but also other cells in mesenteric arteries have reduced expression of Kir2.1. In order to determine whether the effect of Kir2.1 on FIV is endothelium-dependent, I tested vasodilation in endothelium denuded arteries by SNP, a well-known NO donor (Fig. 3-9 A and B). The rationale of this experiment is that NO induces relaxation of smooth muscles directly, resulting in vasodilation. Mesenteric arteries were cannulated to the organ chamber and perfused with 10 ml of air bubbles to remove the endothelium. Figure 3-9 A shows the representative trace and B shows the summary of the SNP dose-dependent vasodilation data. There was no difference observed in vasodilation respond to NO increase between the arteries from WT and Kir2.1<sup>+/-</sup> mice. To verify the endothelium denudation, I tested acetylcholine dose-dependent vasodilation in the same arteries before SNP dose-dependent vasodilation measurement, and there was no dilation detected up to 100  $\mu$ M of acetylcholine in denuded mesenteric arteries from both WT and Kir2.1<sup>+/-</sup> mice (Fig. 3-9 C). In contrast, endothelium intact WT arteries showed acetylcholine dose-dependent vasodilation as

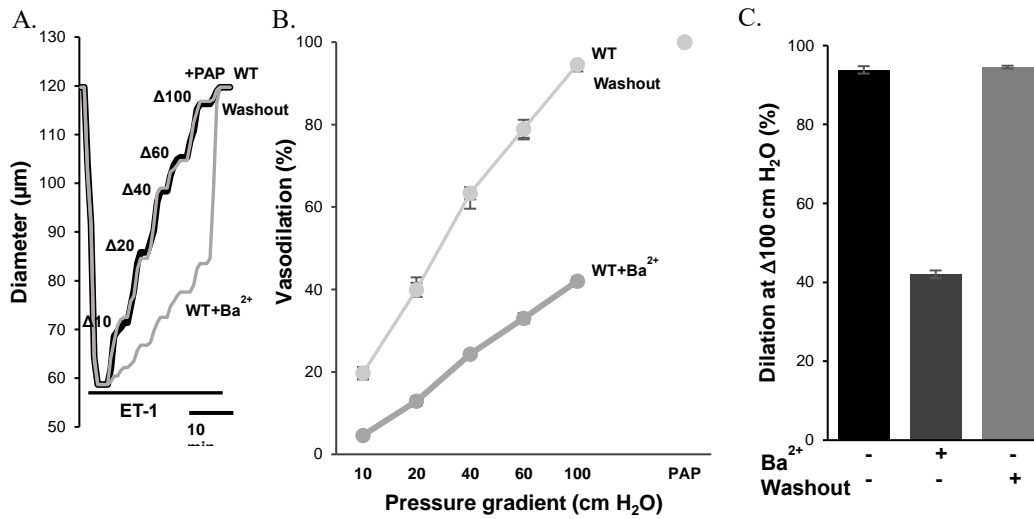


Figure 3-8 Reversible effect of Ba<sup>2+</sup> in flow-induced vasodilation. (A) Representative FIV trace of pre-constricted mesenteric arteries harvested from WT before, during and after the washout 300 µM Ba<sup>2+</sup>. (B) Average flow-induced dilations of mesenteric arteries described above (n=4 per group) (C) Average dilations at Δ100 cm H<sub>2</sub>O pressure gradient for the same experimental conditions as described in B. (ET-1=endothelin-1, PAP=Papaverine, added at the end of experiments to test the vessels' maximal dilation.)

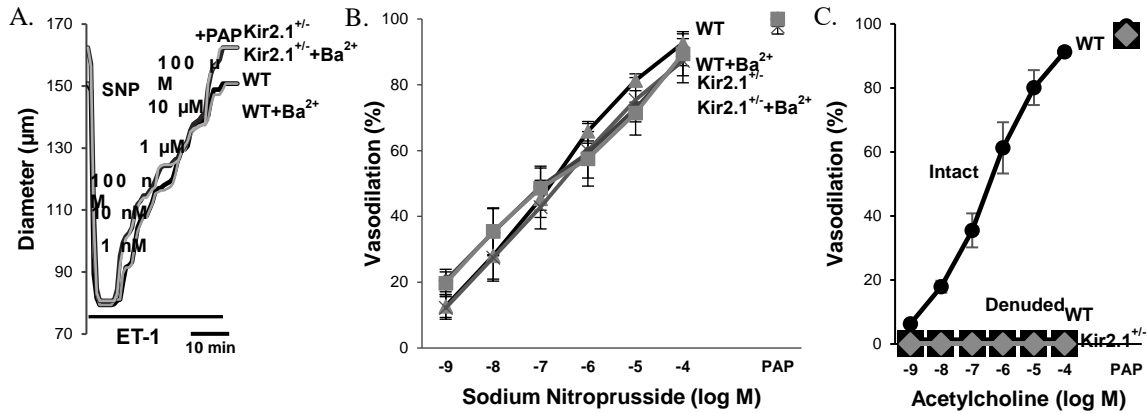


Figure 3-9 Kir2.1 does not affect sodium nitroprusside dependent dilation in endothelium denuded mesenteric arteries. (A) Representative sodium nitroprusside (SNP) induced vasodilation of pre-constricted denuded mesenteric arteries. SNP is perfused extravascularly. The endothelium was mechanically denuded by forcing air through the vessel lumen. (B) Average dilations as a function of SNP dose. (n=5 per group). (C) Average dilations of intact and denuded vessels in response to ACh. (n=4 per group) (ET-1=endothelin-1, PAP=Papaverine, added at the end of experiments to test the vessels' maximal dilation.)

expected.

Additionally, I measured  $K^+$  induced vasodilation in denuded arteries to test whether smooth muscle Kir channels play a role in the regulation of FIV. Earlier studies showed that increase of extracellular  $K^+$  may activate Kir channels and  $Na^+-K^+$  ATPase in VSMCs, inducing the hyperpolarization of smooth muscle in cerebral and coronary arterial beds (Burns *et al.*, 2004; Filosa *et al.*, 2006). Although I showed that Kir2.1 is not expressed in vascular smooth muscles of mesenteric arteries, it is possible that smooth muscles in mesenteric arterial beds can express other Kir channels, which can respond to extracellular  $K^+$  to induce vasodilation. Mesenteric arteries were denuded by 10 ml of air bubbling, and tested the vasodilation with 10, 16, 20 and 40 mM of total  $K^+$  concentration in buffer by adding KCl solution (Fig. 3-10 A, B, and C). Vasodilation was increased dose-dependently up to 20 mM of total  $K^+$  concentration in denuded WT arteries, and there was no difference between WT and Kir2.1<sup>+/-</sup> arteries.  $Ba^{2+}$  also had no effect. In contrast, ouabain, a well-known  $Na^+-K^+$  ATPase inhibitor, blocked  $K^+$ -dependent vasodilation in denuded mesenteric arteries from the both WT and Kir2.1<sup>+/-</sup> mice. These data suggest that  $K^+$ -dependent vasodilation in mesenteric arteries is  $Na^+-K^+$  ATPase dependent, but not Kir channels dependent. As expected, higher than 20 mM of  $K^+$  caused vasoconstriction due to the depolarization of smooth muscles.

In order to know if these observations in mesenteric arteries were tissue specific, I tested  $K^+$  dose-dependent vasodilation in denuded WT cerebral arteries (Fig. 3-11 A and B). I observed decreased vasodilation by  $Ba^{2+}$ , and there was no further decrease between 30 and 300  $\mu M$  of  $Ba^{2+}$ , which implies that  $K^+$  dose-dependent vasodilation relies on the vascular smooth muscle Kir channels. Combination of ouabain with  $Ba^{2+}$  significantly

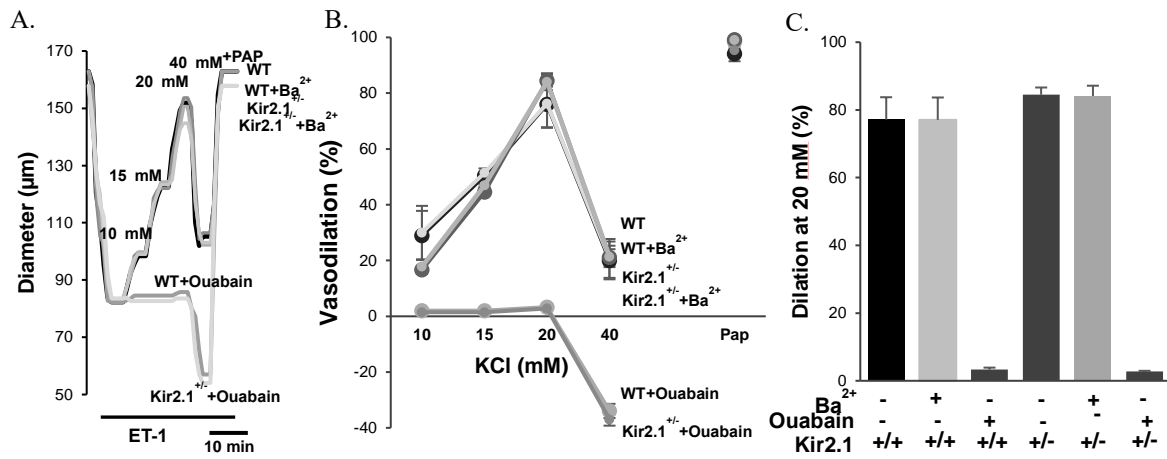


Figure 3-10 Kir2.1 does not affect K<sup>+</sup>-dependent dilation in endothelium denuded mesenteric arteries. (A) Representative K<sup>+</sup>-induced vasodilation of pre-constricted denuded mesenteric arteries from WT and Kir2.1<sup>+/-</sup> mice. (B) Average dilations of arteries from WT and Kir2.1<sup>+/-</sup> mice as a function of K<sup>+</sup> dose (KCl) (n=5 arteries per condition). (C) Average dilations at 20 mM KCl. (PAP=Papaverine, which is added at 40 mM KCl to check the vessels' maximum dilation.)

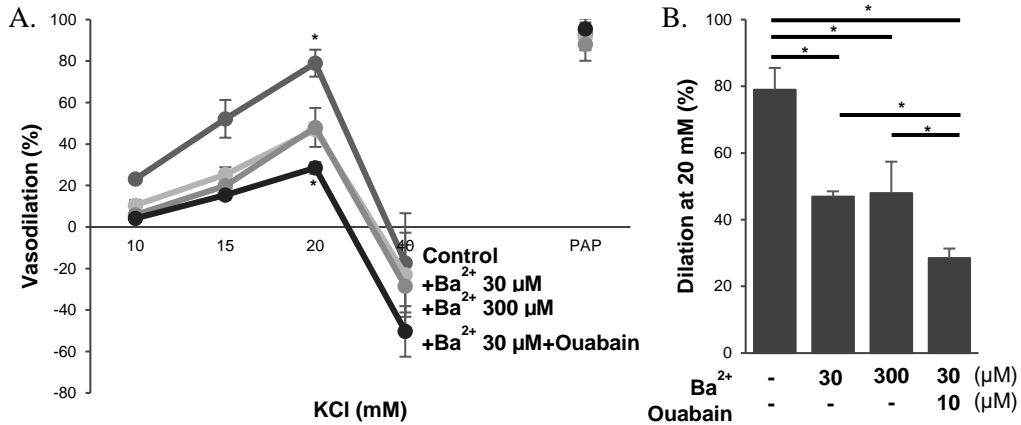


Figure 3-11 Loss of Kir2.1 activity reduces K<sup>+</sup>-dependent dilation in endothelium denuded cerebral arteries. (A) Average K<sup>+</sup>-induced dilation of pre-constricted denuded cerebral arteries from WT mice as a function of K<sup>+</sup> doses of 10, 15, 20, and 40 mM (n=5 arteries per condition, \*p<0.05). (B) Average dilations to 20 mM KCl. (n=5 arteries per condition, \*p<0.05) (PAP=Papaverine, which is added at 40 mM KCl to check the vessels' maximum dilation.)

further decreased the vasodilation by 20 mM of K<sup>+</sup>, which shows that not only Kir channels but also Na<sup>+</sup>-K<sup>+</sup> ATPase in VSMCs regulate K<sup>+</sup> dose-dependent vasodilation in cerebral arteries. Taken all together, these data indicate that my observation in Kir2.1 regulation of FIV is endothelial-dependent in mesenteric arteries.

### **3.3.3 Rescue of FIV in Kir2.1<sup>+/-</sup> arteries by endothelial-specific Kir2.1 expression**

My next question was if the recovery of Kir2.1 channels can rescue the FIV in the Kir2.1<sup>+/-</sup> mouse model. This question was addressed using adenoviral vector, which express WT Kir2.1 channels with HA-tag (WT Kir2.1-HA) using VE-Cad promoter (Vector Biolabs, CA). VE-Cadherin is a well-known endothelial cell specific protein and the promoter of this protein is only activated in ECs. Therefore, this adenoviral vector only expresses WT Kir2.1-HA channels in ECs. The endothelial specific expression of WT Kir2.1-HA channels was tested by immunofluorescence staining in our lab, and it was shown that anti-HA fluorescence signal was only detected from ECs, but not in VSMCs by the transfection of EC-specific WT Kir2.1 (Ahn *et al.*, 2017). Additionally, functional recovery of Kir2.1 currents in Kir2.1<sup>+/-</sup> ECs was observed after the transfection of WT Kir2.1-HA adenoviral vector in our lab (Ahn *et al.*, 2017).

Mesenteric arteries freshly-isolated from Kir2.1<sup>+/-</sup> mice were transfected with EC-specific WT Kir2.1-HA for 24 hours, and FIV was measured (Fig. 3-12 A, B, and C). As expected, empty viral vector transfected arteries from Kir2.1<sup>+/-</sup> mice showed the reduced FIV (less than 40% dilation at maximal flow), and there was no Ba<sup>2+</sup> sensitivity. However, most importantly, EC-specific WT Kir2.1-HA transfected Kir2.1<sup>+/-</sup> arteries showed fully

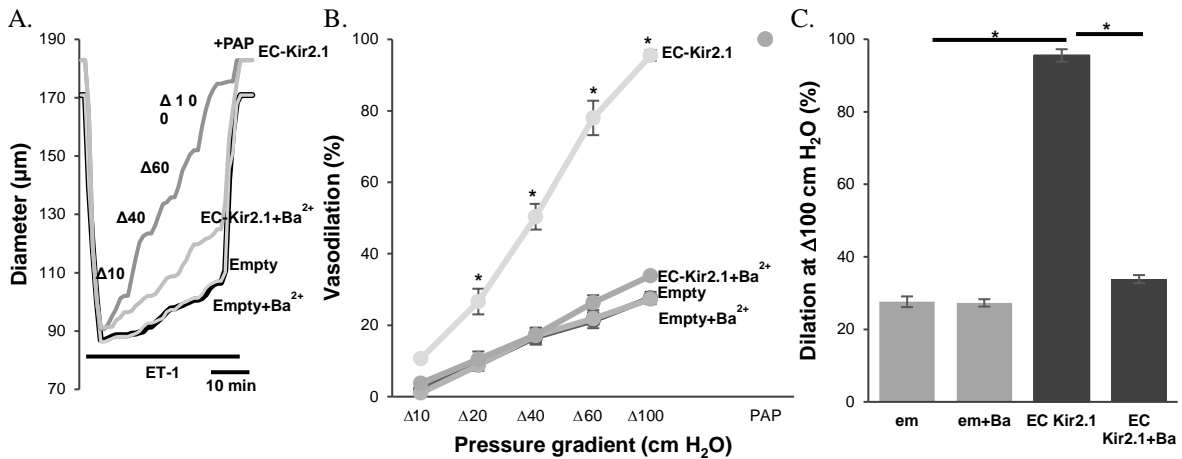


Figure 3-12 Recovery of Kir2.1 function with EC-specific WT Kir2.1-HA adenoviral vector in mesenteric arteries from Kir2.1<sup>+/-</sup> mice. (A) Representative FIV trace of empty or EC specific WT Kir2.1-HA transfected mesenteric arteries harvested from Kir2.1<sup>+/-</sup> mice. (B) Average flow-induced dilations of empty or EC specific WT Kir2.1-HA transfected mesenteric arteries harvested from Kir2.1<sup>+/-</sup> mice with and without 30 µM Ba<sup>2+</sup> (n=4 per group, \*p<0.05). (C) Average dilations of virus-transfected arteries at Δ100 cm H<sub>2</sub>O.

recovered FIV, and the recovered FIV was sensitive to  $Ba^{2+}$ . These results show that endothelial specific WT Kir2.1 recovery by adenoviral vector rescued the FIV impairment due to the Kir2.1 deficiency. Combine these data with previous data, I suggest that endothelial Kir2.1 channel is the major key component in FIV.

### **3.3.4 Complementary roles of Kir2.1 and $K_{Ca}$ channels in flow-induced vasodilation**

I showed endothelial Kir2.1 regulates the flow-induced vasodilation in resistance arteries. Earlier studies showed that SK channels play a significant role in FIV (Brahler *et al.*, 2009; Milkau *et al.*, 2010; Wulff & Köhler, 2013). My next question was to determine whether Kir and SK channels regulate FIV through the same pathway. Mesenteric arteries from WT and Kir2.1<sup>+/-</sup> mice were cannulated in the organ chamber, and then, the arteries were pressurized and pre-constricted to measure the FIV. To test the role of SK channels in FIV, apamin (20 nM), a well-known inhibitor of SK channels, was incubated for 30 mins before the FIV measurement. As expected, the significant reduction (about 50%) of FIV was observed in WT mesenteric arteries treated with apamin (Fig. 3-13 A, B, and C). In the same vessels,  $Ba^{2+}$  also decreased the FIV also about 50%. Interestingly, combination of apamin and  $Ba^{2+}$  completely abrogated FIV, which implies that FIV in mouse mesenteric arteries have two regulatory pathways: 1) Kir channel-dependent pathway and 2) SK channel-dependent pathway. To confirm the data, apamin was incubated with Kir2.1<sup>+/-</sup> arteries, and the residual vasodilation by flow (around 40%) was inhibited completely as same as WT arteries treated with  $Ba^{2+}$  and apamin together (Fig. 3-13 D, E, and F). More importantly, at the end of all experiments, the application of papaverin induced full dilation in all arteries, which showed that the arteries maintained their ability

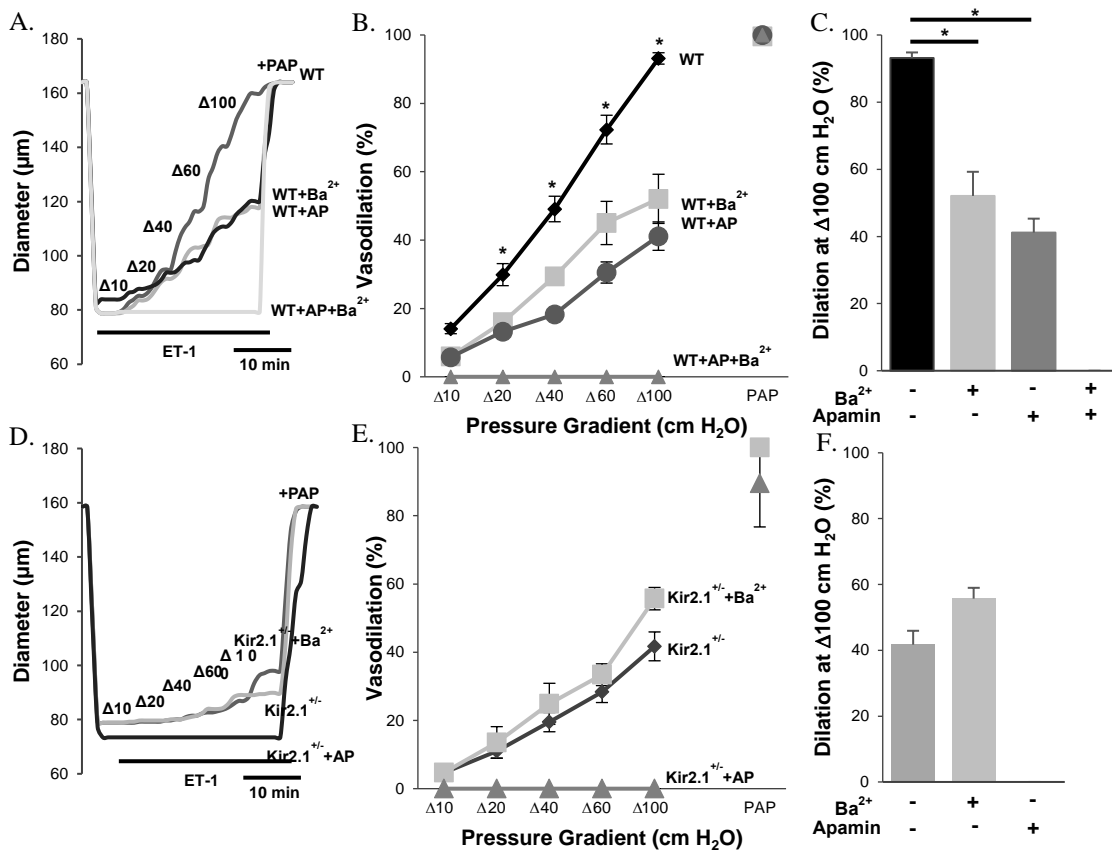


Figure 3-13 SK channels regulate flow-induced vasodilation in parallel pathway to Kir channels. (A) Representative FIV trace of pre-constricted (ET-1) mesenteric arteries harvested from WT mice with and without 20 nM apamin (AP), 300  $\mu$ M Ba<sup>2+</sup>, or both. (B) Average flow-induced dilations of arteries harvested from WT mice with the same experimental conditions described in A (n=4 arteries per condition, \*p<0.05). (D) Representative FIV trace of mesenteric arteries harvested from Kir2.1<sup>+/-</sup> mice exposed to the same experimental conditions described in A. (E) Average flow-induced dilations arteries harvested from Kir2.1<sup>+/-</sup> mice exposed to the same experimental conditions described in A (n=4 arteries per condition, \*p<0.05). C and F: Average dilations at  $\Delta$ 100 cm H<sub>2</sub>O for the same experimental conditions as described in B and E. Apamin was perfused extravascularly. (ET-1=endothelin-1, PAP=Papaverine, which is added at  $\Delta$ 100 cm H<sub>2</sub>O to test the vessels' maximal dilation)

to relax.

In order to test whether the concentration of apamin (20 nM) used to determine the contribution of SK channels to FIV response in mesenteric arteries results in full inhibition of SK, I tested the dose-response of apamin induced inhibition of FIV in WT mesenteric arteries (Fig. 3-14 A and B). Apamin was applied 0, 0.2, 2, 20, and 50 nM for 30 mins prior to measure FIV in the same mesenteric arteries, respectively. After the measurement of each dose of apamin, the vessel was fully washed out by perfusion to remove any residual effect of the dose applied before. During the repeated measurements, different order of dose-dependent, such as increase of dose or decrease of dose of apamin, FIV in WT mesenteric arteries were measured, and the order of dose increase or decrease did not affect the results of FIV. Apamin showed around 11 nM of IC<sub>50</sub>, and there was no further decreased FIV measured after 20 nM, which showed that 20 nM of apamin completely eliminated the contribution of SK channels in FIV of mesenteric arteries during the previous experiments.

In terms of mechanism, SK channels are known to contribute FIV via endothelial-derived hyperpolarizing factors. I showed that Kir channels regulate FIV in SK channel-independent pathway; thus, my next question was if Kir2.1 channels regulate FIV by an NO-dependent mechanism. As discussed in the Chapter 1, NO is produced by eNOS in ECs. To address my question, I measured FIV with N $\omega$ -Nitro-L-arginine-methyl-ester hydrochloride (L-NAME) (100  $\mu$ M), a well-known inhibitor for eNOS, in mesenteric arteries from both WT and Kir2.1<sup>+/-</sup> mice (Fig. 3-15 A, B, and C). As expected, FIV were significantly decreased with L-NAME in WT arteries. Interestingly, there was no further decrease of FIV observed with the combination of L-NAME and Ba<sup>2+</sup>, which suggests that

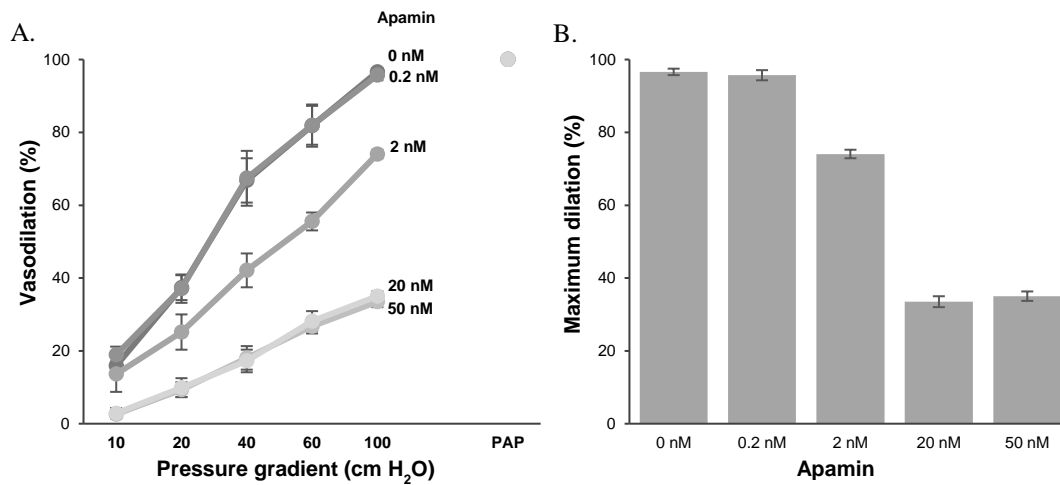


Figure 3-14 Dose-response to apamin of flow-induced vasodilation in WT mesenteric arteries. (A) Average flow-induced dilations of arteries harvested from WT mice with apamin-dose dependent effect (n=4 arteries per condition, \*p<0.05). (B) Dose-response to apamin of FIV in WT mesenteric arteries at average dilations at  $\Delta 100$  cm H<sub>2</sub>O (n=4, \*p<0.05). Apamin was perfused extravascularly. (ET-1=endothelin-1, PAP=Papaverine, which is added at  $\Delta 100$  cm H<sub>2</sub>O to test the vessels' maximal dilation)

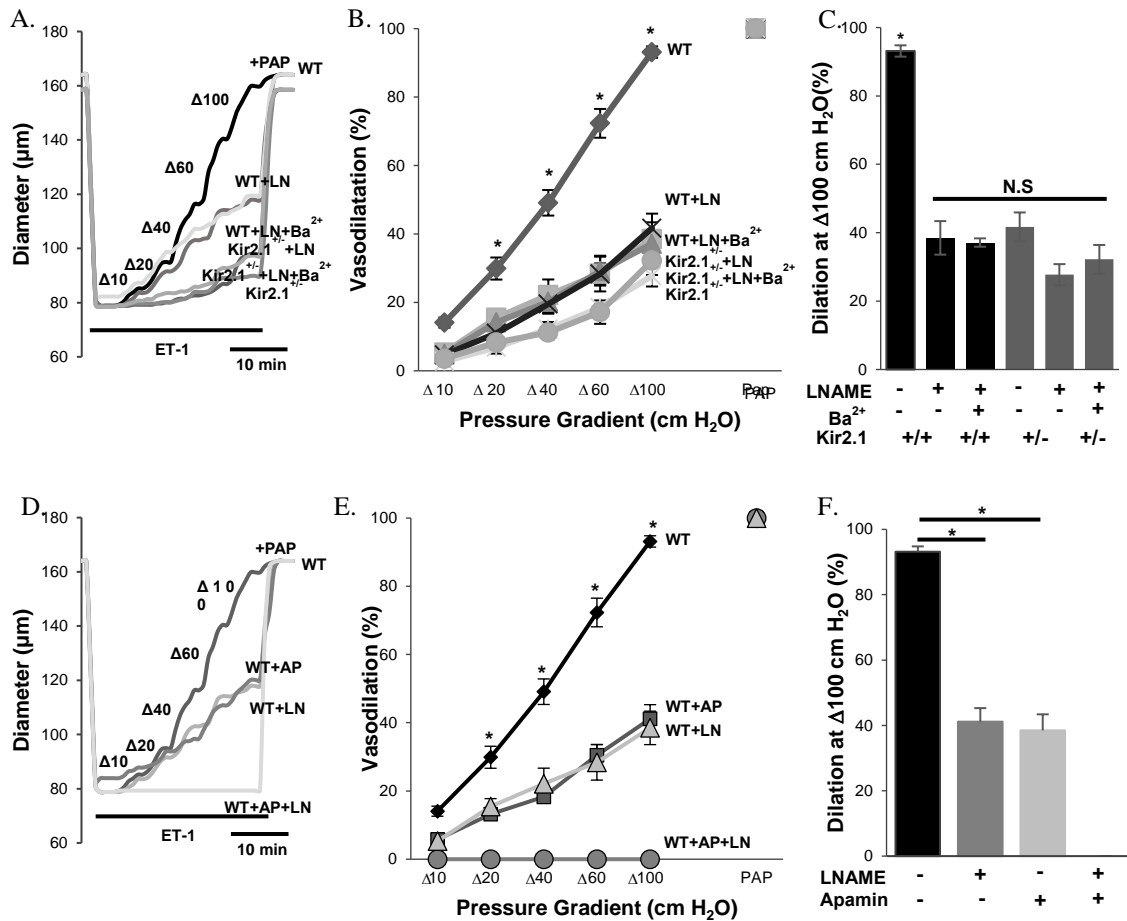


Figure 3-15 Kir2.1 regulate flow-induced vasodilation by a NO-dependent and a SK-independent pathway. (A) Representative FIV trace of arteries harvested from WT or Kir2.1<sup>+/-</sup> mice with and without 100  $\mu$ M L-NAME (LN). (B) Average flow-induced dilations of arteries from WT or Kir2.1<sup>+/-</sup> mice with the same experimental conditions described in A (n=4 arteries per condition). (D) Representative FIV trace of arteries harvested from WT mice with and without 20 nM apamin, 100  $\mu$ M L-NAME, or both. (E) Average flow-induced dilations of mesenteric arteries harvested from WT mice with the same experimental conditions described in D (n=5 arteries per condition, \*p<0.05). C and F: Average dilations at  $\Delta 100$  cm H<sub>2</sub>O for the same experimental conditions as described in B and E. Apamin and LNAME were perfused extravascularly. (ET-1=endothelin-1, PAP=Papaverine, which is added at  $\Delta 100$  cm H<sub>2</sub>O to test the vessels' maximal dilation)

the regulation of Kir channels is via the NO production. The FIV measurement of Kir2.1<sup>+/-</sup> arteries with L-NAME or combination of L-NAME and Ba<sup>2+</sup> showed no further decrease, which supports the previous suggestion that endothelial Kir2.1 regulation of FIV is through the NO pathway.

In order to know if the SK channel dependent pathway in FIV is involved to NO pathway, I tested FIV in WT mesenteric arteries with the combination of L-NAME and apamin (Fig. 3-15 D, E, and F). Interestingly, similar to the application of the combination of Ba<sup>2+</sup> and apamin, the FIV was completely abrogated. In all the experiments, papaverin-induced dilation was not affected by apamin, L-NAME, Ba<sup>2+</sup>, and the combination of any listed components, which showed that mesenteric arteries used in these experiments maintained the ability to relax under the inhibition condition of SK channels, eNOS, and/or Kir channels. Taken all together, these results suggest that endothelial Kir channels regulate FIV via NO production, and the regulation of FIV by SK channels follows NO- and Kir channel-independent pathways.

### **3.3.5 Flow-induced eNOS activation is regulated by Kir2.1 via Akt1 phosphorylation**

The results from FIV measurements suggest that the regulation of endothelial Kir2.1 channels in FIV is via NO production; therefore, my next question was the molecular mechanism of eNOS regulation under flow by Kir2.1 channels.

In order to address this question, primary cultured ECs of mesenteric arteries from WT and Kir2.1<sup>+/-</sup> mice were exposed under 20 dynes/cm<sup>2</sup> of the shear stress, which simulates physiological condition of the resistance artery, generated by the cone apparatus for 30

mins. Due to the strict regulation of eNOS activation, ECs were lysed on ice immediately after flow exposure with RIPA buffer containing protease and phosphatase inhibitor. The activation of eNOS was tested by western blot analysis (Fig. 3-16 A and C). As expected in WT ECs, the shear stress exposure increased the phosphorylation of S1177 residue in eNOS, which is a well-known phosphorylation site (Fisslthaler *et al.*, 2000), compared to the phosphorylation under the static condition. In contrast, the phosphorylation of S1177 in eNOS by shear stress was not increased in Kir2.1<sup>+/-</sup> ECs. Consistent with these observation, Ba<sup>2+</sup> decreased eNOS phosphorylation in WT ECs, and there was no further decrease of flow-induced eNOS activation in Kir2.1<sup>+/-</sup> ECs, which confirms the Kir2.1 regulates flow-induced eNOS phosphorylation. According to Dimmeler *et al.*, flow-induced eNOS activation is governed by Akt phosphorylation (Dimmeler *et al.*, 1999). To test if the eNOS regulation by Kir2.1 is via Akt phosphorylation, I tested flow-induced eNOS phosphorylation with MK2202, a well-known Akt inhibitor. Inhibition of Akt showed no flow-induced increase of eNOS phosphorylation in WT ECs, and interestingly, no flow-induced eNOS activation was also observed in Kir2.1<sup>+/-</sup> ECs without further decrease. These results imply that flow-induced eNOS activation is regulated by Kir2.1 channels via Akt activation. Therefore, I tested the regulation of flow-induced Akt1 activation by Kir2.1 (Fig. 3-16 B and D). Similar to eNOS activation, WT ECs showed the significant phosphorylation increase of S473 residue in Akt1, which is a well-known phosphorylation site to activate Akt, under the shear stress. Whereas, there was no increase of Akt1 phosphorylation in Kir2.1<sup>+/-</sup> ECs with and without Ba<sup>2+</sup> and WT ECs with Ba<sup>2+</sup>. Additionally, the MK2202 treatment did not further decrease the flow-induced Akt1 phosphorylation in both of WT and Kir2.1<sup>+/-</sup> ECs. In order to determine if the overexpression of WT Kir2.1

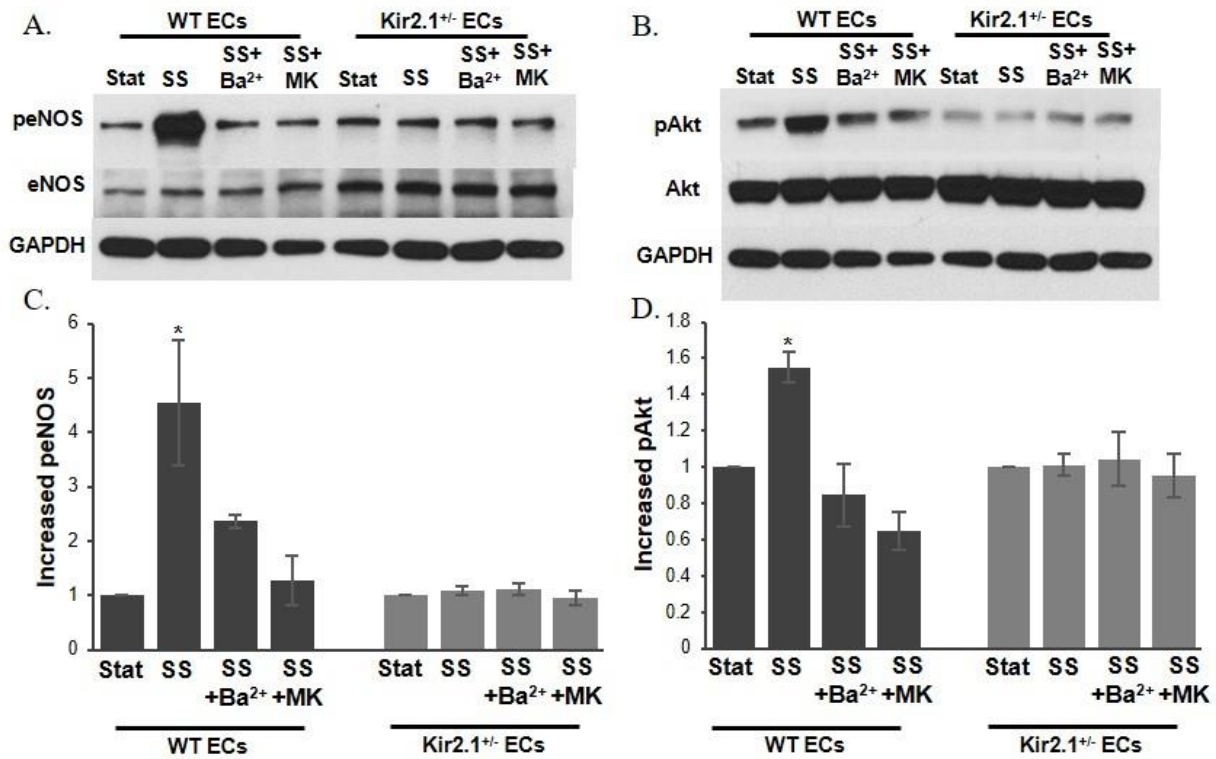


Figure 3-16 Kir channels regulate flow-induced eNOS activation by Akt phosphorylation. (A) Representative western blot for eNOS phosphorylation by shear stress (20 dyn/cm<sup>2</sup>, 30 min) with or without Ba<sup>2+</sup> or Akt inhibitor (MK2206) in murine mesenteric arterial ECs isolated from WT and Kir2.1<sup>+/-</sup> mice. (B) Representative western blot for Akt phosphorylation in the same experimental samples shown in A. (C) Densitometry for group data represented in A (n=4 per group, \*p<0.05) (D) Densitometry for the group data represented in E (n=4 per group, \*p<0.05). (SS: shear stress, MK: MK2206)

channels recover the flow-induced eNOS activation via Akt phosphorylation in Kir2.1<sup>+/-</sup> ECs, I transfected Kir2.1<sup>+/-</sup> ECs with WT Kir2.1-HA adenoviral vectors, and tested the shear stress induced eNOS and Akt phosphorylation by western blot analysis (Fig. 3-17). As expected, empty vector transfected Kir2.1<sup>+/-</sup> ECs showed no increase of flow-induced phosphorylation of eNOS with or without Ba<sup>2+</sup>, and also there was no increase with Akt inhibitor. In contrast, the flow-induced eNOS phosphorylation was fully recovered in WT Kir2.1-HA transfected Kir2.1<sup>+/-</sup> ECs, and there was no flow-induced eNOS phosphorylation in these cells with Ba<sup>2+</sup> or MK2202 (Fig. 3-17 A and C). The flow-induced Akt1 activation was also recovered by the transfection of WT Kir2.1-HA in Kir2.1<sup>+/-</sup> ECs (Fig. 3-17 B and D). Based in these data, Kir2.1 in ECs regulates flow-induced eNOS activation via Akt phosphorylation to produce NO resulting in FIV.

### **3.3.6 Kir 2.1 but not K<sub>Ca</sub> regulate flow-induced NO generation in mesenteric arteries**

Although my data presented above suggest that endothelial Kir2.1 regulates FIV via eNOS regulation, my next objective was to determine whether the flow-induced NO production is affected by Kir2.1 deficiency, and follows the K<sub>Ca</sub>-independent pathway.

I tested flow-induced NO production in mesenteric arteries with a membrane permeable NO-sensitive fluorescent dye, Diaminorhodamine-4M (DAR4M). Intact mesenteric arteries from WT and Kir2.1<sup>+/-</sup> mice were loaded with DAR4M, and then pressurized and exposed to flow generated by a pressure gradient ( $\Delta 60$  cm H<sub>2</sub>O) for 30 min. As expected, WT arteries showed significant increase of NO-fluorescent signal after flow exposure compared to after static condition. In contrast, there was no significant increase of flow-

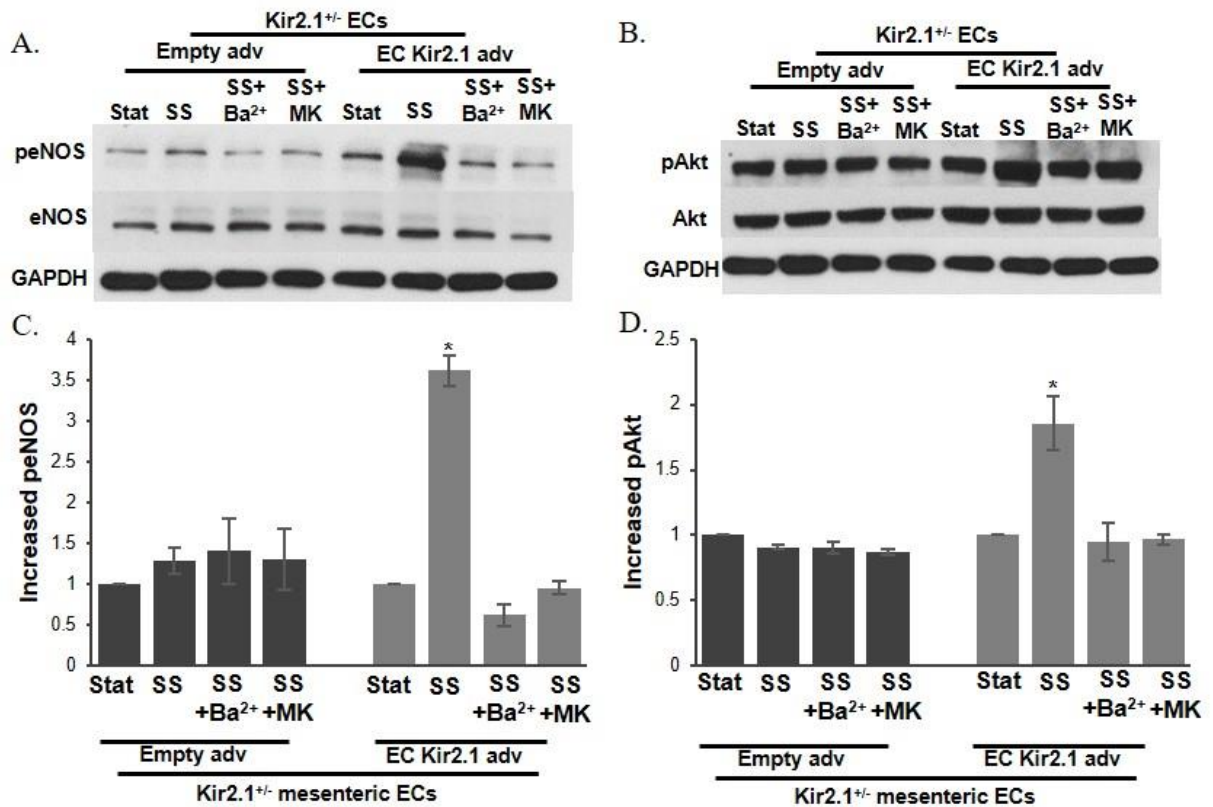


Figure 3-17 Recovery of flow-induced eNOS activation by Akt phosphorylation in Kir2.1<sup>+/-</sup> endothelial cells by the transfection of EC-specific WT-Kir2.1. (A) Representative western blot for eNOS phosphorylation by shear stress (20 dyn/cm<sup>2</sup>, 30 min) with or without Ba<sup>2+</sup> or Akt inhibitor (MK2206) in the adenoviral vector (empty or Kir2.1-HA) transfected murine mesenteric arterial ECs from Kir2.1<sup>+/-</sup> mice. (B) Representative western blot for Akt phosphorylation in the same experimental samples shown in A. (C) Densitometry for the group data represented in A (n=4 per group, \*p<0.05). (D) Densitometry for the group data represented in C (n=4 per group, \*p<0.05). (SS: shear stress, MK: MK2206)

induced NO production in Kir2.1<sup>+/-</sup> arteries and WT arteries with Ba<sup>2+</sup>. To verify that the increased DAR4M signal in WT arteries under flow was by NO production, I tested flow-induced NO production with L-NAME in WT arteries, and the flow-induced NO signal was abrogated, which proves that the increased DAR4M signal is due to the flow-induced NO increase (Fig. 3-18 A and B). As a negative control, endothelium denuded arteries from WT and Kir2.1<sup>+/-</sup> mice were also tested to measure flow-induced NO production, and there were no detectable signals at all under both static and flow conditions (Fig. 3-18 C). These data provide the direct evidence that Kir2.1 channels are essential for the flow-induced NO production.

In order to test the role of SK in flow-induced NO production, the flow-induced NO production was measured in WT arteries with and without 20 nM of apamin in a parallel series of experiments (Fig. 3-19 A and B). As shown in the above, 20 nM of apamin reduced FIV significantly under the fluid shear stress generated by 60 cm H<sub>2</sub>O pressure gradient, whereas the flow-induced production of NO was not affected by apamin (20 nM) under the same shear stress condition.

These data suggest that flow-induced NO production is regulated by Kir2.1 rather than SK, and the contribution of SK channels in FIV follows the Kir2.1- and NO- independent pathway.

### **3.3.7 Kir2.1 contributes to the control of blood pressure**

Blood pressure is determined with two major factors: 1) peripheral vascular resistance and 2) cardiac outputs (Messerli, 1982). All my results shown above suggest that the loss

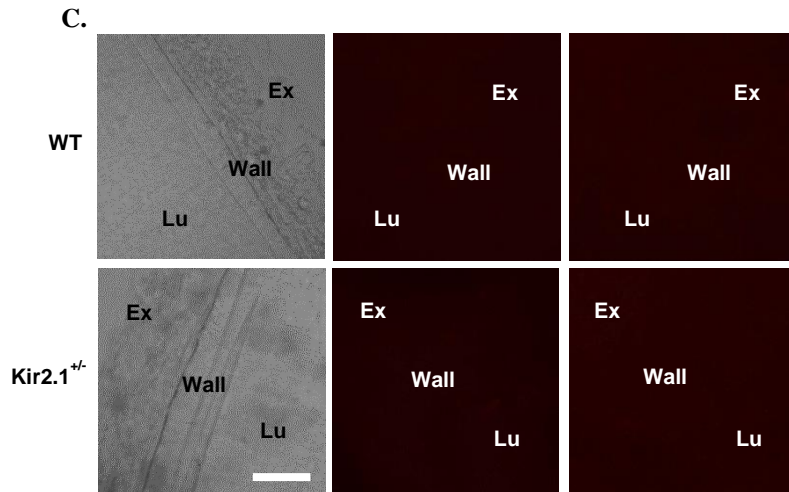
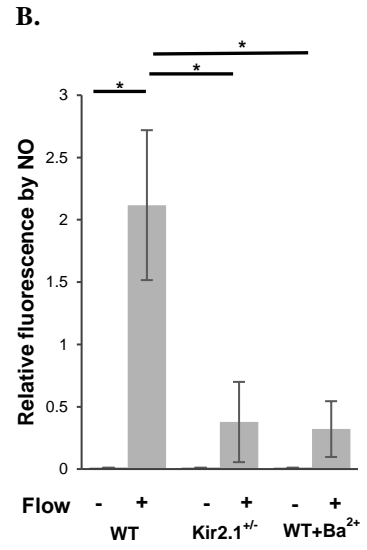
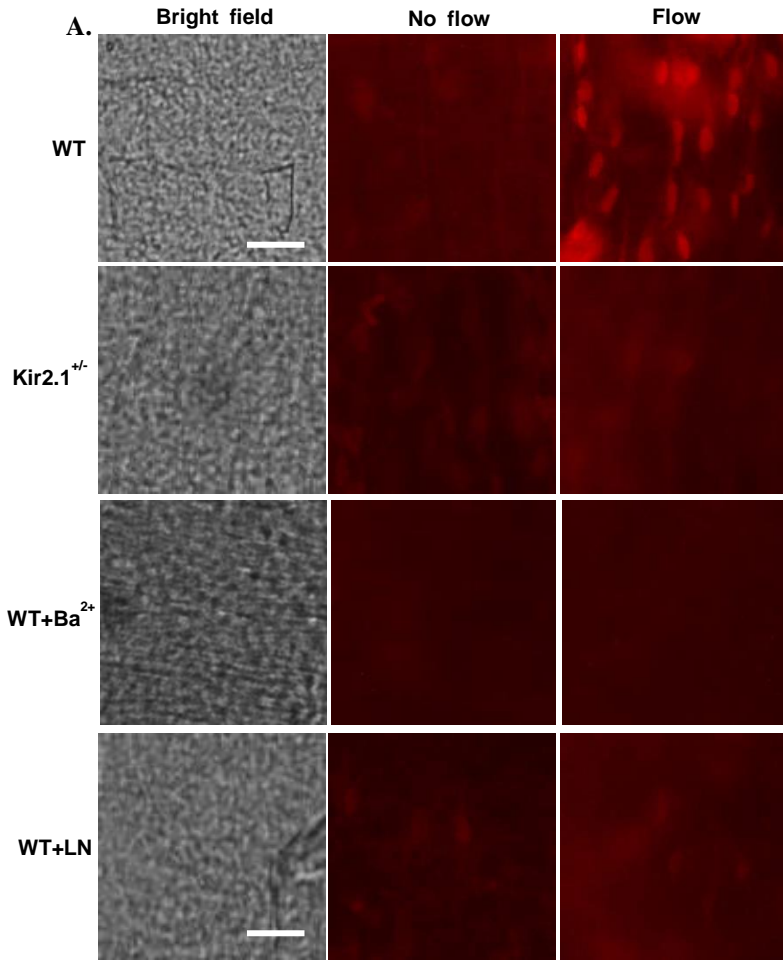


Figure 3-18 Kir2.1 controls flow-induced nitric oxide production. (A) Images of NO-specific fluorescence in response to flow in WT and Kir2.1<sup>+/-</sup> mesenteric arteries: left panels show the inner surface of the arteries in bright field, middle panels show NO-specific fluorescence stained by DAR4M in arteries not exposed to flow, right panels show NO-specific fluorescence in arteries exposed to flow generated by a pressure gradient of  $\Delta 60$  cm H<sub>2</sub>O for 30 min with or without Ba<sup>2+</sup> (30  $\mu$ M) or LNAME (100  $\mu$ M) (scale = 50  $\mu$ m). (B) Quantification of NO specific fluorescence in the same arteries normalized to “No flow” control (n=6 arteries per condition, \*p<0.05). (C) Images of NO specific fluorescence of endothelium denuded WT and Kir2.1<sup>+/-</sup> arteries maintained under static conditions (middle panels) or exposed to 30 min of flow (right panels) (n=4).

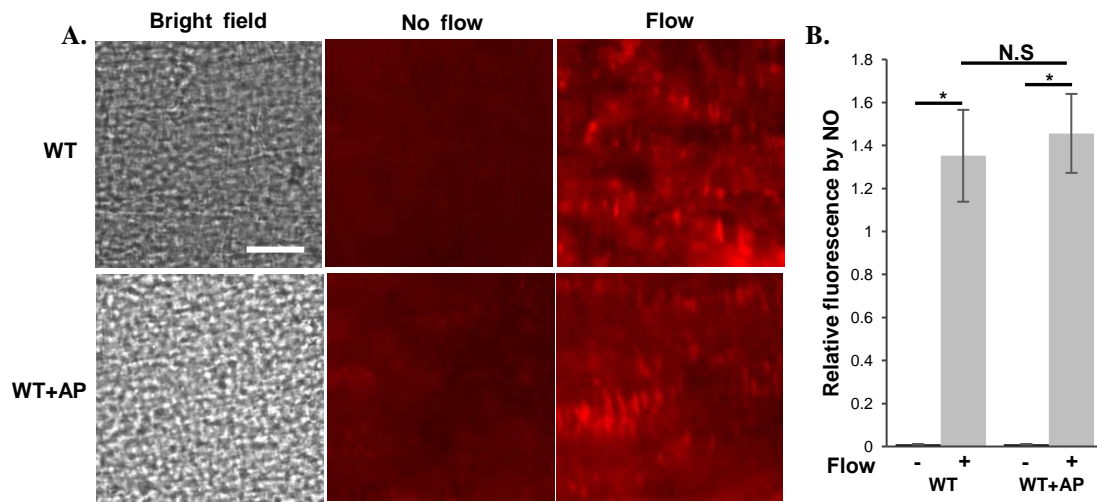


Figure 3-19 Flow-induced nitric oxide production is regulated by SK-independent pathway. (A) Images of NO specific fluorescence of WT arteries maintained under static conditions (middle panels) or exposed to 30 min of flow (right panels) with or without application of apamin (20 nM). (B) Quantification of NO specific fluorescence in the same arteries (n=5 arteries per condition, \*p<0.05).

of Kir2.1 reduces FIV in resistance arteries, which causes the increase of peripheral resistance. My next question in this study, thus, was if the reduced FIV in resistance arteries by the loss of Kir2.1 affects the increase of blood pressure. To address this question, mean arterial pressure (MAP) was measured in carotid arteries using carotid cannulation procedure in WT and Kir2.1<sup>+/-</sup> mice (Fig. 3-20 A). Compared to the MAP in WT mice (62 mm Hg), the MAP of Kir2.1<sup>+/-</sup> mice increased 20 mm Hg higher, which was also statistically significant. These experiments were performed on age-matched male mice and in the same range of body weights (Fig. 3-20 B). In order to know that the increase of the MAP is due to the increased peripheral resistance, the tail blood flow rates were measured from WT and Kir2.1<sup>+/-</sup> mice using volume-pressure recording tail-cuff measurement (Fig. 3-20 C), and the vascular resistance was calculated as a ratio of blood flow to mean blood pressure taken from the same animal (Fig. 3-20 D). Consistent with the increase in the blood pressure, tail blood flow rates were decreased significantly and the vascular resistance significantly increased in Kir2.1<sup>+/-</sup> mice. These results show that loss of FIV in Kir2.1 deficient mice causes higher peripheral vascular resistance, resulting in higher blood pressure.

Loss of Kir channel function is known to cause long-QT syndrome (Tristani-Firouzi *et al.*, 2002). Kir2.1<sup>+/-</sup> mouse model is a global genetic knock down mouse model. To determine if the global deficiency of Kir2.1 channels contributes to the increased blood pressure by affecting cardiac functions in Kir2.1<sup>+/-</sup> mouse model, I tested the cardiac functions in WT and Kir2.1<sup>+/-</sup> mice including stroke volume, heart rate, and cardiac output using echocardiogram.

These parameters were measured using an echocardiogram on lightly sedated mice (1.5%

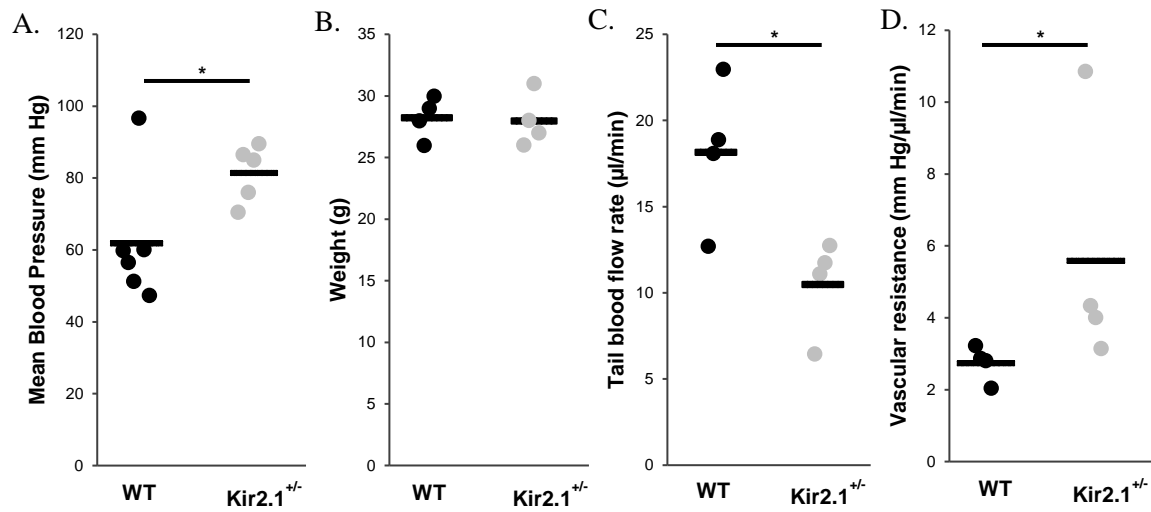


Figure 3-20 Kir2.1 impairment increases blood pressure and peripheral vascular resistance. (A) Mean arterial blood pressure measured in anesthetized mice via carotid arteries catheterization (each point represents one animal, WT, n=6, Kir2.1<sup>+/-</sup>, n=5, \*p<0.05) (B) Body weights of WT and Kir2.1<sup>+/-</sup> animals (n=4 per group). (C) Tail blood flow rates are determined by volumetric pressure recording tail-cuff. (n=4 per group, \*p<0.05) (D) Peripheral vascular resistance calculated from mean blood pressure divided by blood flow rate, measured by volumetric pressure recording tail-cuff (n=4 per group, \*p<0.05).

isoflurane). Typical left ventricular M-mode images of the echocardiogram for WT and Kir2.1<sup>+/-</sup> mice are shown in Figure 3-21 A and B. More specifically, the images show the oscillatory movement of the ventricular wall that occur during the cardiac cycle (i.e., systole and diastole), and the stroke volume is calculated based on the difference between the chamber volumes during diastole and systole. As shown in the representative left ventricular M-mode images, there was no significant difference observed in stroke volume between WT and Kir2.1 mice, and the heart rate of both WT and Kir2.1<sup>+/-</sup> mice was in the regular range of ~500 beats per minute (Fig. 3-21 C and D). Additionally, there was no cardiac output differences in both WT and Kir2.1<sup>+/-</sup> mice (Fig. 3-21 E). The echocardiogram results suggest that the increase of blood pressure in Kir2.1<sup>+/-</sup> mice is mainly due to the increase of peripheral vascular resistance, and the global deficiency of Kir2.1 does not affect the cardiac function in the Kir2.1<sup>+/-</sup> mouse model.

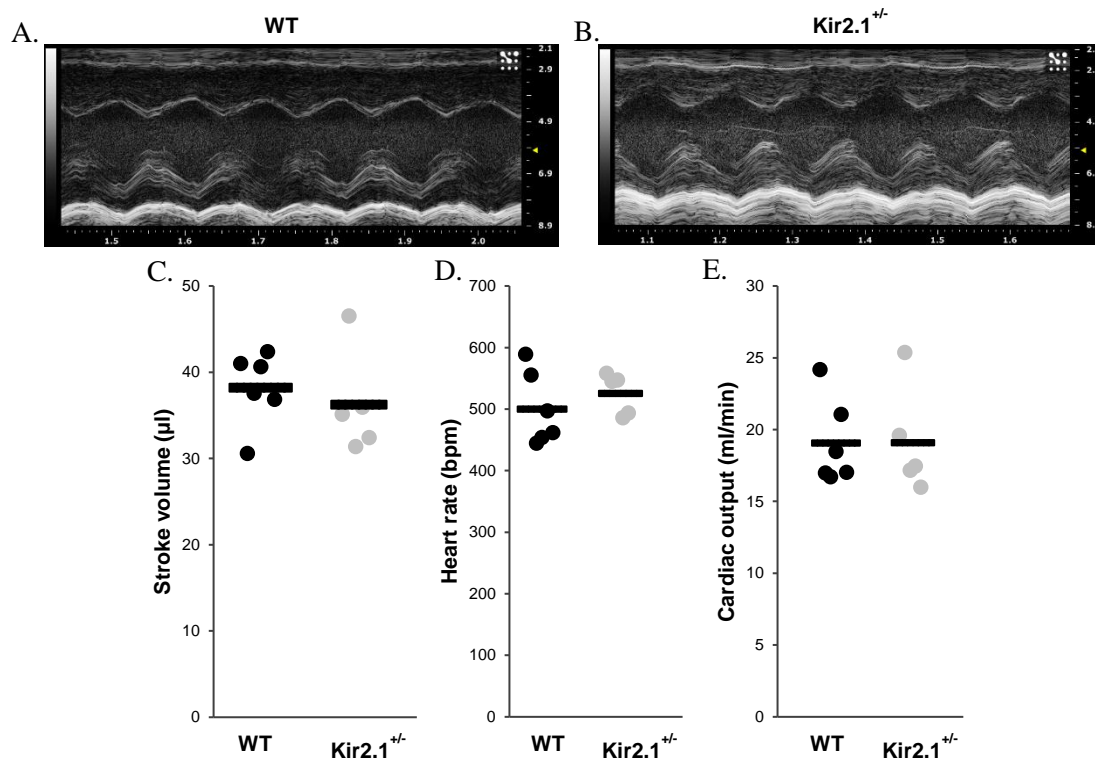


Figure 3-21 Cardiac function does not contribute to increased blood pressure in Kir2.1 deficient mice. (A) Representative M-mode echocardiogram of the left ventricle from WT mouse. (B) Representative M-mode echocardiogram of the left ventricle from Kir2.1<sup>+/-</sup> mouse. (C) Stroke volumes of WT and Kir2.1<sup>+/-</sup> mice are measured by M-mode echocardiogram from the parasternal short axis view. (WT, n=6, Kir2.1<sup>+/-</sup>, n=5) (D) Heart rates are measured during M-mode echocardiogram. (WT, n=6, Kir2.1<sup>+/-</sup>, n=5) (E) Cardiac outputs of WT and Kir2.1<sup>+/-</sup> mice are determined from stroke volume multiplied by heart rate. (WT, n=6, Kir2.1<sup>+/-</sup>, n=5)

### **3.4 Discussion**

In this study, I present the first specific evidence for the role of endothelial Kir channels in FIV of resistance arteries. My major findings of this study are: i) functionally expressed Kir channels in primary endothelial cells from resistance arteries show clear flow sensitivity, ii) Kir2.1 channels in Kir channels are essential for FIV of murine mesenteric arteries through NO production by eNOS and Akt phosphorylation, iii) genetic deficiency of Kir2.1 channels in mouse increases peripheral vascular resistance and blood pressure, iv) Kir and  $K_{Ca}$  act independently through two distinct NO-dependent and NO-independent pathway in FIV. These findings address that Kir channels play a major role in endothelium-dependent FIV and provide the first insights into the mechanism of this effect.

#### **3.4.1 Expression of Kir2 channels in microvascular endothelial cells**

The presence of Kir currents with  $Ba^{2+}$ -sensitivity in multiple subtypes of endothelial cells from different species were reported in multiple studies (Rusko *et al.*, 1992; Romanenko *et al.*, 2002; Crane *et al.*, 2003; Fang *et al.*, 2005b; Ledoux *et al.*, 2008). In this study, I present a molecular profile of Kir2 channels in mouse mesenteric endothelial cells. At the transcriptional level, I observed the expression of three subtypes of Kir2 channels in mesenteric endothelial cells, which are Kir2.1, Kir2.2, and Kir2.3; however, the expression level of Kir2.1 is several orders of magnitude higher than that of the other two channels. Expression of Kir2.1 is also confirmed on the translational level. Functionally, our lab show for the first time that primary mesenteric ECs express shear stress-sensitive Kir currents (Ahn *et al.*, 2017). These currents significantly reduced in mesenteric arterial ECs isolated

from Kir2.1<sup>+/-</sup> heterozygous mice. Based on these observations, Kir2.1 is the major functional Kir channel in mesenteric endothelium.

### **3.4.2 Consideration of the Kir2.1<sup>+/-</sup> mouse model**

Since the global knock out of Kir2.1 channels is lethal, and the mice die within a few hours after birth (Zaritsky *et al.*, 2000), I considered using a Kir2.1 heterozygous mouse model (Kir2.1<sup>+/-</sup>), which is fully viable for the life span same as WT mouse. I found that mesenteric arterial endothelial cells from Kir2.1<sup>+/-</sup> mice express significantly decreased levels of Kir2.1 channels on both transcriptional (~65% decreased) and translational (~50% decreased) levels, as well as functional currents (electrophysiological data ~50% decreased). The decreased Kir2.1 expression in Kir2.1<sup>+/-</sup> mice leads the increase (2-3 folds increase) in the expression of Kir2.2 and Kir2.3 channels; however, because the expression level of Kir2.2 and Kir2.3 channels is much lower than Kir2.1 channels, this increase does not compensate for the functional Kir channel currents. Interestingly, the decreased expression of Kir channels results in the decreased sensitivity to shear stress, but the basis of this decreased sensitivity to shear is unclear.

### **3.4.3 Role of endothelial Kir2.1 in flow-induced vasodilation**

In this study, I demonstrated that the loss of Kir2.1 channels expression with the corresponding reduction of flow-sensitive Kir currents results in a dramatic decrease in FIV of murine mesenteric arteries. It was known that Ba<sup>2+</sup> decreased flow-induced vasodilation in human brachial arteries, rabbit cerebral arteries, and rabbit facial veins

(Wellman & Bevan, 1995; Xie & Bevan, 1998; Dawes *et al.*, 2002). These observations suggested the role of Kir channels in FIV, but it was unclear whether endothelial Kir channels regulate FIV. To address the role of endothelial Kir channels in FIV, I tested Kir2.1 expression in smooth muscles of mouse mesenteric arteries. Consistent with previous studies (Crane *et al.*, 2003; Smith *et al.*, 2008), I observed that mouse mesenteric VSMCs do not express Kir2.1 channels, which allows me to take advantage isolating the effects of endothelial Kir2.1 channels on the vascular function in this resistance artery model. However, there is always a concern about the tissue specificity in the interpretation of the observed effects in a global knock out model. Due to this concern, I provided several lines of evidence to support the conclusion that the observed effects should be attributed to the lack of Kir in endothelial cells. First, endothelium-denuded arteries maintain their full reactivity in response to SNP, an NO donor, an assay that is typically used to ascertain the smooth muscle reactivity to NO (Ignarro & Kadowitz, 1985). Additionally, whereas the expression of Kir channels in VSMCs is shown to be tissue specific, it was reported in previous studies that Kir2.1 channels was not detected in VSMCs of murine mesenteric arteries (Crane *et al.*, 2003; Jackson, 2005; Smith *et al.*, 2008; Dunn & Nelson, 2010). Consistent with these studies, I also show in this study that no detectable Kir2.1 channel expresses in mouse mesenteric VSMCs. However, there is a possibility that other subtypes of Kir2 channels might be expressed in mesenteric VSMCs and contribute to FIV via an NO-independent mechanism; thus, I tested K<sup>+</sup>-induced vasodilation to exclude this possibility. The rationale of this approach is that Kir2 channels in VSMCs may contribute to FIV through NO-independent K<sup>+</sup>-induced vasodilation due to the Kir channel sensitivity to extracellular K<sup>+</sup>, which is elevated due to

the K<sup>+</sup> efflux from adjacent endothelial cells responded to flow (Quayle *et al.*, 1993; Edwards *et al.*, 1998; Burns *et al.*, 2004; Filosa *et al.*, 2006). Alternatively, K<sup>+</sup>-induced vasodilation may also be mediated by Na<sup>+</sup>/K<sup>+</sup>-ATPase (Burns *et al.*, 2004). In order to address this concern, extracellular K<sup>+</sup>-induced vasodilation was tested in endothelium-denuded mesenteric arteries. As expected, increase up to 20 mM of extracellular K<sup>+</sup> resulted in a vasodilatory response, whereas extracellular K<sup>+</sup> concentration higher than 20 mM caused the vasoconstriction, which causes the depolarization of smooth muscle cells triggering constriction. My data show, however, the K<sup>+</sup>-induced vasodilation in these denuded arteries is sensitive to ouabain, but not Ba<sup>2+</sup>. These results indicate that the vasodilation of endothelium-denuded mesenteric arteries by extracellular K<sup>+</sup> should be attributed to the Na<sup>+</sup>/K<sup>+</sup>-ATPase rather than Kir2 channels. In contrast, as expected, I observed the contribution of Kir2 channels of K<sup>+</sup>-induced vasodilation in endothelium denuded cerebral arteries from the same mouse. My data show, therefore, there is tissue specific differences in smooth muscles, which regulate vasodilatory mechanisms differently by tissue functions. Most importantly, by showing the rescued FIV in Kir2.1<sup>+/-</sup> mesenteric arteries with the EC-specific overexpression of WT Kir2.1 channels, I provide compelling evidence for the major role of endothelial Kir2.1 in the mouse mesenteric arterial FIV.

#### **3.4.4 Endothelial Kir2.1 channels control FIV by regulating Akt/eNOS signaling and NO generation**

Previous study suggested that endothelial K<sup>+</sup> channel activation may act as endothelium-derived hyperpolarizing factor (EDHF), which is defined as NO-independent and

cyclooxygenase (COX)-independent mechanism, responsible for a vasodilation observed when both NO synthase and COX are inhibited (Brandes *et al.*, 2000). This mechanism is well-established for  $K_{Ca}$  channels in earlier studies that demonstrate almost complete loss of EDHF-mediated vasodilation in carotid and cremaster arteries by blocking or using genetically knock out mouse models of small and intermediate-conductance  $K_{Ca}$  (SK and IK) channels (Miura *et al.*, 2001; Brahler *et al.*, 2009; Wölfle *et al.*, 2009). Interestingly, it was also reported that IK channels dominantly regulate acetylcholine-induced EDHF-mediated vasodilation (Brahler *et al.*, 2009; Wölfle *et al.*, 2009), whereas SK channels are responsible for the flow-induced EDHF-mediated vasodilation (Brahler *et al.*, 2009). However, my data demonstrates that endothelial Kir2 channels regulate FIV by a different mechanism; there was no changes in FIV with the combination of eNOS inhibitor and either blocking of Kir2 channels by  $Ba^{2+}$  in WT mice or the genetic loss of Kir2.1 expression in Kir2.1<sup>+/-</sup> mice, which shows that Kir2 channels have no effect on NO-dependent FIV component. Consistent with these data, I also demonstrate directly that flow-induced NO generation is abolished in mesenteric arteries from Kir2.1<sup>+/-</sup> mice. Endothelium denudation of the arteries, as expected, eliminates even residual NO signals in both WT and Kir2.1<sup>+/-</sup> arteries because eNOS, the major NO synthase in FIV, is expressed selectively in endothelial cells. Taken together, these data indicate that endothelial Kir2 channels regulate FIV by regulating endothelial NO generation.

In terms of the molecular mechanism, I show that impairment of Kir2.1 results in the loss of flow-induced phosphorylation of eNOS and Akt in mesenteric ECs, and WT Kir2.1 overexpression in Kir2.1-deficient ECs fully rescued the flow-induced phosphorylation of these enzymes. Additionally, consistent with previous studies (Fleming *et al.*, 1998;

Dimmeler *et al.*, 1999), flow-induced eNOS phosphorylation was mainly mediated by Akt phosphorylation. Blocking of Akt activation abrogated the rescue effect by overexpressing Kir2.1 channels. Therefore, these data indicated that Kir2.1 channels regulate flow-induced Akt phosphorylation resulting in eNOS activation. However, it is still unclear what the mechanistic link between Kir channels and Akt is. Earlier studies suggested that K<sup>+</sup> channels regulate Ca<sup>2+</sup> influx into the cells and the cellular functions are regulated by influx Ca<sup>2+</sup> (Adams *et al.*, 1989; Luckhoff & Busse, 1990; Lin *et al.*, 1993). However, there were other studies, which showed that FIV is Ca<sup>2+</sup>-independent (Stepp *et al.*, 1999), and that flow-induced eNOS activation is Akt-dependent but Ca<sup>2+</sup>-independent (Dimmeler *et al.*, 1999). It is also reported that not only flow-induced eNOS activation, but also receptor-mediated eNOS activation has a component that Akt-dependent and Ca<sup>2+</sup> independent, which is supporting the Ca<sup>2+</sup>-independent Akt activation (Fleming *et al.*, 1999; Takahashi & Mendelsohn, 2003). Based on these previous studies and my observations described above, I suggest that Kir channels regulate eNOS through Akt but not through Ca<sup>2+</sup>. However, flow-induced Ca<sup>2+</sup> influx should be checked in future studies to clarify this issue. Additionally, as mentioned above, the mechanism by which Kir channels regulate Akt should also be elucidated in future studies. Although previous study by Sonkusare *et al.* suggested that the role of Kir2.1 is a hyperpolarization booster, which is downstream of SK channels in Ca<sup>2+</sup>-mediated vasodilation (Sonkusare *et al.*, 2016), my data clearly show that the NO-dependent components of FIV is regulated by Kir2 and separate from SK-dependent components. This conclusion is consistent with earlier observations that NO-dependent regulation of blood pressure is still existed in SK channel knock out mouse model (Kohler & Ruth, 2010). Importantly, my data that blocking both Kir2 and SK

channels totally abolished FIV in murine mesenteric arteries indicates that Kir2 and SK regulate FIV in two parallel pathways as major contributors, which are fully responsible to flow. Although the mechanism for differential effects of Kir2.1 and SK channels on FIV is unclear, one possibility is that there are differential intracellular distributions of these channels. Earlier studies in our lab showed that Kir2.1 is located in cholesterol-rich membrane domains (Tikku *et al.*, 2007) and in caveolae, where Kir2.1 channels interact with caveolin-1 (Han *et al.*, 2014). It is well-established in previous studies that eNOS interacts caveolin-1 (Garcia-Cardena *et al.*, 1997; Ghosh *et al.*, 1998; Gratton *et al.*, 2000), which implies the possible geometrical regulation of Kir2.1 channels on eNOS activation; however, SK channels were also reported to be in caveolae (Absi *et al.*, 2007; Goedicke-Fritz *et al.*, 2015). Therefore, it is difficult to explain by location only for the functional difference between Kir2.1 and SK channels in eNOS activation. Further studies are needed to understand how different types of K<sup>+</sup> channels regulate FIV by distinct mechanisms.

#### **3.4.5 Role of Kir2.1 channels in regulation of blood pressure and vascular resistance**

My observation that Kir2.1 impairment causes significant mean arterial blood pressure elevation up to 20 mm Hg indicates that Kir2 channels also play a major role in control of vascular tone in vivo. Based on previous research, impairment of K<sub>Ca</sub> also causes the elevation of blood pressure (Brahler *et al.*, 2009). My finding that Kir2 and SK contribute almost equally to FIV is able to explain either Kir2 or K<sub>Ca</sub> affects to the elevation of blood pressure. Interestingly, whereas Kir2 channels play a key role in FIV, we saw no Ba<sup>2+</sup>

effect on the baseline diameters of the mesenteric arteries. Therefore, it implies that other mechanisms are predominantly involved to the resting tone, as should be investigated in the future.

Moreover, since my finding shows that the loss of Kir2.1 channels results in significant impairment of FIV in resistance arteries and since it is known that resistance arteries are a major source of peripheral vascular resistance in the circulation (Mayet & Hughes, 2003), I hypothesized that increased vascular resistance in vivo causes the elevation of the blood pressure in Kir2.1 deficient mice. My data address this hypothesis that Kir2.1<sup>+/-</sup> mice have significantly decreased flow rate resulting in increased vascular resistance by using volumetric pressure recording tail-cuff measurement. Furthermore, since the two major components that contribute to mean arterial pressure (MAP) are cardiac output (CO) and peripheral vascular resistance (PVR) ( $MAP = CO \times PVR$ ) (Mayet & Hughes, 2003), I also tested if Kir2.1 deficiency in Kir2.1<sup>+/-</sup> mice may result in an increase in the stroke volume and/or heart rate resulting in increased cardiac output because Kir channels are known to function in cardiomyocytes as regulating repolarization and maintaining resting membrane potential. My results show, however, that there is no difference in either stroke volume or heart rates between WT and Kir2.1<sup>+/-</sup> mice and that the physiological cardiac parameters are not changed in Kir2.1<sup>+/-</sup> mice. Taken together, these observations indicate that Kir2.1 deficiency results in increased blood pressure via increased peripheral vascular resistance rather than cardiac functions.

## Reference

- Absi M, Burnham MP, Weston AH, Harno E, Rogers M & Edwards G. (2007). Effects of methyl beta-cyclodextrin on EDHF responses in pig and rat arteries; association between SK(Ca) channels and caveolin-rich domains. *Br J Pharmacol*.
- Adams DJ, Barakeh J, Laskey R & Van Breemen C. (1989). Ion channels and regulation of intracellular calcium in vascular endothelial cells. *FASEB J* **3**, 2389-2400.
- Ahn SJ, Fancher IS, Bian JT, Zhang CX, Schwab S, Gaffin R, Phillips SA & Levitan I. (2017). Inwardly rectifying K<sup>+</sup> channels are major contributors to flow-induced vasodilatation in resistance arteries. *J Physiol* **595**, 2339-2364.
- Arfors KE & Bergqvist D. (1974). Influence of blood flow velocity on experimental haemostatic plug formation. *Thromb Res* **4**, 447-461.
- Brahler S, Kaistha A, Schmidt VJ, Wolfle SE, Busch C, Kaistha BP, Kacik M, Hasenau AL, Grgic I, Si H, Bond CT, Adelman JP, Wulff H, de Wit C, Hoyer J & Kohler R. (2009). Genetic deficit of SK3 and IK1 channels disrupts the endothelium-derived hyperpolarizing factor vasodilator pathway and causes hypertension. *Circulation* **119**, 2323-2332.
- Brandes RP, Schmitz-Winnenthal FH, Feletou M, Godecke A, Huang PL, Vanhoutte PM, Fleming I & Busse R. (2000). An endothelium-derived hyperpolarizing factor distinct from NO and prostacyclin is a major endothelium-dependent vasodilator in resistance vessels of wild-type and endothelial NO synthase knockout mice. *Proc Natl Acad Sci U S A* **97**, 9747-9752.
- Burns WR, Cohen KD & Jackson WF. (2004). K<sup>+</sup>-induced dilation of hamster cremasteric arterioles involves both the Na<sup>+</sup>/K<sup>+</sup>-ATPase and inward-rectifier K<sup>+</sup> channels. *Microcirculation* **11**, 279-293.
- Crane GJ, Walker SD, Dora KA & Garland CJ. (2003). Evidence for a Differential Cellular Distribution of Inward Rectifier K Channels in the Rat Isolated Mesenteric Artery. *Journal of Vascular Research* **40**, 159.

- Dai G, Kaazempur-Mofrad MR, Natarajan S, Zhang Y, Vaughn S, Blackman BR, Kamm RD, Garcia-Cardena G & Gimbrone MA, Jr. (2004). Distinct endothelial phenotypes evoked by arterial waveforms derived from atherosclerosis-susceptible and -resistant regions of human vasculature. *Proc Natl Acad Sci U S A* **101**, 14871-14876.
- Dawes M, Sieniawska C, Delves T, Dwivedi R, Chowienczyk PJ & Ritter JM. (2002). Barium reduces resting blood flow and inhibits potassium-induced vasodilation in the human forearm. *Circulation* **105**, 1323-1328.
- Dimmeler S, Fleming I, Fisslthaler B, Hermann C, Busse R & Zeiher AM. (1999). Activation of nitric oxide synthase in endothelial cells by Akt-dependent phosphorylation. *Nature* **399**, 601-605.
- Dunn KM & Nelson MT. (2010). Potassium channels and neurovascular coupling. *Circ J* **74**, 608-616.
- Edwards G, Dora KA, Gardener MJ, Garland CJ & Weston AH. (1998). K<sup>+</sup> is an endothelium-derived hyperpolarizing factor in rat arteries. *Nature* **396**, 269-272.
- Fang Y, Mohler ER, 3rd, Hsieh E, Osman H, Hashemi SM, Davies PF, Rothblat GH, Wilensky RL & Levitan I. (2006). Hypercholesterolemia suppresses inwardly rectifying K<sup>+</sup> channels in aortic endothelium in vitro and in vivo. *Circ Res* **98**, 1064-1071.
- Fang Y, Romanenko VG, Davies PF & Levitan I. (2005a). Flow sensitivity of inwardly-rectifying K channels in human aortic endothelium. In *3d IASTED International Conference on Biomechanics*, pp. 163-167. ACTA Press, Benidorm, Spain.
- Fang Y, Schram G, Romanenko VG, Shi C, Conti L, Vandenberg CA, Davies PF, Nattel S & Levitan I. (2005b). Functional expression of Kir2.x in human aortic endothelial cells: the dominant role of Kir2.2. *Am J Physiol Cell Physiol* **289**, C1134-1144.
- Filosa JA, Bonev AD, Straub SV, Meredith AL, Wilkerson MK, Aldrich RW & Nelson MT. (2006). Local potassium signaling couples neuronal activity to vasodilation in the brain. *Nat Neurosci* **9**, 1397.

- Fisslthaler, Dimmeler, Hermann, Busse & Fleming. (2000). Phosphorylation and activation of the endothelial nitric oxide synthase by fluid shear stress. *Acta Physiologica Scandinavica* **168**, 81-88.
- Fleming I, Bauersachs J, Fisslthaler B & Busse R. (1998). Ca<sup>2+</sup>-Independent Activation of the Endothelial Nitric Oxide Synthase in Response to Tyrosine Phosphatase Inhibitors and Fluid Shear Stress. *Circ Res* **82**, 686-695.
- Fleming I, Bauersachs J, Schafer A, Scholz D, Aldershvile J & Busse R. (1999). Isometric contraction induces the Ca<sup>2+</sup>-independent activation of the endothelial nitric oxide synthase. *Proc Natl Acad Sci U S A* **96**, 1123-1128.
- Garcia-Cardena G, Martasek P, Masters BS, Skidd PM, Couet J, Li S, Lisanti MP & Sessa WC. (1997). Dissecting the interaction between nitric oxide synthase (NOS) and caveolin. Functional significance of the nos caveolin binding domain in vivo. *J Biol Chem* **272**, 25437-25440.
- Ghosh S, Gachhui R, Crooks C, Wu C, Lisanti MP & Stuehr DJ. (1998). Interaction between caveolin-1 and the reductase domain of endothelial nitric-oxide synthase. Consequences for catalysis. *J Biol Chem* **273**, 22267-22271.
- Goedicke-Fritz S, Kaistha A, Kacik M, Markert S, Hofmeister A, Busch C, Banfer S, Jacob R, Grgic I & Hoyer J. (2015). Evidence for functional and dynamic microcompartmentation of Cav-1/TRPV4/K(Ca) in caveolae of endothelial cells. *Eur J Cell Biol* **94**, 391-400.
- Goslowski M, Piano MR, Bian J-T, Church EC, Szczurek M & Phillips SA. (2013). Binge Drinking Impairs Vascular Function in Young Adults. *Journal of the American College of Cardiology* **62**, 201.
- Gratton JP, Fontana J, O'Connor DS, Garcia-Cardena G, McCabe TJ & Sessa WC. (2000). Reconstitution of an endothelial nitric-oxide synthase (eNOS), hsp90, and caveolin-1 complex in vitro. Evidence that hsp90 facilitates calmodulin stimulated displacement of eNOS from caveolin-1. *J Biol Chem* **275**, 22268-22272.
- Grizelj I, Cavka A, Bian JT, Szczurek M, Robinson A, Shinde S, Nguyen V, Braunschweig C, Wang E,

- Drenjancevic I & Phillips SA. (2015). Reduced flow-and acetylcholine-induced dilations in visceral compared to subcutaneous adipose arterioles in human morbid obesity. *Microcirculation* **22**, 44-53.
- Han H, Rosenhouse-Dantsker A, Gnanasambandam R, Epshtein Y, Chen Z, Sachs F, Minshall RD & Levitan I. (2014). Silencing of Kir2 channels by caveolin-1: cross-talk with cholesterol. . *J of Physiology* **592**, 4025-4038.
- Hoger JH, Ilyin VI, Forsyth S & Hoger A. (2002). Shear stress regulates the endothelial Kir2.1 ion channel. *Proc Natl Acad Sci U S A* **99**, 7780-7785.
- Ignarro LJ & Kadowitz PJ. (1985). The pharmacological and physiological role of cyclic GMP in vascular smooth muscle relaxation. *Annu Rev Pharmacol Toxicol* **25**, 171-191.
- Jackson WF. (2005). Potassium channels in the peripheral microcirculation. *Microcirculation* **12**, 113-127.
- Kohler R & Ruth P. (2010). Endothelial dysfunction and blood pressure alterations in K<sup>+</sup>-channel transgenic mice. *Pflügers Archiv - European Journal of Physiology* **459**, 969-976.
- Ledoux J, Bonev AD & Nelson MT. (2008). Ca<sup>2+</sup>-activated K<sup>+</sup> Channels in Murine Endothelial Cells: Block by Intracellular Calcium and Magnesium. *The Journal of General Physiology* **131**, 125-135.
- Lin PJ, Pearson PJ & Chang CH. (1993). Endothelium-derived contracting factors. *Changeng Yi Xue Za Zhi* **16**, 140-153.
- Liu G, Vogel SM, Gao X, Javaid K, Hu G, Danilov SM, Malik AB & Minshall RD. (2011). Src phosphorylation of endothelial cell surface intercellular adhesion molecule-1 mediates neutrophil adhesion and contributes to the mechanism of lung inflammation. *Arterioscler Thromb Vasc Biol* **31**, 1342-1350.
- Liu GX, Derst C, Schlichthorl G, Heinen S, Seeböhm G, Bruggemann A, Kummer W, Veh RW, Daut J & Preisig-Müller R. (2001). Comparison of cloned Kir2 channels with native inward rectifier K<sup>+</sup> channels from guinea-pig cardiomyocytes. *J Physiol* **532**, 115-126.

- Liu SM, Cogny A, Kockx M, Dean RT, Gaus K, Jessup W & Kritharides L. (2003). Cyclodextrins differentially mobilize free and esterified cholesterol from primary human foam cell macrophages. *J Lipid Res* **44**, 1156-1166.
- Luckhoff A & Busse R. (1990). Calcium influx into endothelial cells and formation of endothelium-derived relaxing factor is controlled by the membrane potential. *Pflugers Archiv : European journal of physiology* **416**, 305-311.
- Mayet J & Hughes A. (2003). Cardiac and vascular pathophysiology in hypertension. *Heart* **89**, 1104-1109.
- Messerli FH. (1982). Cardiovascular effects of obesity and hypertension. *Lancet* **1**, 1165-1168.
- Milkau M, Kohler R & de Wit C. (2010). Crucial importance of the endothelial K<sup>+</sup> channel SK3 and connexin40 in arteriolar dilations during skeletal muscle contraction. *Faseb J* **24**, 3572-3579.
- Miura H, Wachtel RE, Liu Y, Loberiza FR, Jr., Saito T, Miura M & Gutterman DD. (2001). Flow-Induced Dilation of Human Coronary Arterioles : Important Role of Ca<sup>2+</sup>-Activated K<sup>+</sup> Channels. *Circulation* **103**, 1992-1998.
- Olesen SP, Clapham DE & Davies PF. (1988). Haemodynamic shear stress activates a K<sup>+</sup> current in vascular endothelial cells. *Nature* **331**, 168-170.
- Phillips SA, Hatoum OA & Gutterman DD. (2007). The mechanism of flow-induced dilation in human adipose arterioles involves hydrogen peroxide during CAD. *Am J Physiol Heart Circ Physiol* **292**, H93-100.
- Pistner A, Belmonte S, Coulthard T & Blaxall B. (2010). Murine echocardiography and ultrasound imaging. *J Vis Exp*.
- Quayle JM, McCarron JG, Brayden JE & Nelson MT. (1993). Inward rectifier K<sup>+</sup> currents in smooth muscle cells from rat resistance-sized cerebral arteries. *Am J Physiol* **265**, C1363-1370.

- Rindler TN, Lasko VM, Nieman ML, Okada M, Lorenz JN & Lingrel JB. (2011). Knockout of the Na,K-ATPase alpha2-isoform in cardiac myocytes delays pressure overload-induced cardiac dysfunction. *Am J Physiol Heart Circ Physiol* **304**, H1147-1158.
- Romanenko VG, Rothblat GH & Levitan I. (2002). Modulation of endothelial inward rectifier K<sup>+</sup> current by optical isomers of cholesterol. *Biophys J* **83**, 3211-3222.
- Rusko J, Tanzi F, van Breemen C & Adams DJ. (1992). Calcium-activated potassium channels in native endothelial cells from rabbit aorta: conductance, Ca<sup>2+</sup> sensitivity and block. *J Physiol* **455**, 601-621.
- Schram G, Pourrier M, Melnyk P & Nattel S. (2002). Differential distribution of cardiac ion channel expression as a basis for regional specialization in electrical function. *Circ Res* **90**, 939-950.
- Sharma H, Pathan RA, Kumar V, Javed S & Bhandari U. (2011). Anti-apoptotic potential of rosuvastatin pretreatment in murine model of cardiomyopathy. *Int J Cardiol* **150**, 193-200.
- Smith PD, Brett SE, Luykenaar KD, Sandow SL, Marrelli SP, Vigmond EJ & Welsh DG. (2008). KIR channels function as electrical amplifiers in rat vascular smooth muscle. *J Physiol* **586**, 1147-1160.
- Sonkusare SK, Dalsgaard T, Bonev AD & Nelson MT. (2016). Inward rectifier potassium (Kir2.1) channels as end-stage boosters of endothelium-dependent vasodilators. *J Physiol* **594**, 3271-3285.
- Stepp DW, Nishikawa Y & Chilian WM. (1999). Regulation of shear stress in the canine coronary microcirculation. *Circulation* **100**, 1555-1561.
- Takahashi S & Mendelsohn ME. (2003). Calmodulin-dependent and -independent activation of endothelial nitric-oxide synthase by heat shock protein 90. *J Biol Chem* **278**, 9339-9344.
- Tikku S, Epshtein Y, Collins H, Travis AJ, Rothblat GH & Levitan I. (2007). Relationship between Kir2.1/Kir2.3 activity and their distribution between cholesterol-rich and cholesterol-poor membrane domains. *Am J Physiol Cell Physiol* **293**, C440-450.

- Tristani-Firouzi M, Jensen JL, Donaldson MR, Sansone V, Meola G, Hahn A, Bendahhou S, Kwiecinski H, Fidzianska A, Plaster N, Fu YH, Ptacek LJ & Tawil R. (2002). Functional and clinical characterization of KCNJ2 mutations associated with LQT7 (Andersen syndrome). *J Clin Invest* **110**, 381-388.
- Wölfle SE, Schmidt VJ, Hoyer J, Köhler R & C. dW. (2009). Prominent role of KCa3.1 in endothelium-derived hyperpolarizing factor-type dilations and conducted responses in the microcirculation in vivo. *Cardiovasc Res* **82**, 476-483.
- Wellman GC & Bevan JA. (1995). Barium inhibits the endothelium-dependent component of flow but not acetylcholine-induced relaxation in isolated rabbit cerebral arteries. *J Pharmacol Exp Ther* **274**, 47-53.
- Wu C, Huang R-T, Kuo C-H, Kumar S, Kim CW, Lin Y-C, Chen Y-J, Birukova A, Birukov KG, Dulin NO, Civelek M, Lusic AJ, Loyer X, Tedgui A, Dai G, Jo H & Fang Y. (2015). Mechanosensitive PPAP2B Regulates Endothelial Responses to Atherorelevant Hemodynamic Forces. *Circulation Research* **117**, e41-e53.
- Wulff H & Köhler R. (2013). Endothelial small-conductance and intermediate-conductance KCa channels: an update on their pharmacology and usefulness as cardiovascular targets. *J Cardiovasc Pharmacol* **61**, 102-112.
- Xie H & Bevan JA. (1998). Barium and 4-aminopyridine inhibit flow-initiated endothelium-independent relaxation. *J Vasc Res* **35**, 428-436.
- Zaritsky JJ, Eckman DM, Wellman GC, Nelson MT & Schwarz TL. (2000). Targeted disruption of Kir2.1 and Kir2.2 genes reveals the essential role of the inwardly rectifying K(+) current in K(+)-mediated vasodilation. *Circ Res* **87**, 160-166.

## **Chapter 4. Inwardly rectifying K<sup>+</sup> channels plays a key role to agonist-induced vasodilation in resistance arteries**

### **4.1 Introduction**

Endothelium-dependent vasodilation is not only mediated by flow but also mediated by vasoactive factors, such as bradykinin, acetylcholine, and sphingosine-1-phosphate, which bind to their specific receptors (kinin receptor, cholinergic muscarinic receptor, sphingosine-1-phosphate receptor, respectively), which induce Ca<sup>2+</sup> influx into the endothelial cells, which activate Ca<sup>2+</sup>-activated K<sup>+</sup> (K<sub>Ca</sub>) channels (Sun & Ye, 2012). These receptors are known to be G protein-coupled receptors, and they are also known to activate Akt phosphorylation through the activation of phosphoinositide 3-kinase (PI3K) resulting in endothelial nitric oxide synthase (eNOS) activation (Sessa, 2004).

Bradykinin is a type of kinins and endogenous vasoactive peptides (Malowney *et al.*, 2015). Bradykinin is known as an important vasoactive factor in many types of vascular beds, such as coronary and resistance arteries (Groves *et al.*, 1995). When bradykinin binds to the receptor, the cytosolic Ca<sup>2+</sup> concentration increases leading the activation of K<sub>Ca</sub> channels. Activated endothelial K<sub>Ca</sub> channels activate vascular smooth muscle Kir channels and Na<sup>+</sup>-K<sup>+</sup> ATPase, which result in hyperpolarization of vasodilation (Hangaard *et al.*, 2015).

Bradykinin is also known to activate eNOS through Akt activation. Binding of bradykinin to the receptor induces the G protein-coupled receptor mediated PI3K activation, which phosphorylates Akt resulting in eNOS activation by the phosphorylation of S1177 residue

of eNOS. In the Chapter 3, I presented the data showing that endothelial Kir channels regulate flow-induced vasodilation through eNOS activation by regulating Akt phosphorylation. Previous studies showed that bradykinin-induced vasodilation is also regulated by eNOS activation via Akt phosphorylation (Ndiaye *et al.*, 2004; Sessa, 2004); therefore, I hypothesized that endothelial Kir channels may also regulate NO production in the receptor-mediated vasodilation. To address my hypothesis, I tested: i) bradykinin-induced vasodilation in mesenteric arteries from WT and Kir2.1<sup>+/-</sup> mice, ii) acetylcholine mediated vasodilation in the same arteries, and iii) bradykinin-induced NO production from endothelial cells isolated from WT and Kir2.1<sup>+/-</sup> mesenteric arteries by real-time electrical NO detection.

## 4.2 Methods

### 4.2.1 Receptor-mediated vasodilation measurement

Resistance arteries (between 75-150  $\mu\text{m}$ ) from mesenteric arteriole beds were isolated and cannulated to glass micropipettes filled with Krebs solution (pH 7.40). Both ends of the cannulated vessel were connected to two separate Krebs reservoirs, and the vessel was stabilized at 60 cm H<sub>2</sub>O intraluminal pressure by elevating two Krebs-containing reservoirs 60 cm above the organ chamber. The reservoirs and the vessel lumen generate an open circuit. Vessels are equilibrated in this way for 30 minutes. After the 30-min equilibration period, vessels were constricted (up to 50% of baseline diameter) with endothelin (ET-1) (120 to 160 pM final concentration), and receptor-mediated vasodilation was determined by exposing the vessels to incremental dosages of 1 nM, 10 nM, 100 nM, 1  $\mu\text{M}$ , 10  $\mu\text{M}$ , and 100  $\mu\text{M}$  for acetylcholine stimulation, and 10 pM, 100 pM, 1 nM, 10 nM, 100 nM, and 1  $\mu\text{M}$  for bradykinin stimulation. Intraluminal pressure is maintained at 60 cm H<sub>2</sub>O during the experiment. Receptor-mediated vasodilation was determined in the presence and absence of external perfusion of BaCl<sub>2</sub> (30  $\mu\text{M}$ ), L-NAME (100  $\mu\text{M}$ ), apamin (20 nM), and combination of BaCl<sub>2</sub> and L-NAME, and BaCl<sub>2</sub> and apamin. All inhibitors and blockers were incubated with the arteries for 30 mins before the application of flow. Papaverine (100  $\mu\text{M}$ ) was added during exposure at the maximal dosage (at 100  $\mu\text{M}$  for acetylcholine and at 1  $\mu\text{M}$  for bradykinin) to test maximal endothelium-independent dilation. Resistance arteries were monitored continuously, and internal diameters were measured at the maximal diameter after each pressure gradient applied. Preparations were visualized with video cameras and monitors (model VIA-100, Boeckeler).

#### **4.2.2 Receptor-mediated NO production electrical measurement**

Mouse mesenteric arterial endothelial cells were isolated as described in Chapter 2. Briefly, mouse mesenteric arteries were extracted from 3 mice and incubated in digestion solution for 1 hour in 37 °C. Digested cells were incubated with magnetic beads conjugated anti-mouse CD31 IgG for endothelial cell purification. Purified ECs were cultured to passage 5 to use. Isolated ECs were seeded in a 24-well plate with  $2 \times 10^5$  cells.

Receptor-mediated NO production were measured using a porphyrinic NO electrode as described previously (Maniatis *et al.*, 2006). Briefly, the electrode was created by coating carbon fibers with a metalloporphyrinic conductive polymer and subsequently sealed with Nafion. Each electrode is calibrated using a stock solution of NO-saturated water. NO diffuses into the Nafion membrane where it is oxidized to the nitrosyl ion. The electron is transferred to the porphyrin of the conductive polymer and proceeds along the copper wire to a detector. The NO electrode is placed onto the surface of an endothelial cell monolayer and 2 additional electrodes are added to the solution to generate a 650-mV potential. The system was coupled with a FAS1 femtostat and a personal computer with electrochemical software (Gamry Instruments, Warminster, Pa). Electrode current, which is proportional to NO concentration, is measured as a function of time. The cell culture medium temperature is kept at 37°C. ECs from WT and Kir2.1<sup>+/-</sup> mice were treated with 100 nM BK or 100 μM Ach, and produced NO were measured. Pharmaceutical Kir2.1 inhibitor, Ba<sup>2+</sup> (30 μM), and Akt inhibitor, MK2202, were incubated for 30 minutes in 37 °C, and NO production measured with BK (100 nM).

**Rescue experiment:** Kir2.1<sup>+/-</sup> ECs were incubated with adenoviral vector of WT-Kir2.1 for 24 hours in 37 °C. ECs were stimulated with BK (100 nM) and NO was measured.

Empty viral vector transfected Kir2.1<sup>+/-</sup> ECs were used for control. Rescued Ba<sup>2+</sup>-sensitivity was tested with Ba<sup>2+</sup> (30 μM).

## 4.3 Results

### **4.3.1 Role of Kir2.1 in receptor-mediated vasodilation**

My first question in this study was whether Kir2.1 channels also regulate the receptor mediated vasodilation; hence, I tested bradykinin-induced vasodilation in mesenteric arteries from WT and Kir2.1<sup>+/-</sup> mice. As expected, WT mesenteric arteries dilated respond to bradykinin dose-dependently (Fig. 4-1 A, B, and C), whereas Kir2.1<sup>+/-</sup> mesenteric arteries showed significantly reduced vasodilation (up to 50%) respond to bradykinin (Fig. 4-1 D, E, and F). The application of Ba<sup>2+</sup> (30 μM) in WT arteries also reduced around 50% of vasodilation. These observations support that Kir2.1 channels play a major role in receptor-mediated vasodilation. Additionally, there was no further decrease of bradykinin-induced vasodilation in Kir2.1<sup>+/-</sup> mesenteric arteries with Ba<sup>2+</sup>, which suggests that there was no Kir2.1 channel distribution in bradykinin-induced vasodilation of Kir2.1<sup>+/-</sup> mesenteric arteries.

In the previous chapter, I showed that Kir2.1 channels regulate flow-induced vasodilation through NO production. To test whether Kir2.1 channels also regulate receptor-mediated vasodilation through NO production, I measured bradykinin-induced vasodilation with L-NAME (100 μM), a well-known eNOS inhibitor (Fig. 4-1). As expected, I observed around 50% reduction of vasodilation respond to bradykinin. There was no further decrease in bradykinin-induced vasodilation observed in Kir2.1<sup>+/-</sup> mesenteric arteries with L-NAME or the combination of L-NAME and Ba<sup>2+</sup>, or in WT mesenteric arteries with the combination of Ba<sup>2+</sup> and L-NAME. These data show that Kir2.1 channels regulate receptor-mediated vasodilation through NO production, likely to Kir2.1 regulation in flow-induced vasodilation. Previous studies showed that receptor-mediated vasodilation induces K<sub>Ca</sub> channel

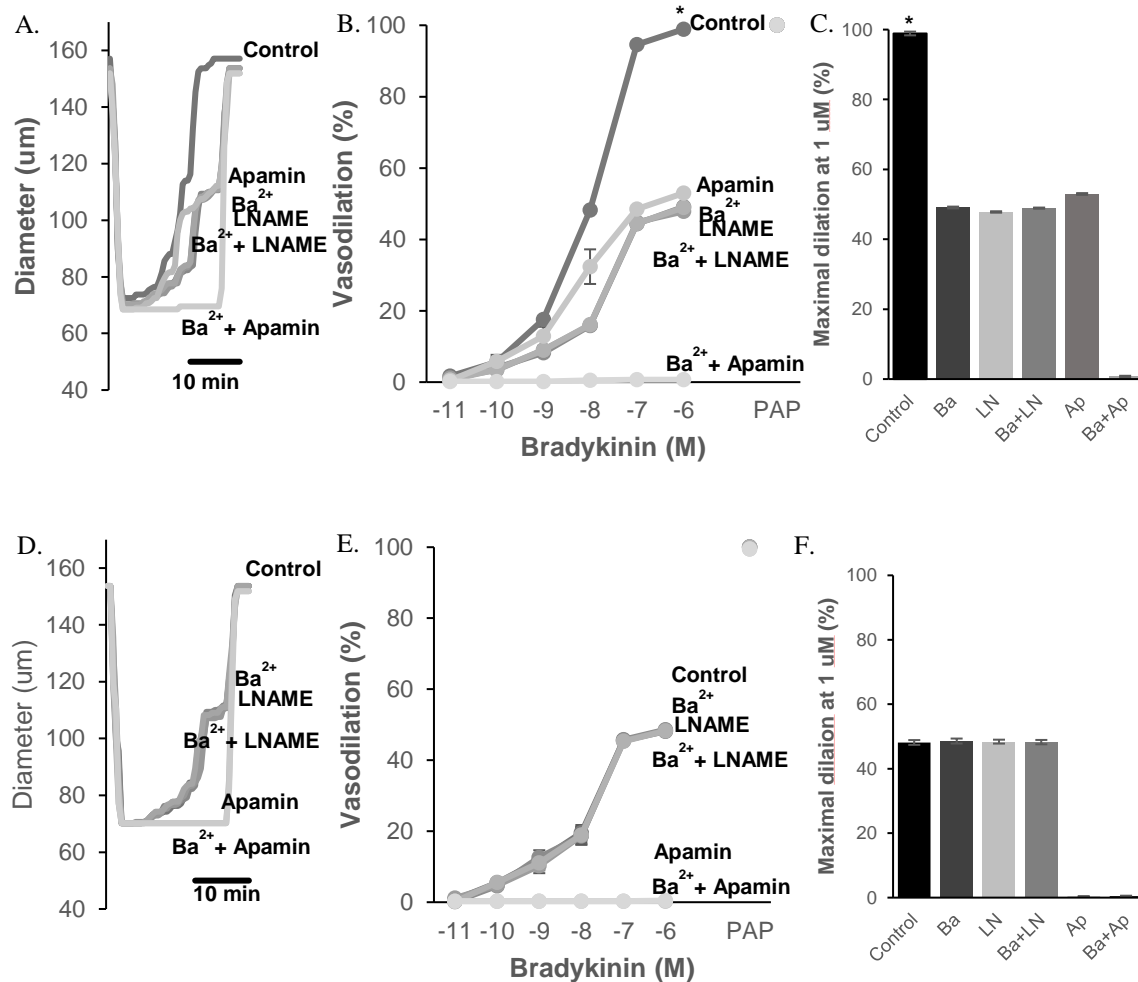


Figure 4-1 Role of Kir2.1 in bradykinin-induced vasodilation in mouse mesenteric arteries. (A) Representative bradykinin-induced trace of pre-constricted mesenteric arteries harvested from WT mice with and without 30  $\mu\text{M}$   $\text{Ba}^{2+}$ , 100  $\mu\text{M}$  LNAME, 20 nM apamin, or combination of each. (B) Average bradykinin-induced dilation (%) of mesenteric arteries harvested from WT mice with and without 30  $\mu\text{M}$   $\text{Ba}^{2+}$ , 100  $\mu\text{M}$  LNAME, 20 nM apamin, or combination of each. (n=4 per group, \*p<0.05) (D) Representative bradykinin-induced trace of pre-constricted mesenteric arteries harvested from Kir2.1<sup>+/-</sup> mice in the same condition of A. (E) Average bradykinin-induced dilation (%) of mesenteric arteries harvested from Kir2.1<sup>+/-</sup> mice in the same condition of B. (n=4 per group) C, F: Maximal dilation at 1 $\mu\text{M}$  bradykinin for the same experimental conditions as described in B and E, respectively. (ET-1=endothelin-1, PAP= Papaverine, added at the end of experiments to test the vessels' maximal dilation.)

activation leading vasodilation. Thus, my next question was whether Kir2.1 channels and  $K_{Ca}$  channels regulate receptor-mediated vasodilation in the same pathway. To address this question, I tested bradykinin-induced vasodilation with apamin, a well-known blocker of small-conductance  $Ca^{2+}$ -activated  $K^+$  channels (SK) (Fig. 4-1). As expected, apamin reduced around 50% of vasodilation respond to bradykinin in WT mesenteric arteries. Interestingly, bradykinin-induced vasodilation was disrupted in Kir2.1<sup>+/-</sup> mesenteric arteries with apamin and in WT mesenteric arteries with the combination of  $Ba^{2+}$  and apamin. These data show that Kir2.1 channels regulate receptor-mediated vasodilation in mesenteric arteries in a  $K_{Ca}$  channel-independent pathway.

I also tested the role of Kir2.1 channels in acetylcholine-induced vasodilation to address that Kir2.1 channels also regulate in other major vasoactive factor mediated vasodilation (Fig. 4-2 A). As expected, WT mesenteric arteries showed increase of vasodilation respond to applied acetylcholine concentrations. Kir2.1<sup>+/-</sup> mesenteric arteries showed significantly reduced vasodilation (up to 50%) respond to acetylcholine, and additional  $Ba^{2+}$  did not further decrease the vasodilation. Interestingly, WT mesenteric arteries with  $Ba^{2+}$  showed further decrease in vasodilation (up to 38%) compared to Kir2.1<sup>+/-</sup> mesenteric arteries, but there was no statistical significance. To determine whether Kir2.1 channels regulate acetylcholine-induced vasodilation through NO production, I tested acetylcholine-induced vasodilation with L-NAME in a different set of experiments (Fig. 4-2 B). As expected, WT mesenteric arteries showed significant reduction of acetylcholine-induced vasodilation with L-NAME. In Kir2.1<sup>+/-</sup> mesenteric arteries, there was no further decrease of acetylcholine-induced vasodilation observed with L-NAME. These results show that acetylcholine-induced vasodilation is also regulated by Kir2.1 channels through

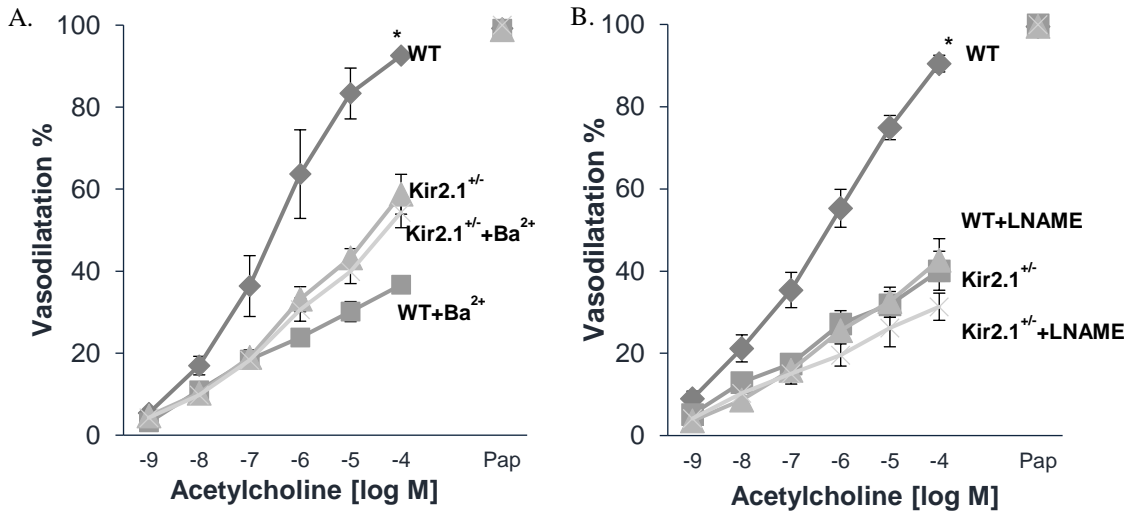


Figure 4-2 Role of Kir2.1 in acetylcholine-induced vasodilation in mouse mesenteric arteries. (A) Average acetylcholine-induced dilation (%) of mesenteric arteries harvested from WT and Kir2.1<sup>+/-</sup> mice with and without 30  $\mu$ M Ba<sup>2+</sup>. (n=4 per group, \*p<0.05) (B) Average acetylcholine-induced dilation (%) of mesenteric arteries harvested from WT and Kir2.1<sup>+/-</sup> mice with and without 100  $\mu$ M LNAME. (n=4 per group, \*p<0.05) (ET-1=endothelin-1, PAP= Papaverine, added at the end of experiments to test the vessels' maximal dilation.)

NO production.

#### **4.3.2 Kir regulation in receptor-mediated NO production**

As I observed that the vasodilation mediated by vasoactive factors is regulated by Kir2.1 channels through NO production, my next question was if the bradykinin-induced NO production in endothelial cells is regulated by Kir channels. To address this question, I measured bradykinin-induced NO production using real-time electrical NO detection in ECs from mesenteric arteries of WT and Kir2.1<sup>+/-</sup> mice. Porphyrinic NO probe detects NO and provides electrical signal, which can be converted to the amounts of NO production in real-time from ECs. Bradykinin (100 nM)-induced NO production was recorded for 10 minutes in the both of WT and Kir2.1<sup>+/-</sup> ECs. The representative trace of NO production from WT and Kir2.1<sup>+/-</sup> ECs is presented (Fig. 4-3 A). WT mesenteric arterial ECs produced 890 ± 70 nM of NO for 10 minutes respond to bradykinin (Fig. 4-3 B). In 2 minutes after bradykinin treatment, NO production hit the maximum release of 220 ± 15 nM (Fig. 4-3 C). Kir2.1<sup>+/-</sup> ECs showed reduced production of bradykinin-induced NO production (total 325 ± 35 nM in 10 minutes, and max 95 ± 15 nM). Ba<sup>2+</sup> reduced bradykinin-induced NO production in WT ECs (Fig. 4-3 D, E, and F). In Kir2.1<sup>+/-</sup> ECs, whereas, Ba<sup>2+</sup> had no significant reduction for both the total and maximal bradykinin-induced NO production. Taken together, my observation suggests that Kir2.1 channels regulate NO production in EC cells.

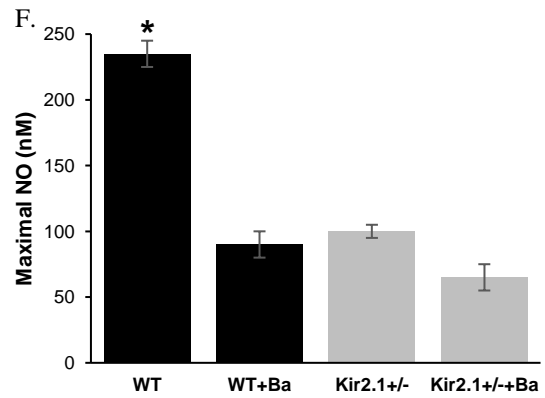
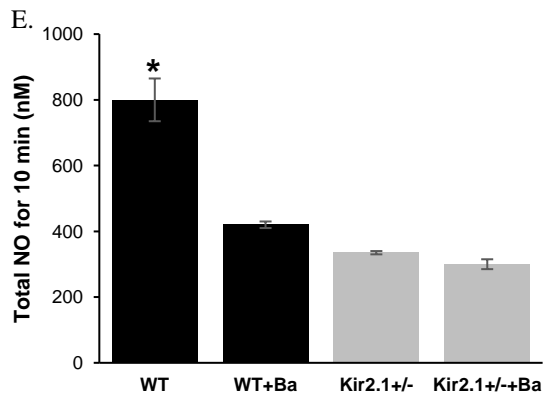
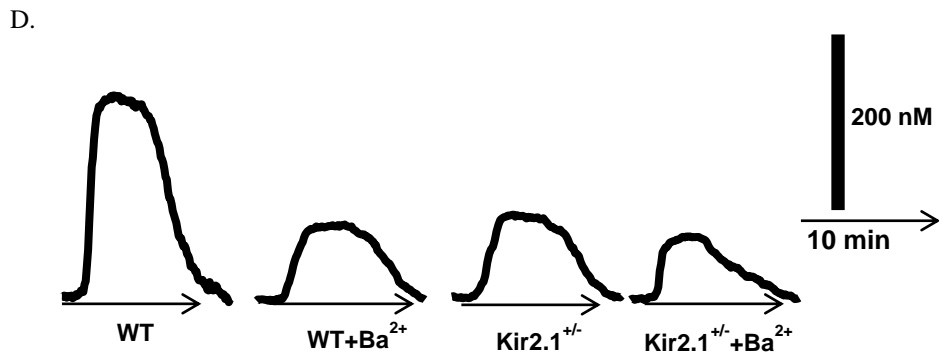
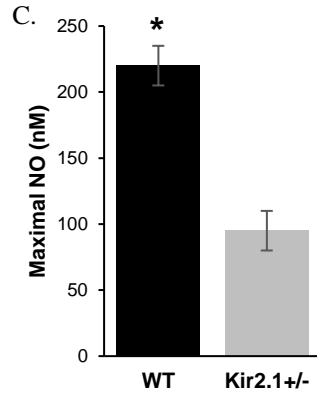
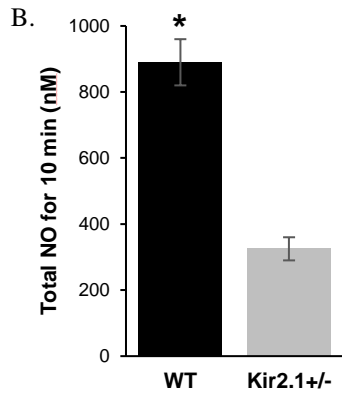
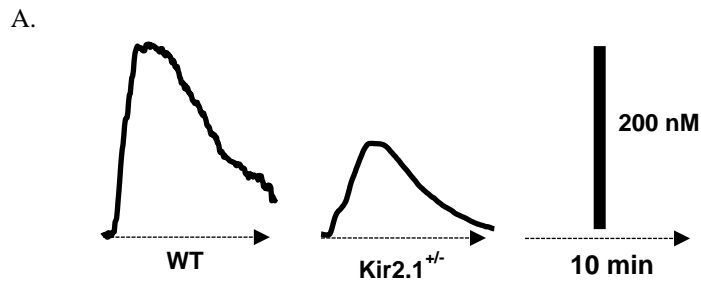


Figure 4-3 Role of Kir2.1 in bradykinin-induced NO production from mesenteric arterial endothelial cells. (A) Representative trace of bradykinin-induced (100 nM) NO production in mesenteric arterial endothelial cells from WT and Kir2.1<sup>+/-</sup> mice. (B) Average amounts of total NO production for 10 min in endothelial cells from WT and Kir2.1<sup>+/-</sup> mice by 100 nM of bradykinin. (n=4 per group, \*p<0.05) (C) Average amounts of maximal NO production in endothelial cells from WT and Kir2.1<sup>+/-</sup> mice by 100 nM of bradykinin. (n=4 per group, \*p<0.05) (D) Representative trace of bradykinin-induced (100 nM) NO production in mesenteric arterial endothelial cells from WT and Kir2.1<sup>+/-</sup> mice with and without Ba<sup>2+</sup> (30 μM). (E) Average amounts of total NO production for 10 min in endothelial cells from WT and Kir2.1<sup>+/-</sup> mice with and without Ba<sup>2+</sup> (30 μM) by 100 nM of bradykinin. (n=4 per group, \*p<0.05) (F) Average amounts of maximal NO production in endothelial cells from WT and Kir2.1<sup>+/-</sup> mice with and without Ba<sup>2+</sup> (30 μM) by 100 nM of bradykinin. (n=4 per group, \*p<0.05)

### **4.3.3 Rescued NO production in Kir channel impaired ECs by WT-Kir2.1 overexpression**

My next question was whether the reduced bradykinin-induced NO production in Kir2.1<sup>+/-</sup> ECs could be rescued by WT-Kir2.1 channel overexpression. To address this question, Kir2.1<sup>+/-</sup> ECs were transfected by adenoviral vectors (10 MOI) with empty or WT-Kir2.1 channels. WT-Kir2.1 transfected Kir2.1<sup>+/-</sup> ECs showed fully recovered bradykinin-induced NO production in both total and maximal NO production (Fig. 4-4 A and B). The maximal NO production from WT-Kir2.1 transfected Kir2.1<sup>+/-</sup> ECs respond to bradykinin was similar to the amounts of WT ECs (225 ± 25 nM and 210 ± 25 nM in WT and recovered Kir2.1<sup>+/-</sup> ECs, respectively). Although the total production of bradykinin-induced NO in WT-Kir2.1 transfected Kir2.1<sup>+/-</sup> ECs were lower than that of WT ECs (890 ± 70 and 690 ± 60 in WT and recovered Kir2.1<sup>+/-</sup> ECs, respectively), the rescued bradykinin-induced NO production was significantly higher than that of empty vector transfected Kir2.1<sup>+/-</sup> ECs. Rescued bradykinin-induced NO production showed Ba<sup>2+</sup> sensitivity, which implies that Kir2.1 channels distribute to this recovery effect. Taken all together, my observations strongly suggest that Kir2.1 channels mainly regulate NO production in endothelial cells resulting in vasodilation.

### **4.3.4 Kir channel regulation on NO production via Akt activation**

My next question was how Kir2.1 channels regulate bradykinin-induced NO production. In Chapter 3, I observed that Kir channel regulation in flow-induced eNOS activation was through Akt phosphorylation. Therefore, in order to determine whether Kir channel

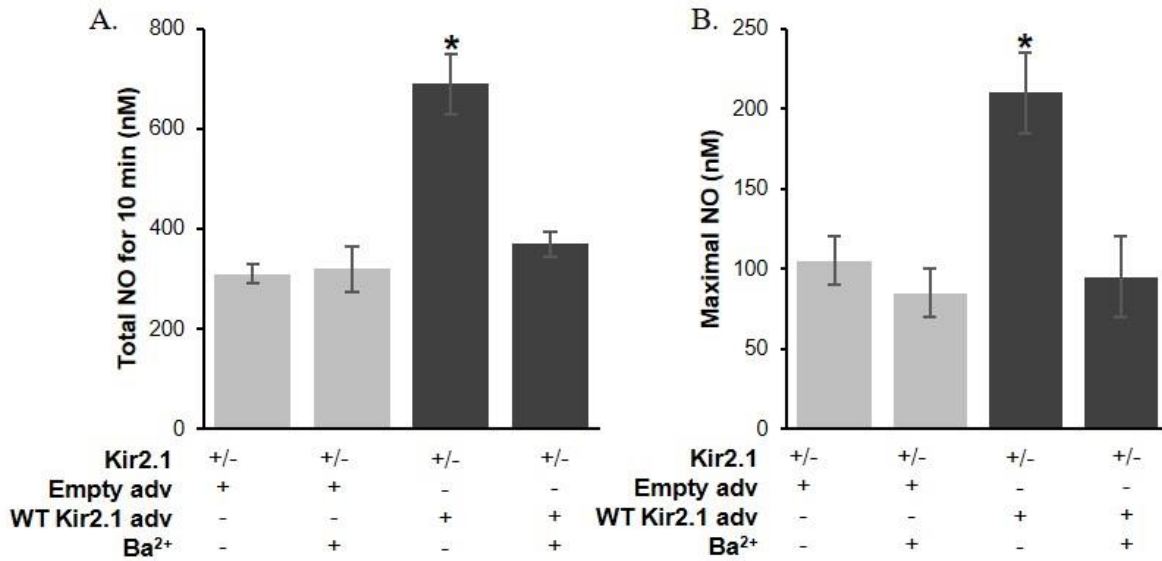


Figure 4-4 WT-Kir2.1 transfection recovers bradykinin-induced NO production in endothelial cells from Kir2.1<sup>+/-</sup> mice. (A) Average amounts of total bradykinin-induced (100 nM) NO production for 10 min in endothelial cells from Kir2.1<sup>+/-</sup> mice transfected by empty and WT-Kir2.1 adenoviral vector. (n=4 per group, \*p<0.05) (B) Average amounts of maximal bradykinin-induced (100 nM) NO production in endothelial cells from Kir2.1<sup>+/-</sup> mice transfected by empty and WT-Kir2.1 adenoviral vector. (n=4 per group, \*p<0.05)

regulation in bradykinin-induced NO production was also through Akt, I tested bradykinin-induced NO production with Akt inhibitor, MK2202, in WT and Kir2.1<sup>+/-</sup> ECs (Fig. 4-5 A and B). MK2202 (100 nM) inhibited NO production significantly in WT ECs in both total ( $310 \pm 15$  nM) and maximal ( $85 \pm 10$  nM) bradykinin-induced NO production. However, there was no significant decrease of NO production in Kir2.1<sup>+/-</sup> ECs. No further decrease of NO in Kir2.1<sup>+/-</sup> ECs with Akt inhibitor implies that Kir channel regulation in the receptor-mediated NO production is via Akt activation. Therefore, Kir channel regulates not only the flow-induced but also the receptor-mediated NO production through Akt activation.

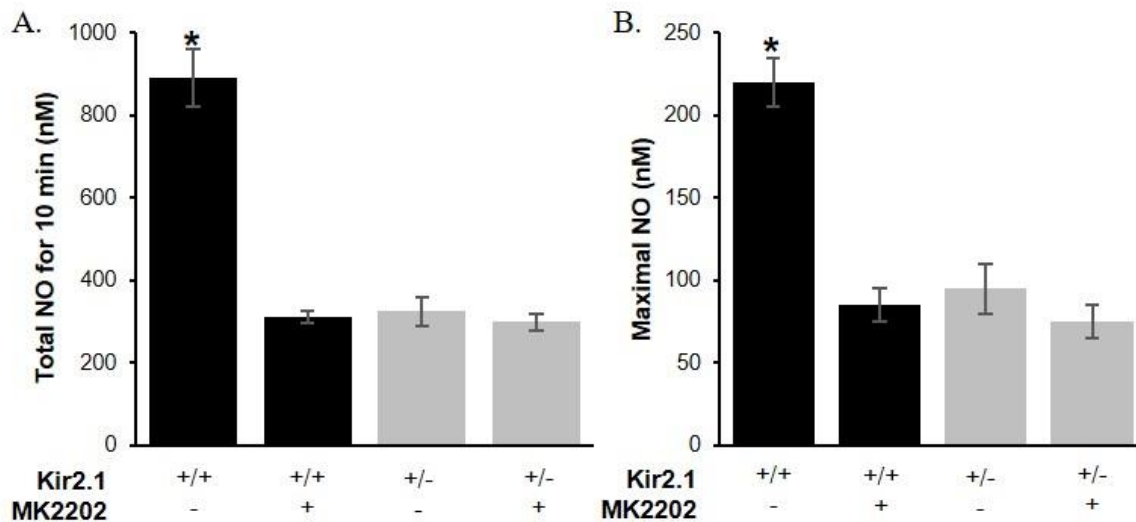


Figure 4-5 Kir2.1 regulation in Bradykinin-induced NO production from endothelial cells via Akt-dependent pathway. (A) Average amounts of total bradykinin-induced (100 nM) NO production for 10 min in endothelial cells from WT and Kir2.1<sup>+/-</sup> mice with and without Akt inhibitor (MK2202). (n=4 per group, \*p<0.05) (B) Average amounts of maximal bradykinin-induced (100 nM) NO production in endothelial cells from WT and Kir2.1<sup>+/-</sup> mice with and without Akt inhibitor (MK2202). (n=4 per group, \*p<0.05)

## **4.4 Discussion**

In this study, I present evidence that Kir2.1 channels regulate not only flow-induced vasodilation but also receptor-mediated vasodilation through NO production via Akt activation in resistance arteries. My major findings in this part of the study are: i) Kir2.1 channels are essential for bradykinin-induced vasodilation of murine mesenteric arteries through NO production, ii) Kir and  $K_{Ca}$  act independently through two distinct pathways (NO-dependent and NO-independent) in bradykinin-induced vasodilation, and iii) Kir2.1 channels regulate bradykinin-induced NO production through Akt activation. These findings indicate that Kir channels are essential for the NO production in endothelium-dependent vasodilation of both flow-induced and receptor-mediated.

### **4.4.1 Role of endothelial Kir2.1 channels in bradykinin-induced vasodilation**

Previous studies reported that bradykinin-induced vasodilation was reduced by  $Ba^{2+}$  in porcine coronary arteries and human brachial arteries (Rivers *et al.*, 2001; Vigili de Kreutzenberg *et al.*, 2003); however, the contribution of endothelial Kir channels in bradykinin-induced vasodilation was unclear. In this study, I showed the impairment of bradykinin-induced vasodilation in mesenteric arteries from Kir2.1 deficient mice. Notably, as was shown in Chapter 3, Kir2.1 channels are expressed in endothelial cell, not in smooth muscle cells. Therefore, my observation of Kir channel regulation in bradykinin-induced mouse mesenteric arterial vasodilation is the first evidence that Kir channels in endothelial cells regulate receptor-mediated vasodilation. Additionally, my results show that Kir channels in endothelium regulate not only bradykinin-induced vasodilation but

also vasodilation induced by acetylcholine, which are known to be the major vasoactive factors in vascular physiology. Based on these results, I suggest that endothelial Kir channels are essential for receptor-mediated vasodilation.

In this study, I also observed that bradykinin-induced vasodilation was completely disrupted with apamin in Kir2.1<sup>+/-</sup> mouse mesenteric arteries. Additionally, WT mesenteric arteries with combination of Ba<sup>2+</sup> and apamin also showed complete disruption of bradykinin-induced vasodilation. While, I observed there was no further decrease in bradykinin-induced vasodilation with L-NAME in Kir2.1<sup>+/-</sup> mesenteric arteries. Additionally, there was no difference between WT arteries with Ba<sup>2+</sup> and with combination of Ba<sup>2+</sup> and L-NAME. These data show that the effect of Kir2.1 channels on bradykinin-induced vasodilation is mediated by a NO-dependent pathway and a K<sub>Ca</sub>-independent pathway. Furthermore, I observed that there was no further decrease in acetylcholine-induced vasodilation with L-NAME in Kir2.1<sup>+/-</sup> arteries; hence, based on my observations, I conclude that Kir channels regulate receptor-mediated vasodilation through NO production.

#### **4.4.2 Role of Kir2.1 in endothelial NO production in response to bradykinin**

In this study, I present evidence that Kir2.1 channels are essential for bradykinin-induced NO production in mouse mesenteric arterial endothelial cells. The lack of Kir2.1 channel activity significantly reduced bradykinin-induced NO production in these cells. Furthermore, adenoviral transfection of WT-Kir2.1 channels fully recovered bradykinin-induced NO production in Kir2.1 deficient ECs. Bradykinin-induced eNOS activation is

known to be regulated by Akt phosphorylation (Ndiaye *et al.*, 2004; Sessa, 2004). As expected, Akt inhibitor significantly reduced bradykinin-induced NO production in WT ECs. Interestingly, there was no further reduction of bradykinin-induced NO production with Akt inhibitor in Kir2.1 deficient ECs. These data imply that Kir2.1 channels regulate eNOS activation by bradykinin through an Akt-dependent pathway. I also showed in Chapter 3 that Kir2.1 channels regulate flow-induced eNOS activation through Akt phosphorylation. However, it is still unclear what is the mechanistic link between Kir2.1 channels and Akt activation in response to both flow and bradykinin. Therefore, the detailed mechanism how Kir2.1 channels regulate Akt activation should be addressed in further studies. Bradykinin is also known to induce Ca<sup>2+</sup> influx into ECs (Hangaard *et al.*, 2015), and intracellular Ca<sup>2+</sup> is also essential for eNOS activation. However, it is unclear whether Kir2.1 channels are involved to Ca<sup>2+</sup> influx into ECs; hence, the relation between Kir2.1 channel activity and Ca<sup>2+</sup> influx respond to bradykinin should be studied in the future.

## Reference

- Groves P, Kurz S, Just H & Drexler H. (1995). Role of endogenous bradykinin in human coronary vasomotor control. *Circulation* **92**, 3424-3430.
- Hangaard L, Jessen PB, Kamaev D, Aalkjaer C & Matchkov VV. (2015). Extracellular Calcium-Dependent Modulation of Endothelium Relaxation in Rat Mesenteric Small Artery: The Role of Potassium Signaling. *Biomed Res Int* **2015**, 758346.
- Malowney M, Keltz S, Fischer D & Boyd JW. (2015). Availability of outpatient care from psychiatrists: a simulated-patient study in three U.S. cities. *Psychiatr Serv* **66**, 94-96.
- Maniatis NA, Brovkovich V, Allen SE, John TA, Shajahan AN, Tirupathi C, Vogel SM, Skidgel RA, Malik AB & Minshall RD. (2006). Novel mechanism of endothelial nitric oxide synthase activation mediated by caveolae internalization in endothelial cells. *Circ Res* **99**, 870-877.
- Ndiaye M, Chataigneau T, Chataigneau M & Schini-Kerth VB. (2004). Red wine polyphenols induce EDHF-mediated relaxations in porcine coronary arteries through the redox-sensitive activation of the PI3-kinase/Akt pathway. *Br J Pharmacol* **142**, 1131-1136.
- Rivers RJ, Hein TW, Zhang C & Kuo L. (2001). Activation of barium-sensitive inward rectifier potassium channels mediates remote dilation of coronary arterioles. *Circulation* **104**, 1749-1753.
- Sessa WC. (2004). eNOS at a glance. *J Cell Sci* **117**, 2427-2429.
- Sun L & Ye RD. (2012). Role of G protein-coupled receptors in inflammation. *Acta Pharmacol Sin* **33**, 342-350.
- Vigili de Kreutzenberg S, Kiwanuka E, Tiengo A & Avogaro A. (2003). Visceral obesity is characterized by impaired nitric oxide-independent vasodilation. *Eur Heart J* **24**, 1210-1215.

## Chapter 5. Role of Kir2.1 channels in hyperlipidemia

### 5.1 Introduction

Hyperlipidemia is the number one risk factor causing severe cardiovascular disease, such as atherosclerosis, hypertension, and coronary artery disease. In previous studies from our lab, inwardly rectifying K<sup>+</sup> (Kir) channels are known to be strongly suppressed by the increase of cellular cholesterol (Romanenko *et al.*, 2002; Levitan, 2009; Singh *et al.*, 2009). In these studies, Kir currents were reduced by cholesterol enrichment, and it was shown that cholesterol directly binds to Kir channels. Additionally, it was shown that cholesterol inhibited flow-induced Kir currents in porcine aortic endothelial cells (Fang *et al.*, 2006).

Since my data demonstrated that Kir channels are essential for flow-induced vasodilation. I hypothesized that shear stress induced vasodilation may be impaired because of the hyperlipidemia-induced downregulation of Kir channel activity. Furthermore, I suggest that the loss of Kir channel activity may enhance the development of atherosclerosis. To address my hypothesis, I tested: i) flow-induced vasodilation in mesenteric arteries from ApoE<sup>-/-</sup> mice and ApoE<sup>-/-</sup>/Kir2.1<sup>+/-</sup> mice, and ii) aortic lesion formation under high fat diet condition in ApoE<sup>-/-</sup> and ApoE<sup>-/-</sup>/Kir2.1<sup>+/-</sup> mice.

## 5.2 Methods

### 5.2.1 Aortic lesion formation

ApoE<sup>-/-</sup> and ApoE<sup>-/-</sup>/Kir2.1<sup>+/-</sup> FVB mice were used. Mice were fed with western high fat diet for 6 months and 9 months. Mice were euthanized by high dose isoflurane, and the heart perfusion was performed right after expiring. PBS were circulated to remove the blood for 10 minutes, and 4% paraformaldehyde were circulated to fix the aorta for 10 minutes. Fixed aortas were extracted with hearts and kept in 4% paraformaldehyde to further fix for 24 hours, 4 °C. After fixation, the surrounding tissues of aortas were cleaned in PBS, and aortas were detached from hearts.

Oil red O *en face* staining was used to stain aortic lesions. Oil red O stock solution (5% w/v) was prepared in 100% isopropanol. Working solution was prepared in 2:3 ratio of water and stock solution, and filtered through 0.2 µm membrane for ready-to-use. Washing solution was prepared with 60% isopropanol. Aortas were opened to make intraluminal side up to be stained. To fix the shape of aortas during staining, outer diameter 100 µm pins were used. Each aorta was exposed to 200 µl of Oil red O working solution for 10 minutes in room temperature, and washed with washing solution for 3 times. Not to dry the samples, stained aortas, then, emerged with PBS. The pictures were taken through DFK 41 CCD camera (World Precision Instrument) with stereotype microscope. Lesion areas were analyzed by ImageJ based on total areas of the aortas.

## 5.3 Results

### **5.3.1 Hyperlipidemia reduces flow-induced vasodilation by blocking of Kir channels**

Previous studies in our lab showed that Kir currents were suppressed by direct cholesterol binding to Kir channels (Romanenko *et al.*, 2002; Levitan, 2009; Singh *et al.*, 2009). Additionally, our lab showed that flow-induced Kir currents were also significantly reduced by cholesterol (Fang *et al.*, 2006). Based on these results, my first question in this part of the study was whether FIV in mesenteric arteries is reduced by hyperlipidemia through Kir channel impairment. To address this question, I tested FIV in mesenteric arteries from ApoE<sup>-/-</sup> and ApoE<sup>-/-</sup>/Kir2.1<sup>+/-</sup> (DKO) mice (Fig. 5-1). ApoE<sup>-/-</sup> mouse model is a well-known hyperlipidemic mouse model. It was reported that FIV in ApoE<sup>-/-</sup> mouse cutaneous vessels were significantly reduced (Yang *et al.*, 1999). Consistent with this study, I observed significantly decreased FIV in mesenteric arteries from ApoE<sup>-/-</sup> mice (Fig. 5-1 A and B). To determine if the loss of Kir channel activity contribute to the decreased FIV in ApoE<sup>-/-</sup> arteries, FIV was measured in mesenteric arteries from DKO mouse (Fig. 5-1 C and D). Interestingly, there was no further decrease in FIV of DKO mesenteric arteries compared to that of ApoE<sup>-/-</sup> arteries. Additionally, the sensitivity of FIV to Ba<sup>2+</sup> was not observed in mesenteric arteries from both of ApoE<sup>-/-</sup> and DKO mice. These results suggest that the reduction of FIV caused by hyperlipidemia is due to the loss of Kir channel activity in endothelial cells. In the Chapter 3 and 4, I have shown that Kir channel regulation in vasodilation is through a NO-dependent and a K<sub>Ca</sub>-independent pathway; hence, I tested FIV with L-NAME or apamin in mesenteric arteries from ApoE<sup>-/-</sup> and DKO mice. There was no significant decrease of FIV observed in both ApoE<sup>-/-</sup> and DKO arteries, whereas

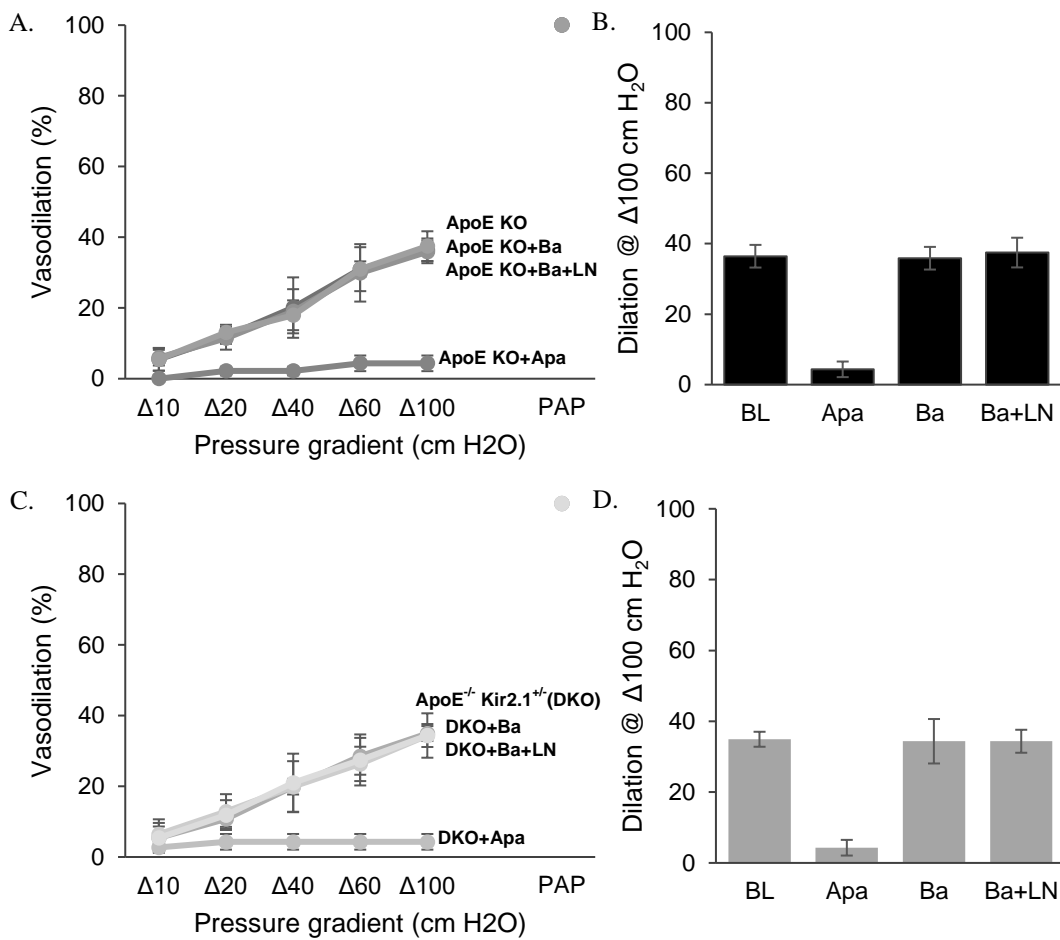


Figure 5-1 Impaired flow-induced vasodilation in dyslipidemia is due to the loss of Kir2.1 activity. (A) Average flow-induced dilation of pre-constricted mesenteric arteries harvested from ApoE<sup>-/-</sup> mice with and without Ba<sup>2+</sup> (30 μM), LNAME (100 μM), apamin (20 nM) or combination of Ba<sup>2+</sup> and LNAME, as a function of pressure gradient. (n=4 per group) (B) Average dilations at Δ100 cm H<sub>2</sub>O of A. (C) Average flow-induced dilation of pre-constricted mesenteric arteries harvested from ApoE<sup>-/-</sup>/Kir2.1<sup>+/-</sup> mice with and without Ba<sup>2+</sup> (30 μM), LNAME (100 μM), apamin (20 nM) or combination of Ba<sup>2+</sup> and LNAME, as a function of pressure gradient. (n=4 per group) (D) Average dilations at Δ100 cm H<sub>2</sub>O of C.

apamin disrupted FIV in mesenteric arteries from both ApoE<sup>-/-</sup> and DKO mice. Therefore, these data strongly suggest that hyperlipidemia reduces FIV through suppression of Kir channels in a NO-dependent pathway.

### **5.3.2 Kir2.1 channel deficiency causes more lesions in hyperlipidemia**

Multiple studies showed that ApoE<sup>-/-</sup> mice develop aortic lesions (Afek *et al.*, 1999; Lee *et al.*, 1999; Paul *et al.*, 1999), and that western-style high fat diet is known to accelerate the formation of lesions in these mice. My next question was if Kir channel impairment by hyperlipidemia enhances lesion formation. To address this question, I tested aortic lesion formation in ApoE<sup>-/-</sup> and DKO mice with 6 months and 9 months of western-style high fat diet (HFD). As expected, aortic lesions were formed in arteries from both ApoE<sup>-/-</sup> and DKO mice after 6 months of HFD (Fig. 5-2 A, B, C, D, and E). No significant difference was observed in total aortic lesion area between aortas from ApoE<sup>-/-</sup> and DKO mice in this time point (Fig. 5-2 A, B, and C). Furthermore, I also analyzed lesion formation in two separate regions of aortas: i) arch of aorta, known to be atheroprone region, in which lesion forms in larger area due to the disturbed shear stress, and ii) thoracic aorta, known to be atheroprotective region because of the laminar shear stress. However, while there were more lesions in arch of aortas from both ApoE<sup>-/-</sup> and DKO mice as compared to thoracic, there was no difference between ApoE<sup>-/-</sup> and DKO mice (Fig. 5-2 D and E). After 9 months of western-style HFD, the aortic lesions were dramatically increased in aortas from both ApoE<sup>-/-</sup> and DKO mice compared to those of 6 months HFD (Fig. 5-2 F and G). Interestingly, aortas from DKO mice showed significantly larger lesion area than aortas from ApoE<sup>-/-</sup> mice in total, arch regions, and thoracic regions. Especially, the

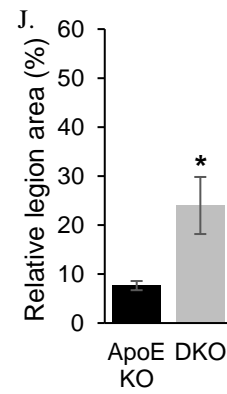
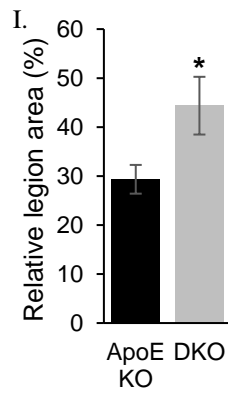
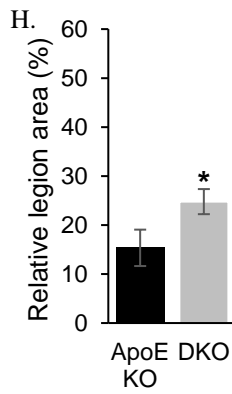
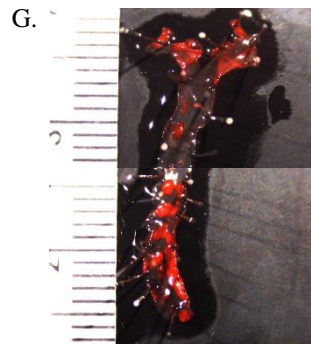
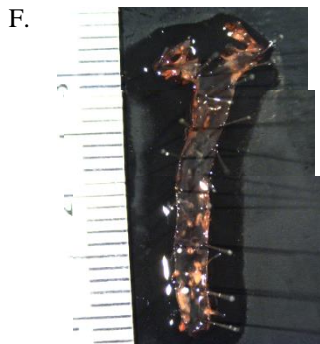
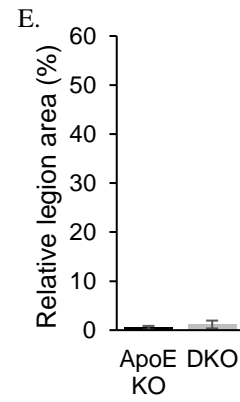
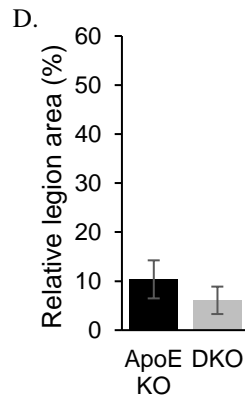
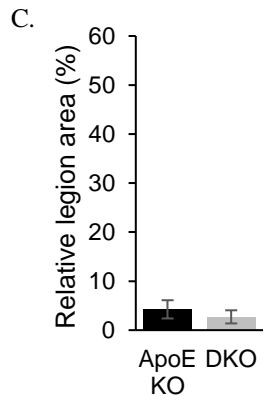
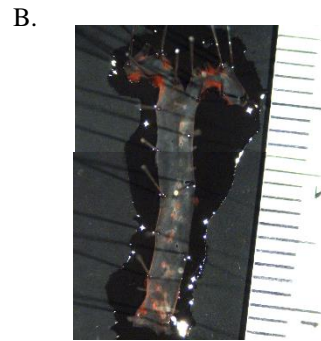
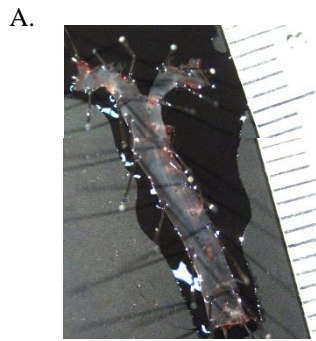


Figure 5-2 Kir2.1 is essential to prevent lesion formation. (A) Representative oil red O en face stained aorta from ApoE<sup>-/-</sup> mouse with 6 months of high fat diet. (B) Representative oil red O en face stained aorta from ApoE<sup>-/-</sup>/Kir2.1<sup>+/-</sup> mouse with 6 months of high fat diet. (C) Average of total lesion area normalized by total area of aortas with 6 months of high fat diet. (n=4 per group). (D) Average of lesion area in arch of aortas normalized by total arch area with 6 months of high fat diet. (n=4 per group) (E) Average of lesion area in thoracic of aorta normalized by total thoracic area with 6 months of high fat diet. (n=4 per group) (F) Representative oil red O en face stained aorta from ApoE<sup>-/-</sup> mouse with 9 months of high fat diet. (B) Representative oil red O en face stained aorta from ApoE<sup>-/-</sup>/Kir2.1<sup>+/-</sup> mouse with 9 months of high fat diet. (C) Average of total lesion area normalized by total area of aortas with 9 months of high fat diet. (n=4 per group, \*p<0.05). (D) Average of lesion area in arch of aortas normalized by total arch area with 9 months of high fat diet. (n=4 per group, \*p<0.05) (E) Average of lesion area in thoracic of aorta normalized by total thoracic area with 9 months of high fat diet. (n=4 per group, \*p<0.05)

atheroprotective thoracic aortas were covered by lesions up to 24%. These results showed that genetic deficiency of Kir2.1 channels results in increased formation of atherosclerotic lesions.

## **5.4 Discussion**

In this study, I presented evidence for the role of Kir channels in endothelial dysfunction and lesion formation in hyperlipidemia. Our lab showed the loss of Kir channel activity by cholesterol in previous studies. Impaired FIV in microcirculation under dyslipidemia was observed in multiple studies (Lopes *et al.*, 2013; Ozkor *et al.*, 2015; Reimann *et al.*, 2015). However, it was unclear the role of endothelial Kir channels in impaired FIV under dyslipidemic condition. In my observation, as consistent with previous studies, mesenteric arteries from dyslipidemic mice showed impaired FIV. Interestingly, mesenteric arteries from Kir2.1 deficient mice with dyslipidemia showed no further decreased FIV. These data combined with previous studies suggest that dyslipidemia reduces Kir channel activity resulting in impairment of FIV. However, many other studies are still required to support this statement, such as whether other components of FIV rather than Kir channels are affected by dyslipidemia, where and how cholesterol binds to Kir channels, and if the impaired FIV in dyslipidemia can be recovered by endothelial Kir2.1 overexpression.

### **5.4.1 Larger lesion formation in Kir2.1 deficient ApoE knock out mice**

It is well-known that dyslipidemia elevates lesion formation in blood vessels resulting in atherosclerosis. Multiple studies suggest that increased low-density lipoprotein (LDL) uptake into endothelial cells in dyslipidemia enhances the athero-lesion formation (Linton *et al.*, 2000); hence, other studies observed the reduced lesion formation in caveolin-1 or scavenger receptor (components related to LDL uptake) knock out mouse models in dyslipidemia (Hu *et al.*, 2008; Kuchibhotla *et al.*, 2008; Das & Das, 2012). Deletion of

certain genes elevated lesion formation, such as syndecan 4 in endothelial cells, which serves as a coreceptor for extracellular matrix proteins and growth factors, and maintains endothelial function (Baeyens *et al.*, 2014); therefore, the loss of syndecan 4 leads to endothelial dysfunction, and results in severe atherosclerosis. Additionally, endothelial specific overexpression of caveolin-1 increased lesion formation in dyslipidemic condition (Fernandez-Hernando *et al.*, 2010). Interestingly, I observed that the loss of Kir2.1 also exacerbated lesion formation in dyslipidemia. Based on these observations, there are several possibilities for the role of Kir2.1 in atherosclerosis: i) Kir2.1 may be essential for endothelial function; therefore, the loss of Kir2.1 may result in endothelial dysfunction leading to atherosclerosis, ii) Kir2.1 may regulate LDL uptake into endothelial cells; hence, the loss of Kir2.1 may enhance LDL uptake, and iii) since these mice are global Kir2.1 deficient mice, the loss of Kir2.1 in other types of cells, such as macrophages, may play a key role in the observed elevated lesion formation. All of these possibilities should be studied to understand the role of Kir2.1 in atherosclerosis.

## Reference

- Afek A, George J, Shoenfeld Y, Gilburd B, Levy Y, Shaish A, Keren P, Janackovic Z, Goldberg I, Kopolovic J & Harats D. (1999). Enhancement of atherosclerosis in beta-2-glycoprotein I-immunized apolipoprotein E-deficient mice. *Pathobiology* **67**, 19-25.
- Baeyens N, Mulligan-Kehoe MJ, Corti F, Simon DD, Ross TD, Rhodes JM, Wang TZ, Mejean CO, Simons M, Humphrey J & Schwartz MA. (2014). Syndecan 4 is required for endothelial alignment in flow and atheroprotective signaling. *Proc Natl Acad Sci U S A* **111**, 17308-17313.
- Das M & Das DK. (2012). Caveolae, caveolin, and cavins: potential targets for the treatment of cardiac disease. *Ann Med* **44**, 530-541.
- Fang Y, Mohler ER, 3rd, Hsieh E, Osman H, Hashemi SM, Davies PF, Rothblat GH, Wilensky RL & Levitan I. (2006). Hypercholesterolemia suppresses inwardly rectifying K<sup>+</sup> channels in aortic endothelium in vitro and in vivo. *Circ Res* **98**, 1064-1071.
- Fernandez-Hernando C, Yu J, Davalos A, Prendergast J & Sessa WC. (2010). Endothelial-specific overexpression of caveolin-1 accelerates atherosclerosis in apolipoprotein E-deficient mice. *Am J Pathol* **177**, 998-1003.
- Hu C, Dandapat A, Sun L, Chen J, Marwali MR, Romeo F, Sawamura T & Mehta JL. (2008). LOX-1 deletion decreases collagen accumulation in atherosclerotic plaque in low-density lipoprotein receptor knockout mice fed a high-cholesterol diet. *Cardiovasc Res* **79**, 287-293.
- Kuchibhotla S, Vanegas D, Kennedy DJ, Guy E, Nimako G, Morton RE & Febbraio M. (2008). Absence of CD36 protects against atherosclerosis in ApoE knock-out mice with no additional protection provided by absence of scavenger receptor A I/II. *Cardiovasc Res* **78**, 185-196.
- Lee TS, Shiao MS, Pan CC & Chau LY. (1999). Iron-deficient diet reduces atherosclerotic lesions in apoE-deficient mice. *Circulation* **99**, 1222-1229.
- Levitan I. (2009). Cholesterol and Kir channels. *IUBMB Life* **61**, 781-790.

- Linton MF, Yancey PG, Davies SS, Jerome WGJ, Linton EF & Vickers KC. (2000). The Role of Lipids and Lipoproteins in Atherosclerosis. In *Endotext*, ed. De Groot LJ, Chrousos G, Dungan K, Feingold KR, Grossman A, Hershman JM, Koch C, Korbonits M, McLachlan R, New M, Purnell J, Rebar R, Singer F & Vinik A. South Dartmouth (MA).
- Lopes FG, Bottino DA, Oliveira FJ, Mecnas AS, Clapauch R & Bouskela E. (2013). In elderly women moderate hypercholesterolemia is associated to endothelial and microcirculatory impairments. *Microvasc Res* **85**, 99-103.
- Ozkor MA, Hayek SS, Rahman AM, Murrow JR, Kavtaradze N, Lin J, Manatunga A & Quyyumi AA. (2015). Contribution of endothelium-derived hyperpolarizing factor to exercise-induced vasodilation in health and hypercholesterolemia. *Vasc Med* **20**, 14-22.
- Paul A, Calleja L, Vilella E, Martinez R, Osada J & Joven J. (1999). Reduced progression of atherosclerosis in apolipoprotein E-deficient mice with phenylhydrazine-induced anemia. *Atherosclerosis* **147**, 61-68.
- Reimann M, Weiss N & Ziemssen T. (2015). Different responses of the retinal and cutaneous microcirculation to transient dysmetabolic conditions. *Atheroscler Suppl* **18**, 1-7.
- Romanenko VG, Rothblat GH & Levitan I. (2002). Modulation of endothelial inward-rectifier K<sup>+</sup> current by optical isomers of cholesterol. *Biophys J* **83**, 3211-3222.
- Singh DK, Rosenhouse-Dantsker A, Nichols CG, Enkvetchakul D & Levitan I. (2009). Direct regulation of prokaryotic Kir channel by cholesterol. *J Biol Chem* **284**, 30727-30736.
- Yang R, Powell-Braxton L, Ogaoawara AK, Dybdal N, Bunting S, Ohneda O & Jin H. (1999). Hypertension and endothelial dysfunction in apolipoprotein E knockout mice. *Arterioscler Thromb Vasc Biol* **19**, 2762-2768.

## Chapter 6. Conclusion

My main project was to identify the role of Kir2.1 channels in vascular function. Kir channels are expressed in variable cell types, and function to maintain the membrane potential. Olesen *et al.* showed that endothelial Kir channels are activated by flow (Olesen *et al.*, 1988); however, the role of endothelial Kir channels in vascular function was unclear. Therefore, my first goal to achieve in this project was to identify the role of endothelial Kir channels in flow-induced vasodilation, which is known as a major function of endothelium in vascular function. I mainly used murine mesenteric arteries to identify the role of endothelial Kir channels in flow-induced vasodilation (FIV). To address the role of Kir channels in vasodilation, I showed that: i) Kir2.1 channels are the major Kir channels expressed in endothelial cells, ii) the loss of Kir2.1 channels results in impaired FIV, iii) transfection of endothelial cell-specific WT-Kir2.1 channels in Kir2.1 deficient arteries fully recovers FIV, which demonstrates endothelial Kir2.1 channels regulate FIV, iv) Kir2.1 channels regulate FIV in a NO-dependent and a  $K_{Ca}$ -independent pathway, v) in terms of mechanism, Kir2.1 channels regulate flow-induced eNOS phosphorylation through Akt phosphorylation, vi) the loss of Kir2.1 channels results in disruption of flow-induced NO production, and vii) the loss of Kir2.1 channels leads hypertension due to the increased peripheral vascular resistance. Based on these results, I concluded that endothelial Kir2.1 channels are essential for FIV. However, to address further about the role of Kir2.1 channels in FIV, many questions are needed to be answered: i) whether Kir2.1 channels regulates flow-induced  $Ca^{2+}$  influx, ii) whether the results shown here can be repeated in endothelial-specific Kir2.1 channel knock out mouse model, and iii) whether the regulation of endothelial Kir2.1 channels in FIV of murine arteries has the same effect in human

microcirculation. Additionally, data that I provided in this thesis are based on experiments from ex vivo studies; hence, new experimental design may be required to support animal in vivo studies. To increase the shear stress of the blood in vivo, there are so many factors, but exercise would be the best physiological factor to induce high shear stress of the blood in vivo naturally to study FIV in vivo. Therefore, I would also like to suggest introducing animal exercise experimental set up in the further study to support my findings.

There is another type of endothelium-dependent vasodilation, which is receptor-mediated vasodilation. Receptor-mediated vasodilation is defined by vasoactive factors binding to their receptors to induce vasodilation. Vasoactive factors are known to induce  $\text{Ca}^{2+}$  influx into the endothelial cells, and increased intracellular  $\text{Ca}^{2+}$  activates  $\text{K}_{\text{Ca}}$  channels in endothelial cells, which causes membrane hyperpolarization of endothelial cells resulting in vasodilation (Sun & Ye, 2012). Additionally,  $\text{K}^{+}$  efflux from endothelial cells by  $\text{K}_{\text{Ca}}$  channel activation induces the activation of Kir channels and  $\text{Na}^{+}\text{-K}^{+}$  ATPase in smooth muscles, which causes membrane hyperpolarization of smooth muscle resulting in vasodilation (Hangaard *et al.*, 2015). Furthermore, vasoactive factors also activate eNOS through Akt activation, resulting in vasodilation by NO (Ndiaye *et al.*, 2004). To address whether Kir2.1 channels also regulate receptor-mediated vasodilation through NO production, I showed that i) the loss of Kir2.1 channels results in impaired receptor-mediated vasodilation, ii) the regulation of Kir channels in receptor-mediated vasodilation follows a NO-dependent and a  $\text{K}_{\text{Ca}}$ -independent pathway, iii) Kir2.1 channels are essential for receptor-mediated NO production, iv) overexpression of WT-Kir2.1 channels in Kir2.1 deficient endothelial cells recovers receptor-mediated NO production, and v) Kir2.1 channel regulation on receptor-mediated NO production is through an Akt-dependent

pathway. Although I showed several lines of evidence, which show endothelial Kir channels play a major role in receptor-mediated vasodilation via NO production, many other studies are required to support this statement, such as i) whether Kir channels are activated by vasoactive factors, ii) whether receptor-mediated  $\text{Ca}^{2+}$  influx into endothelial cells is regulated by Kir channels, iii) whether these results can be repeated in endothelial-specific Kir2.1 channel knock out mice, and iv) whether Kir channel effect on receptor-mediated vasodilation in mouse resistance arteries has the same effect in human microcirculation.

These two findings suggest that when the endothelial cells are stimulated by flow or vasoactive factors, Kir2.1 channels are activated to induce eNOS activation through Akt phosphorylation resulting in a NO-dependent vasodilation (Fig. 6-1). According to Chatterjee et al, change of membrane potential may control the Akt phosphorylation through the activation of voltage-sensitive phosphatase (Chatterjee *et al.*, 2012). Ci-VSP (Ciona intestinalis-voltage sensitive phosphatase) is known to be activated by the membrane depolarization and remove phosphates in PIP3 (phosphatidylinositol (3,4,5)-triphosphate) transforming into PIP2 (phosphatidylinositol (4,5)-diphosphate), which can be used as a substrate for PI3K (phosphoinositide 3-kinase), a well-known kinase for Akt phosphorylation (Halaszovich *et al.*, 2009).

In the same time,  $\text{Ca}^{2+}$  influx is also increased by flow or vasoactive factors, although the relationship between  $\text{Ca}^{2+}$  influx and Kir2.1 activity is still unclear, and the increased intracellular  $\text{Ca}^{2+}$  activates  $\text{K}_{\text{Ca}}$  channels in endothelial cells resulting in a  $\text{K}_{\text{Ca}}$ -dependent vasodilation (Hangaard *et al.*, 2015).

Our lab previously showed that cholesterol strongly suppresses Kir channel activity in

endothelial cells, and my data suggest that impaired FIV in dyslipidemia is due to the loss of Kir channel activity, which is consistent with my previous observation that loss of endothelial Kir channels results in impaired FIV. However, dyslipidemia is known to affect various components in endothelial cells resulting in endothelial dysfunction; therefore, other endothelial components in FIV, such as  $K_{Ca}$ ,  $Ca^{2+}$  channels, eNOS, PI3K, and Akt, should also be studied in the level of expression and functional activity. I also showed that the loss of Kir2.1 channels enhances lesion formation in dyslipidemic mice resulting in severe atherosclerosis. These results imply that Kir2.1 channels are important to prevent atherosclerosis formation in dyslipidemia. Although mechanisms how Kir2.1 channels protect atherosclerosis remain unclear, these results suggest that Kir channels can be a key component to treat atherosclerosis.

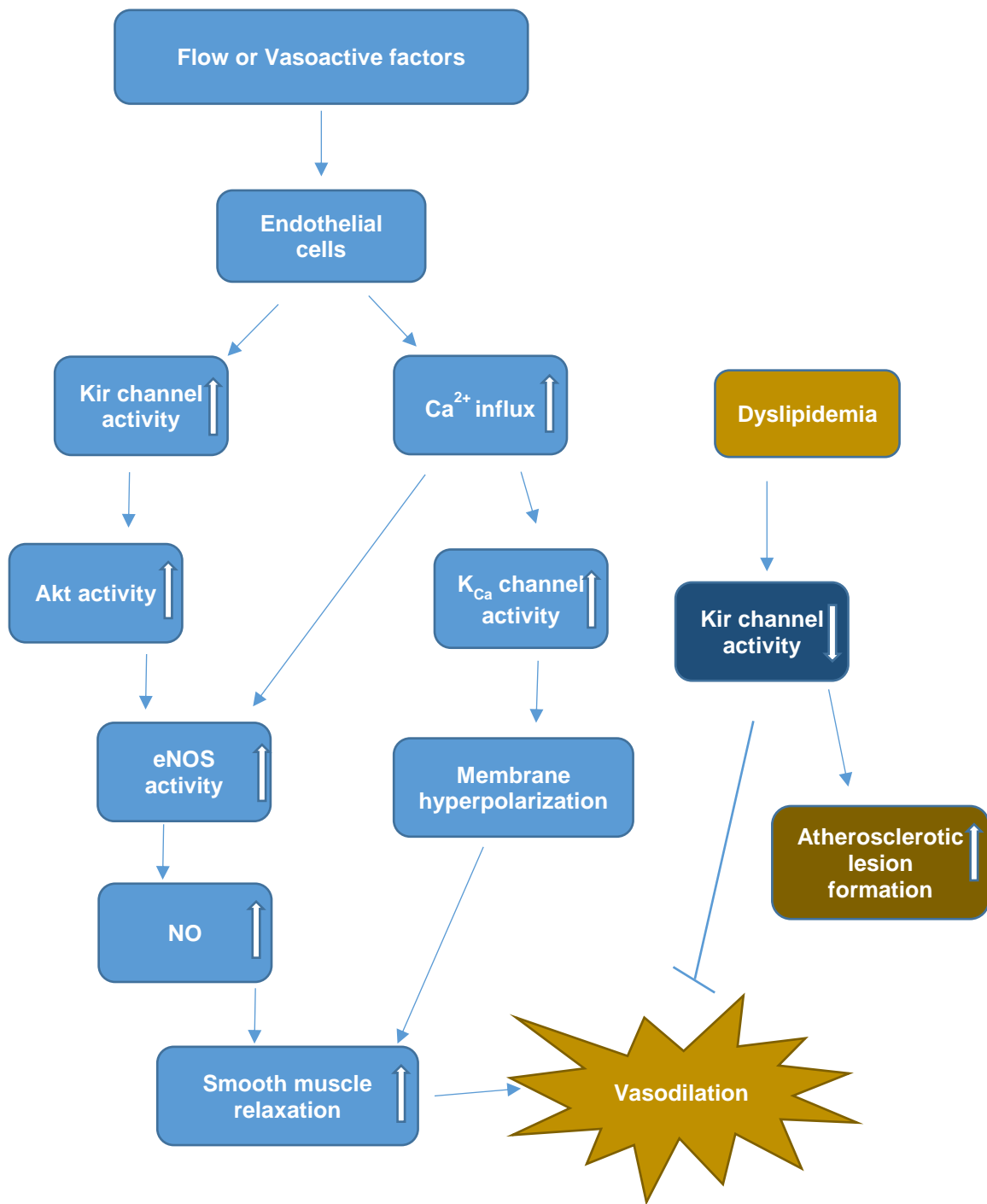


Figure 6-1 Role of endothelial Kir channels in vasodilation under normal and dyslipidemic condition

## Reference

- Chatterjee S, Browning EA, Hong N, DeBolt K, Sorokina EM, Liu W, Birnbaum MJ & Fisher AB. (2012). Membrane depolarization is the trigger for PI3K/Akt activation and leads to the generation of ROS. *American Journal of Physiology - Heart and Circulatory Physiology* **302**, H105-H114.
- Halaszovich CR, Schreiber DN & Oliver D. (2009). Ci-VSP is a depolarization-activated phosphatidylinositol-4,5-bisphosphate and phosphatidylinositol-3,4,5-trisphosphate 5'-phosphatase. *J Biol Chem* **284**, 2106-2113.
- Hangaard L, Jessen PB, Kamaev D, Aalkjaer C & Matchkov VV. (2015). Extracellular Calcium-Dependent Modulation of Endothelium Relaxation in Rat Mesenteric Small Artery: The Role of Potassium Signaling. *Biomed Res Int* **2015**, 758346.
- Ndiaye M, Chataigneau T, Chataigneau M & Schini-Kerth VB. (2004). Red wine polyphenols induce EDHF-mediated relaxations in porcine coronary arteries through the redox-sensitive activation of the PI3-kinase/Akt pathway. *Br J Pharmacol* **142**, 1131-1136.
- Olesen SP, Clapham DE & Davies PF. (1988). Haemodynamic shear stress activates a K<sup>+</sup> current in vascular endothelial cells. *Nature* **331**, 168-170.
- Sun L & Ye RD. (2012). Role of G protein-coupled receptors in inflammation. *Acta Pharmacol Sin* **33**, 342-350.

## Appendix

### JOHN WILEY AND SONS LICENSE TERMS AND CONDITIONS

Jul 03, 2017

---

---

This Agreement between Dr. Sang Joon Ahn ("You") and John Wiley and Sons ("John Wiley and Sons") consists of your license details and the terms and conditions provided by John Wiley and Sons and Copyright Clearance Center.

License Number	4141501486461
License date	Jul 03, 2017
Licensed Content Publisher	John Wiley and Sons
Licensed Content Publication	Journal of Physiology
Licensed Content Title	Inwardly rectifying K <sup>+</sup> channels are major contributors to flow-induced vasodilatation in resistance arteries
Licensed Content Author	Sang Joon Ahn,Ibra S. Fancher,Jing-Tan Bian,Chong Xu Zhang,Sarah Schwab,Robert Gaffin,Shane A. Phillips,Irena Levitan
Licensed Content Date	Dec 26, 2016
Licensed Content Pages	26
Type of use	Dissertation/Thesis
Requestor type	Author of this Wiley article
Format	Print and electronic
Portion	Figure/table
Number of figures/tables	11
Original Wiley figure/table number(s)	Figure 1 Figure 2 Figure 4 Figure 5 Figure 6 Figure 7 Figure 8 Figure 9 Figure 10 Figure 11 Figure 12
Will you be translating?	No
Title of your thesis / dissertation	Role of Endothelial Potassium Channels in Vasodilation Under Normal and Dyslipidemic Condition
Expected completion date	Aug 2017
Expected size (number of pages)	150
Requestor Location	Dr. Sang Joon Ahn 65 Crofton St

NEW HAVEN, CT 06513

United States  
Attn: Dr. Sang Joon Ahn

Publisher Tax ID EU826007151

Billing Type Invoice

Billing Address Dr. Sang Joon Ahn  
65 Crofton St

NEW HAVEN, CT 06513  
United States  
Attn: Dr. Sang Joon Ahn

Total 0.00 USD

[Terms and Conditions](#)

### TERMS AND CONDITIONS

This copyrighted material is owned by or exclusively licensed to John Wiley & Sons, Inc. or one of its group companies (each a "Wiley Company") or handled on behalf of a society with which a Wiley Company has exclusive publishing rights in relation to a particular work (collectively "WILEY"). By clicking "accept" in connection with completing this licensing transaction, you agree that the following terms and conditions apply to this transaction (along with the billing and payment terms and conditions established by the Copyright Clearance Center Inc., ("CCC's Billing and Payment terms and conditions"), at the time that you opened your RightsLink account (these are available at any time at <http://myaccount.copyright.com>).

#### Terms and Conditions

- The materials you have requested permission to reproduce or reuse (the "Wiley Materials") are protected by copyright.
- You are hereby granted a personal, non-exclusive, non-sub licensable (on a stand-alone basis), non-transferable, worldwide, limited license to reproduce the Wiley Materials for the purpose specified in the licensing process. This license, **and any CONTENT (PDF or image file) purchased as part of your order**, is for a one-time use only and limited to any maximum distribution number specified in the license. The first instance of republication or reuse granted by this license must be completed within two years of the date of the grant of this license (although copies prepared before the end date may be distributed thereafter). The Wiley Materials shall not be used in any other manner or for any other purpose, beyond what is granted in the license. Permission is granted subject to an appropriate acknowledgement

given to the author, title of the material/book/journal and the publisher. You shall also duplicate the copyright notice that appears in the Wiley publication in your use of the Wiley Material. Permission is also granted on the understanding that nowhere in the text is a previously published source acknowledged for all or part of this Wiley Material. Any third party content is expressly excluded from this permission.

- With respect to the Wiley Materials, all rights are reserved. Except as expressly granted by the terms of the license, no part of the Wiley Materials may be copied, modified, adapted (except for minor reformatting required by the new Publication), translated, reproduced, transferred or distributed, in any form or by any means, and no derivative works may be made based on the Wiley Materials without the prior permission of the respective copyright owner. **For STM Signatory Publishers clearing permission under the terms of the [STM Permissions Guidelines](#) only, the terms of the license are extended to include subsequent editions and for editions in other languages, provided such editions are for the work as a whole in situ and does not involve the separate exploitation of the permitted figures or extracts,** You may not alter, remove or suppress in any manner any copyright, trademark or other notices displayed by the Wiley Materials. You may not license, rent, sell, loan, lease, pledge, offer as security, transfer or assign the Wiley Materials on a stand-alone basis, or any of the rights granted to you hereunder to any other person.
- The Wiley Materials and all of the intellectual property rights therein shall at all times remain the exclusive property of John Wiley & Sons Inc, the Wiley Companies, or their respective licensors, and your interest therein is only that of having possession of and the right to reproduce the Wiley Materials pursuant to Section 2 herein during the continuance of this Agreement. You agree that you own no right, title or interest in or to the Wiley Materials or any of the intellectual property rights therein. You shall have no rights hereunder other than the license as provided for above in Section 2. No right, license or interest to any trademark, trade name, service mark or other branding ("Marks") of WILEY or its licensors is granted hereunder, and you agree that you shall not assert any such right, license or interest with respect thereto
- NEITHER WILEY NOR ITS LICENSORS MAKES ANY WARRANTY OR REPRESENTATION OF ANY KIND TO YOU OR ANY THIRD PARTY, EXPRESS, IMPLIED OR STATUTORY, WITH RESPECT TO THE

MATERIALS OR THE ACCURACY OF ANY INFORMATION CONTAINED IN THE MATERIALS, INCLUDING, WITHOUT LIMITATION, ANY IMPLIED WARRANTY OF MERCHANTABILITY, ACCURACY, SATISFACTORY QUALITY, FITNESS FOR A PARTICULAR PURPOSE, USABILITY, INTEGRATION OR NON-INFRINGEMENT AND ALL SUCH WARRANTIES ARE HEREBY EXCLUDED BY WILEY AND ITS LICENSORS AND WAIVED BY YOU.

- WILEY shall have the right to terminate this Agreement immediately upon breach of this Agreement by you.
- You shall indemnify, defend and hold harmless WILEY, its Licensors and their respective directors, officers, agents and employees, from and against any actual or threatened claims, demands, causes of action or proceedings arising from any breach of this Agreement by you.
- IN NO EVENT SHALL WILEY OR ITS LICENSORS BE LIABLE TO YOU OR ANY OTHER PARTY OR ANY OTHER PERSON OR ENTITY FOR ANY SPECIAL, CONSEQUENTIAL, INCIDENTAL, INDIRECT, EXEMPLARY OR PUNITIVE DAMAGES, HOWEVER CAUSED, ARISING OUT OF OR IN CONNECTION WITH THE DOWNLOADING, PROVISIONING, VIEWING OR USE OF THE MATERIALS REGARDLESS OF THE FORM OF ACTION, WHETHER FOR BREACH OF CONTRACT, BREACH OF WARRANTY, TORT, NEGLIGENCE, INFRINGEMENT OR OTHERWISE (INCLUDING, WITHOUT LIMITATION, DAMAGES BASED ON LOSS OF PROFITS, DATA, FILES, USE, BUSINESS OPPORTUNITY OR CLAIMS OF THIRD PARTIES), AND WHETHER OR NOT THE PARTY HAS BEEN ADVISED OF THE POSSIBILITY OF SUCH DAMAGES. THIS LIMITATION SHALL APPLY NOTWITHSTANDING ANY FAILURE OF ESSENTIAL PURPOSE OF ANY LIMITED REMEDY PROVIDED HEREIN.
- Should any provision of this Agreement be held by a court of competent jurisdiction to be illegal, invalid, or unenforceable, that provision shall be deemed amended to achieve as nearly as possible the same economic effect as the original provision, and the legality, validity and enforceability of the remaining provisions of this Agreement shall not be affected or impaired thereby.
- The failure of either party to enforce any term or condition of this Agreement shall not constitute a waiver of either party's right to enforce each and every term and condition of this Agreement. No breach under

this agreement shall be deemed waived or excused by either party unless such waiver or consent is in writing signed by the party granting such waiver or consent. The waiver by or consent of a party to a breach of any provision of this Agreement shall not operate or be construed as a waiver of or consent to any other or subsequent breach by such other party.

- This Agreement may not be assigned (including by operation of law or otherwise) by you without WILEY's prior written consent.
- Any fee required for this permission shall be non-refundable after thirty (30) days from receipt by the CCC.
- These terms and conditions together with CCC's Billing and Payment terms and conditions (which are incorporated herein) form the entire agreement between you and WILEY concerning this licensing transaction and (in the absence of fraud) supersedes all prior agreements and representations of the parties, oral or written. This Agreement may not be amended except in writing signed by both parties. This Agreement shall be binding upon and inure to the benefit of the parties' successors, legal representatives, and authorized assigns.
- In the event of any conflict between your obligations established by these terms and conditions and those established by CCC's Billing and Payment terms and conditions, these terms and conditions shall prevail.
- WILEY expressly reserves all rights not specifically granted in the combination of (i) the license details provided by you and accepted in the course of this licensing transaction, (ii) these terms and conditions and (iii) CCC's Billing and Payment terms and conditions.
- This Agreement will be void if the Type of Use, Format, Circulation, or Requestor Type was misrepresented during the licensing process.
- This Agreement shall be governed by and construed in accordance with the laws of the State of New York, USA, without regards to such state's conflict of law rules. Any legal action, suit or proceeding arising out of or relating to these Terms and Conditions or the breach thereof shall be instituted in a court of competent jurisdiction in New York County in the State of New York in the United States of America and

each party hereby consents and submits to the personal jurisdiction of such court, waives any objection to venue in such court and consents to service of process by registered or certified mail, return receipt requested, at the last known address of such party.

## **WILEY OPEN ACCESS TERMS AND CONDITIONS**

Wiley Publishes Open Access Articles in fully Open Access Journals and in Subscription journals offering Online Open. Although most of the fully Open Access journals publish open access articles under the terms of the Creative Commons Attribution (CC BY) License only, the subscription journals and a few of the Open Access Journals offer a choice of Creative Commons Licenses. The license type is clearly identified on the article.

### **The Creative Commons Attribution License**

The [Creative Commons Attribution License \(CC-BY\)](#) allows users to copy, distribute and transmit an article, adapt the article and make commercial use of the article. The CC-BY license permits commercial and non-

### **Creative Commons Attribution Non-Commercial License**

The [Creative Commons Attribution Non-Commercial \(CC-BY-NC\) License](#) permits use, distribution and reproduction in any medium, provided the original work is properly cited and is not used for commercial purposes. (see below)

### **Creative Commons Attribution-Non-Commercial-NoDerivs License**

The [Creative Commons Attribution Non-Commercial-NoDerivs License](#) (CC-BY-NC-ND) permits use, distribution and reproduction in any medium, provided the original work is properly cited, is not used for commercial purposes and no modifications or adaptations are made. (see below)

### **Use by commercial "for-profit" organizations**

Use of Wiley Open Access articles for commercial, promotional, or marketing purposes requires further explicit permission from Wiley and will be subject to a fee.

Further details can be found on Wiley Online Library

<http://olabout.wiley.com/WileyCDA/Section/id-410895.html>

Other Terms and Conditions:

v1.10 Last updated September 2015

Questions? [customercare@copyright.com](mailto:customercare@copyright.com) or +1-855-239-3415 (toll free in the US) or +1-978-646-2777.

## Vitae

# Sang Joon Ahn

## EDUCATION

### Ph. D. Student, Department of Bioengineering, University of Illinois at Chicago, Present

Major: Cell and Tissue Engineering

### M.M.S., Graduate School of East-West Medical Science, Kyung Hee University, Feb. 2005

Major: East-West Oncology

### B.S., Kyung Hee University, Feb. 2003

Major: Genetic Engineering

## EXPERIENCE

### Electro Cell Physiology Lab, Department of Medicine, University of Illinois at Chicago

*May 2013 to present*

**Research Assistant.** Studying in roles and functions of inwardly rectifying potassium ion channel for arteriole endothelial cells. Studying in physiologic and pathogenic role of cholesterol with the related vascular disease, and the cholesterol dependent dysfunction of potassium ion channels in the development of vascular disease. Developing a new mouse model to discover potassium ion channel functions for atherosclerosis in dyslipidemic condition.

### Islet Transplantation Lab, Department of Surgery, University of Illinois at Chicago

*Sep. 2010 to Dec. 2012*

**Research Assistant.** Studying in pancreatic islet beta cell proliferation and reconstruction of its functional cluster for the clinical application. Studying in pancreatic endocrine precursor from exocrine tissue for the alternate insulin producing beta cell source. Assisted in design, animal tissue isolation, 3D tissue culture, and in vivo assessment.

### Regenerative Nanomedicine Lab, Division of Bioengineering, National University of Singapore

*Aug. 2007 to Apr. 2010*

**Research Assistant.** Studying in corneal tissue regeneration with nanotopography using thermoresponsive material. Assisted in design, assembly and maintenance of experimental instruments.

### Graduate School of East-West Medical Science, Kyung Hee University, Department of Herbal

#### Pharmacology

*Feb. 2005 to Jun. 2007*

**Research Assistant.** Studying in development of medicine for diabetic neuropathy and general neuropathy, using neuronal growth factor expression inducing molecules. Assisted in design, assembly and maintenance of experimental instruments. (Not yet published)

*Feb. 2004 to Feb. 2005*

**Research Assistant.** Studied to develop a whitening reagent through screening inhibitor of Melanin biosynthesis. Led in design, assembly and maintenance of experimental instruments. (Published by Chemical Pharmaceutical Bulletin.)

**Graduate School of East-West Medical Science, Kyung Hee University, Department of East-West Oncology**

*Jan. 2003 to Feb. 2004*

**Research Assistant.** Studied in inducing mechanism of soluble ICAM-1. Assisted in maintenance of experimental instruments. (Not yet published)

*Jan. 2003 to Feb. 2004*

**Research Assistant.** Engaged in another study that confirmed the anti-angiogenic effects by extracting molecules from oriental herbal medicine. Assisted in design and maintenance of experimental instruments. (Not yet published)

## **HONORS**

Recipient, Summa Cum Laude, Graduate School of East-West Medical Science Feb. 2005

Recipient, Brain Korea 21 Scholarship. Mar. 2003–Feb. 2005

Recipient, President's Award Feb. 2003

Recipient, Alumni Association Scholarship Sep. 2002

Recipient, Kyung Hee's Best Student Scholarship Feb. 2002

## **Conference Poster Presentation**

**Ahn S. J.,** Bian J. T., Han H., Schwab S., Thomas J., Eddington D., Phillips S. A., and Levitan I. **Lipoprotein-induced suppression of endothelial Kir channels: potential role in agonist- and flow-induced vasodilation of murine and human arteries.** *Vascular Biology 2013* – North American Vascular Biology Organization

**Ahn S. J.,** Bian J. T., Han H., Schwab S., Rosenhouse-Dantsker A., Thomas J., Eddington D., Phillips S. A., and Levitan I. **The potential role of endothelial Kir channels in dyslipidemia-induced endothelial dysfunction.** *GLC ASPET Annual Meeting 2014* – American Society for Pharmacology and Experimental Therapeutics

**Ahn S. J.,** Bian J. T., Schwab S., Szczurek M., Phillips S. A., and Levitan I. **Role of Kir channels in flow-induced vasodilation.** *AHA Scientific Sessions 2014* – American Heart Association

**Ahn S. J.,** Bian J. T., Epshtein Y., Schwab S., Phillips S. A., and Levitan I. **Role of endothelial Kir channels in flow-induced vasodilation via NO production.** *Experimental Biology 2015* – Experimental Biology

**Ahn S. J.,** Fancher I. S., Bian J. T., Schwab S., Phillips S. A., and Levitan I. **Endothelial Kir channels play a key role in flow-induced vasodilation.** *Vascular Biology 2015* – North American Vascular Biology Organization

**Ahn S. J.**, Fancher I. S., Phillips S. A., and Levitan I. **The role of endothelial Kir channels in flow-induced activation of AKT, eNOS and NO release.** International Vascular Biology Meeting 2016 – North American Vascular Biology Organization

## **PUBLICATION**

**Ahn S. J.**, Koketsu M., Ishhara H., Lee S. M., Ha S. K., Lee K. H., Kang T. H. and Kim S. Y. **Regulation of melanin synthesis by selenium-containing carbohydrates.**

*Chem. Pharm. Bull.*(Tokyo). 2006 Mar;54(3):281-6.

Koo S., **Ahn S. J.**, Zhang H., Wang J. C., and Yim E. K. F. **Human Corneal Keratocyte Response to Micro- and Nano-Gratings on Chitosan and PDMS.** (co-first author)

*Cell. Mol. Bioeng.* 2011 Sep;4(3):399-410.

Wang Y., Mendoza-Elias J. E., Qi M., Harvat T. A., **Ahn S. J.**, Lee D., Gutierrez D., Jeon H., Paushter D., Oberholzer J. **Implication of mitochondrial cytoprotection in human islet isolation and transplantation.**

*Biochem. Res. Int.* 2012; 2012:1-16.

Qi M., Wang Y., Formo K., Marchese E., Wang S., McGarrigle J. J., Bochenek M. A., Kinzer K., Vaca P., Davis M., **Ahn S. J.**, Chang K., Bartholomew A., Benedetti E., Oberholzer J. **Implementation of a simplified method of islet isolation for allogeneic islet transplantation in cynomolgus monkeys.**

*Pancreas.* 2014 Mar;43(2):226-35.

Levitan I., **Ahn S. J.**, Fancher I. S. and Rosenhouse-Dantsker. **Physiological roles and cholesterol sensitivity of endothelial inwardly-rectifying K<sup>+</sup> channels: specific cholesterol-protein interactions through non annular binding sites.**

In “Vascular Ion Channels in Health and Disease,” Editors: Levitna I. and Dopico A., *Springer*, 2016

**Ahn S. J.**, Fancher I. S., Bian J. T., Zhang C. X., Schuwab S., Gaffin R., Phillips S. A., and Levitan I.

**Inwardly-rectifying K<sup>+</sup> channels are major contributors to flow-induced vasodilation in resistance arteries.**

*J. Physiol.* 2017 Apr;595(7):2339-2364.

## **SKILLS**

**Computer Skills:** MS Office, ImageJ, Prism

**Research Skills:** Rodent pancreatic islet isolation, Human pancreatic islet isolation, Primary human corneal cell isolation and culture, Primary Human Umbilical Vascular Endothelial Cell isolation and culture, Primary mouse mesenteric arterial endothelial cell isolation and culture, Various cancer cell culture, Human Mesenchymal Stem cell culture, Hanging drop culture, Immunofluorescence Staining, Immunohistochemistry (Paraffin embedding), Western Blot, Polymerase Chain Reaction, DNA and mRNA isolation, DNA sequencing, DNA gel electrophoresis, Reverse Transcriptase Polymerase Chain Reaction, Real-time (Quantitative) Polymerase Chain Reaction, MTT assay, alama blue assay, PDMS sample fabrication, heat-embossing, solvent casting,

electrospinning, Poly Electrolyte Complex fiber fabrication, Animal drug treatment (oral and peripheral), Animal tissue isolation (sciatic nerve), IPGTT for rodent, OGTT for rodent, Islet transplant to kidney pocket for mouse, Nephrectomy for mouse, Whole blood assay for immune response to biomaterial. (All skills above includes both technical and data analytical aspects.)

**Lab Facilities:** Thermocycler, Microscope, Pipette, Pipette aid, UV-Vis spectrometer, Microplate reader, High Performance Liquid Chromatography, X-ray film developer, Scanning Electron Microscope, Freeze drying machine, Biological Safety Cabinet, Fume hood, Oven, Incubator.

## **REFERENCES**

Available upon request